Bing Topology and Casson Handles

2013 Santa Barbara/Bonn Lectures

Michael H. Freedman

Last update: April 14, 2013

Preface

In January and February 2013 Mike Freedman gave a series of 12 lectures at UC Santa Barbara with the goal to explain his proof of the 4-dimensional Poincaré conjecture. The lectures were broadcast live to the Max Planck Institute for Mathematics (MPIM) in Bonn as part of the *Semester on 4-manifolds and their combinatorial invariants* where Frank Quinn and Peter Teichner ran supplementary discussion sessions. Among the Santa Barbara audience was Bob Edwards who not only contributed various helpful remarks but also stepped in as a guest lecturer and presented his take on "the Design" which is probably the most confusing piece of the proof.

The lectures have been recorded and made available online at the MPIM homepage. In addition, Peter Teichner had the idea to create lecture notes. The original idea was to take handwritten notes and make them available directly after the lecture but after the first lecture it became clear to the designated note taker, Teichner's Ph.D. student Stefan Behrens, that this was not feasible. Instead he decided to create LaTeX notes with the help of the video recordings. The result was a mixture of a word-by-word transcription of the lectures and more or less successful attempts to convert some of the more pictorial arguments into written form. Later on, the rough draft of the notes was revised and significantly improved in a collaborative effort of the MPIM audience. The following people were involved in this process:

Chapters 1 & 2	Stefan Behrens and Peter Teichner
Chapter 3	Henrik Rüping
Chapter 4	Xiaoyi Cui and Nathan Sunukjian
Chapter 5	Daniele Zuddas
Chapter 6	Matt Hogancamp and Ju A. Lee
Chapter 7	Thomas Vogel
Chapter 8	Wojciech Politarczyk and Mark Powell
Chapters 9 & 10	Stefan Behrens and Daniel Kasprowski

However, it goes without saying that most of the credit is due to Mike Freedman who did a sublime job at presenting this material which had become considered as almost impossible to understand. It was a pleasure listening to him explain the beautiful ideas involved in his proof and how they all came together. He managed to make things that had been considered almost impossible to understand seem accessible and not scary at all.

Hopefully, these notes along with the videos will make this high point in 4-manifold topology more accessible in the future.

Contents

Preface **2**

I Bing Topology **5**

1 The Schoenflies theorem after Mazur and Morse **5**
1.1 The Schoenflies problem 5
1.2 Mazur's Schoenflies theorem 5
1.3 Removing the standard spot hypothesis 8

2 The Schoenflies theorem via the Bing shrinking principle **10**
2.1 Shrinking cellular sets 10
2.2 Brown's proof of the Schoenflies theorem 13
2.3 The Bing shrinking criterion 13

3 Decomposition space theory and shrinking: examples **15**
3.1 Some decomposition space theory 15
3.2 Applying the Shrinking criteria to shrink an "X" 17
3.3 Three descriptions of the Alexander gored ball 17
3.4 The Bing decomposition: the first shrink ever 20
3.5 Something that cannot be shrunk 23
3.6 The Whitehead decomposition 25

4 Decomposition space theory and shrinking: more examples **26**
4.1 Starlike-equivalent sets and shrinking 27
4.2 A slam dunk for the Bing shrinking criterion 30
4.3 Mixing Bing and Whitehead 31

5 The ball to ball theorem **32**
5.1 The main idea of the proof 32
5.2 Relations 34
5.3 Iterating the main idea: admissible diagrams 35
5.4 Proof of the ball to ball theorem 37

II Casson handles **38**

6 From the Whitney trick to Casson handles **38**
6.1 The Whitney trick in dimension 4 38
6.2 4-manifolds in the early 1970s: surgery and h-cobordism 40
6.3 Finding dual spheres 43
6.4 Casson handles and Kirby calculus 45

7 Exploring Casson handles **51**
7.1 Picture Camp 51
7.2 The boundary of a Casson handle 56
7.3 An exercise in wishful thinking 58
7.4 A glimpse at reimbedding and the Design 59

8 Combinatorics day **61**
8.1 Gropes and transverse spheres 61
8.2 Height raising and reimbedding for Casson towers 65
8.3 Height raising for gropes 66

9 Geometric control and the Design **67**
9.1 Where Casson left us off 67
9.2 Reimbedding in the grope world 68
9.3 The Design in CEQFAS handles 70
9.4 Embedding the Design in the standard handle 73
9.5 Holes, gaps and the Endgame 76

10 Epilogue: Edwards' original shrink **77**

Part I
Bing Topology

1 The Schoenflies theorem after Mazur and Morse

In the 1950s there was pervasive pessimism about the topological category because nobody knew how to tackle even the simplest problems without smooth or piecewise linear charts. The watershed moment was in 1959 when Mazur gave his partial proof of the Schoenflies conjecture [Maz59].

1.1 The Schoenflies problem

The Schoenflies problem is a fundamental question about spheres embedded in Euclidean space. We denote the d-dimensional Euclidean space by $\mathbb{R}^d$, the unit ball by $B^d \subset \mathbb{R}^d$ and the sphere by $S^d = \partial B^{d+1} \subset \mathbb{R}^{d+1}$. We phrase the Schoenflies problem as a conjecture.

Conjecture 1.1 (Schoenflies)**.** *Any continuous embedding of S^d into the $\mathbb{R}^{d+1}$ extends to an embedding of B^{d+1}.*

In 1914, the 1-dimensional case of the conjecture was proven in full generality by Caratheodory and Osgood-Taylor using elaborate methods from complex analysis. The 2-dimensional case was studied in the 1920s by Alexander who first circulated a manuscript claiming a proof but soon discovered a counterexample himself, the famous *horned sphere*. Later Alexander found an extra condition under which the Schoenflies conjecture holds in dimension 2. This extra condition, the existence of a *bicollar*, makes sense in arbitrary dimensions; it means that the embedding of S^d should extend to an embedding of $S^d \times [-1, 1]$ in which S^d sits as $S^d \times \{0\}$.

In the 40 years that followd almost no progress was made which lead to much dismay about the topological category until Mazur gave his argument.

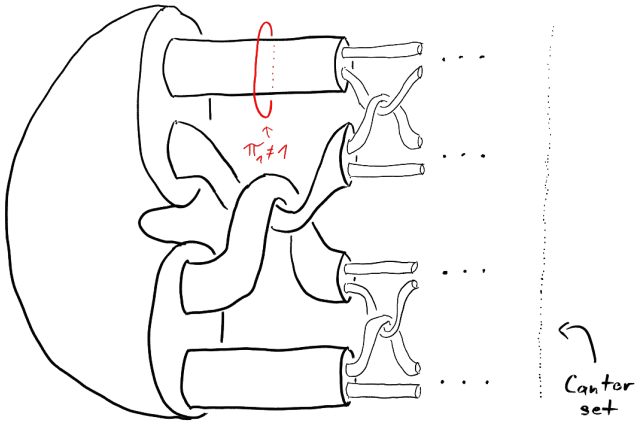

Figure 1: Alexander's horned sphere. (The red circle is not contractible in the exterior.)

1.2 Mazur's Schoenflies theorem

Consider a bicollared embedding $i\colon S^d \times [-1, 1] \to \mathbb{R}^{d+1}$ and fix a point $p \in S^d = S^d \times \{0\}$. Possibly after translation we can assume that $i(p) = 0$. We say that p is a *standard spot*

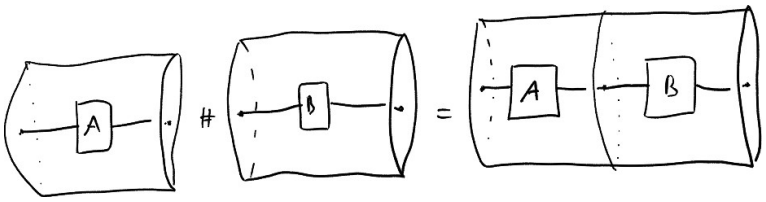

Figure 2: Adding knots.

of i if the following condition is satisfied. There is a disk $D \subset S^d$ around p such that, if we consider $\mathbb{R}^{d+1}$ as $\mathbb{R}^d \times \mathbb{R}$, then

1. i maps $D \times 0$ to $\mathbb{R}^d \times 0$ and
2. for each $q \in D$ the interval $q \times [-1, 1]$ is mapped to $i(q) \times [-1, 1] \subset \mathbb{R}^d \times \mathbb{R}$.

Roughly, this means that i is "as standard as possible" around p.

Theorem 1.2 (Mazur [Maz59])**.** *Let $i\colon S^d \times [-1, 1] \to \mathbb{R}^{d+1}$ be a bicollared embedding which has a standard spot. Then i extends to an embedding of B^{d+1}.*

The strategy of Mazur's proof – which is given in Chapter 1.2.2 below – was based on the *Eilenberg swindle* which is an observation in commutative algebra.

1.2.1 The Eilenberg swindle

Let A be a projective module (over some ring) written as a summand $A \oplus B = F$ of a free module F. Then on the one hand we have

$$(A \oplus B) \oplus (A \oplus B) \oplus (A \oplus B) \oplus \cdots \cong F^\infty$$

while, on the other hand, a different grouping of the summands gives

$$A \oplus (B \oplus A) \oplus (B \oplus A) \oplus (B \oplus A) \oplus \cdots \cong A \oplus F^\infty$$

since the direct sum is associative and commutative (up to isomorphism). Consequently, A becomes a free module after direct summing with an infinitely dimensional free module. In other words, a projective module is *stably free* in the infinite dimensional context.

Before going into Mazur's proof we take a look at a warm up example of an application of this principle in topology.

Example 1.3 (Do knots have inverses?)**.** Knots in $\mathbb{R}^3$ (or S^3) can be added by forming connected sums. The question is whether, given a knot A, there is a knot B such that $A\#B$ is isotopic to the trivial knot I, denoted by $A\#B \cong I$.

If we think of knots as strands in a cylinder connecting one end to the other, then the connect sum operation is realized by simply stacking cylinders next to each other. Note that this operation is also commutative and associative. Indeed, the associativity is obvious and to see the commutativity we can simply shrink B so that it becomes very small compared to A, then slide it along A and let it grow again.

Now let us assume that a knot A has an inverse B, ie $A\#B \cong I$. In this case the swindle works as follows. We sum infinitely many copies of $A\#B$ and think of them as living in a cone which, in turn, lives in a cylinder (see Figure 3). Then we clearly have

$$(A\#B)\#(A\#B)\#(A\#B)\#\cdots \cong I^\infty \cong I$$

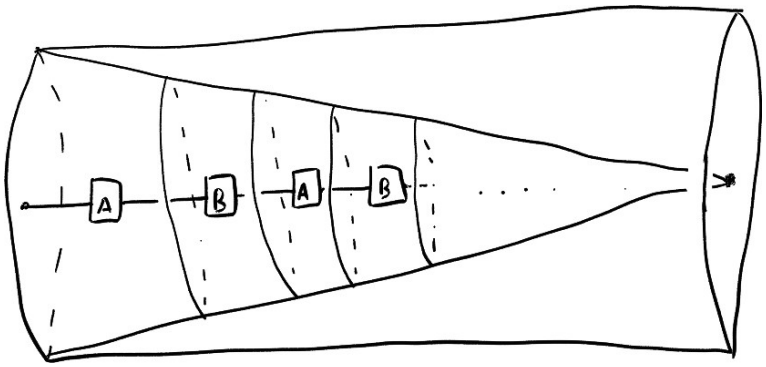

Figure 3: Stacking infinitely many copies of $A\#B$ in a cone.

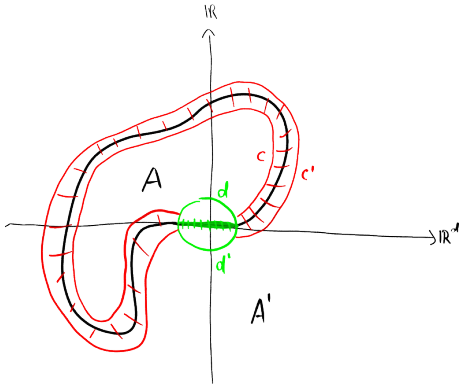

Figure 4: The decomposition used in Mazur's proof.

while a different grouping gives

$$A\#(B\#A)\#(B\#A)\#(B\#A)\#\cdots \cong A\#I^\infty \cong A$$

which proves that A must be the trivial knot.

Remark 1.4. Besides the fact that there are easier proof for the fact that non-trivial knots don't have inverses, the above proof has another drawback in that it "looses category". For example, we might have started with smooth or piecewise linear knots but the conclusion holds only in the topological category since the isotopy we constructed will not be smooth or piecewise linear at the cone point.

1.2.2 The proof of Theorem 1.2

By passing to the one point compactification we can consider i as a flat embedding $S^d \hookrightarrow S^{d+1}$ and we cut out a small (d+1)-ball around the standard spot. What is left is another (d+1)-ball which is cut into two pieces A and A' by the image of i. The standard spot hypothesis implies that the boundary of A (resp. A') is a d-sphere which is decomposed into two standard d-balls c and d (resp. c' and d'), see Figure 4

By construction we have $A \cup_{c\sim c'} A' \cong B^{d+1}$ and, after noticing that gluing two balls along balls (of one dimension lower) gives another ball, it follows that

$$\begin{aligned} B^{d+1} &\cong (A \cup_{c\sim c'} A') \cup_{d'\sim d} (A \cup_{c\sim c'} A') \cup_{d'\sim d} (A \cup_{c\sim c'} A') \cdots \\ &\cong A \cup_{c\sim c'} (A' \cup_{d'\sim d} A) \cup_{c\sim c'} (A' \cup_{d'\sim d} A) \cup_{c\sim c'} (A' \cup_{d'\sim d} A) \cdots \end{aligned}$$

where the regrouping is justified by the associativity of gluing.

This is the setup for another swindle and in order to make it work we have to show that the identification $A' \cup_{d' \sim d} A$ is also a ball. To see this, note that c and d are isotopic in ∂A and, since ∂A is collared by the standard spot hypothesis, this isotopy can be extended to an isotopy of A in the standard way. Analogous results hold for c' and d' in $\partial A'$ and from this we can construct a homeomorphism from $A \cup_{c \sim c'} A'$ to $A \cup_{d \sim d'} A'$ and, since gluing is symmetric, $A' \cup_{d' \sim d} A$ is a ball and the swindle tells us that A is a ball. In fact, by reversing the roles of A and A' we also see that A' is a ball.

Finally, we can glue back in the neighborhood of the standard spot and we see that $S^{d+1} \setminus i(S^d)$ is the union of two open balls which proves the theorem.

1.3 Removing the standard spot hypothesis

After Mazur's work, there was a lot of interest in removing the standard spot hypothesis. This was done in 1960 in a paper by Marston Morse [Mor60].

Theorem 1.5 (Morse [Mor60])**.** *Any flat embedding $S^d \to \mathbb{R}^{d+1}$ has a standard spot after applying a homeomorphism of $\mathbb{R}^{d+1}$.*

Combining the results of Mazur and Morse we immediately get:

Theorem 1.6 (generalized Schoenflies theorem)**.** *Any flat embedding of S^d into $\mathbb{R}^{d+1}$ extends to an embedding of B^{d+1}.*

However, by the time Morse had completed Mazur's argument, Brown had already given an independent proof of Theorem 1.6 which will be discussed in Chapter 2.

Morse used a technique called *push-pull* which was common knowledge around that time. This technique is very general and is valuable in its own right.

1.3.1 Push-pull

We will introduce the technique by proving a theorem which uses it.

Lemma 1.7 (Application of push-pull)**.** *Let X and Y be two compact metric spaces. If $X \times \mathbb{R}$ is homeomorphic to $Y \times \mathbb{R}$, then $X \times S^1$ is homeomorphic to $Y \times S^1$.*

Proof. Let $h \colon X \times \mathbb{R} \to Y \times \mathbb{R}$ be a homeomorphism. Then $Y \times \mathbb{R}$ has two product structures, the intrinsic one and the one induced from $x \times \mathbb{R}$ via h.

By compactness we can find $a, b, c, d \in \mathbb{R}$ such that

- $Y_a = Y \times a$, $Y_c = Y \times c$, $X_b = h(X \times b)$ and $X_c = h(X \times d)$ are disjoint in $Y \times \mathbb{R}$ and
- $X_b \subset Y \times [a, c]$ and $Y_c \subset h(X \times [b, d])$

as illustrated on the left side of Figure 5. The idea is to find a homeomorphism Π of $Y \times \mathbb{R}$ such that the composition $\Pi \circ h \colon X \times \mathbb{R} \to Y \times \mathbb{R}$ has enough periodicity to create a homeomorphism $X \times S^1 \to Y \times S^1$. We construct Π as a composition

$$\Pi = C^{-1} \circ P_Y \circ P_X \circ C$$

where the steps are illustrated in Figure 5. The maps P_X and P_Y will constitute the actual pushing and pulling while C, which we might call *cold storage*, makes sure that nothing is pushed or pulled unless it's supposed to be.

The maps are defined as follows:

- C rescales the intrisic $\mathbb{R}$-coordinate of $Y \times \mathbb{R}$ such that $C(Y \times [a, c])$ lies below the level of X_b and leaves X_d untouched.

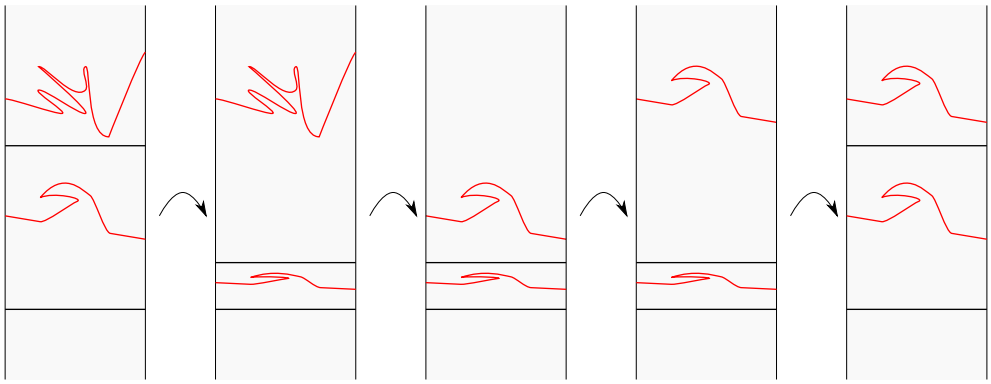

Figure 5: The push pull construction. The red lines indicate the X-levels.

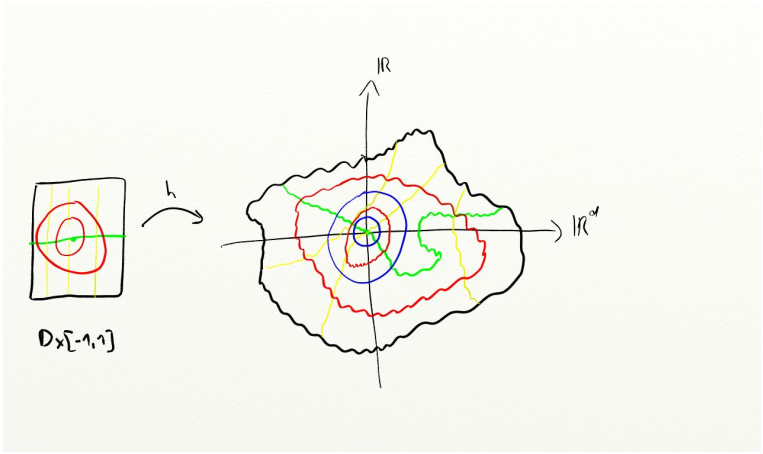

Figure 6: Creating a standard spot.

- P_X pushes X_d down to X_b along the $\mathbb{R}$-coordinate induced by h.
- P_Y pulls X_b up along the intrinsic $\mathbb{R}$-coordinate by the amount $c - a$.

Observe that Π leaves X_b untouched and that $\Pi(X_d)$ appears as a translate of X_b in the intrinsic $\mathbb{R}$-coordinate. By repeating this construction we can create periods with respect to both translations which proves the claim. □

Exercise 1.8. (a) Fill in the details in the proof.
(b) Find spaces X and Y, such that $X \times S^1 \cong Y \times S^1$ but $X \times \mathbb{R} \ncong Y \times \mathbb{R}$.

1.3.2 The proof of Theorem 1.5

Consider an embedding $h\colon S^d \times [-1,1] \to \mathbb{R}^{d+1}$ and fix a point $p \in S^d \times 0$. By translation we can assume that $i(p) = 0$. We choose local coordinates on a disk $D \subset S^d$ containing p and observe that we get an induced local coordinate system on $h(D \times [-1,1]) \subset \mathbb{R}^{d+1}$, see Figure 6.

In this new local coordinate system, the embedded sphere clearly has a standard spot, so it remains to extend it to a global coordinate system.

To achieve this we can use a push-pull argument. The idea is to compare the standard polar coordinates in $\mathbb{R}^{d+1}$ with the ones induced by h. Again, by compactness we can find interlaced pairs standard spheres and curved spheres and, using push pull, we can find an isotopy such that transforms one of the curved sphere into a translate of the other along

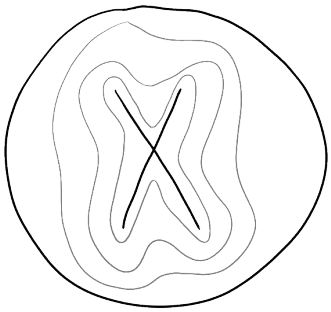

Figure 7: An example of a cellular set.

the standard radial coordinate and preserves a neighborhood of the origin. Moreover, now we can extend the local chart by periodicity to cover all of $\mathbb{R}^{d+1}$.

1.3.3 More about push-pull

A way to think of the push-pull argument is that it gives control over a homeomorphism in one linear direction. A major technical problem when working with topological manifolds is to gain control of a homeomorphism in many directions simultaneously. The culminating step in this direction was Kirby's work on the torus trick which we will take up later

We end this lecture by giving some more applications, probably also due to Brown, of push-pull.

Theorem 1.9 (Brown)**.** *A locally bicollared codimension one embedding is globally bicollared.*

Theorem 1.10 (Brown)**.** *Collars for codimension one submanifolds are unique up to isotopy.*

2 The Schoenflies theorem via the Bing shrinking principle

In this lecture we are getting closer to the material that will be at the core of the 4-dimensional arguments, namely *decomposition space theory*. We will introduce these ideas through the notion of *cellular sets* (see Definition 2.1 below)

2.1 Shrinking cellular sets

Most of the following is due to Brown [Bro60]. We begin by introducing two central notions.

Definition 2.1. A subset $X \subset B^d$ is called *cellular* if it can be written as the intersection of countably many nested balls in B^d, that is, if there embedded d-balls $B_i \subset B^d$, $i = 1, 2, \ldots$, such that $B_{i+1} \subset \text{int}B_i$ and $X = \cap_i B_i$.

As an example, Figure 7 illustrates that the letter X is a cellular subset of B^2.

Exercise 2.2. Which capital letters are cellular sets?

Remark 2.3. Note that cellularity is not an intrinsic property of the space X but depends on the specific embedding.

We will see that the notion of cellular sets is closely related to maps whose point preimages are mostly singletons while some points have larger preimages. One can think of such maps as close to being homeomorphisms. The following terminology will be useful.

Definition 2.4. Let $f\colon X \to Y$ be a map. A point preimage $f^{-1}(y)$, $y \in Y$, is called an *inverse set* of f it contains more than one element.

Eventually, we will obtain a characterization of cellular sets in terms of inverse sets. We start by showing that isolated inverse sets are cellular.

Lemma 2.5. *Let $f\colon B^d \to \mathcal{B}^d$ be a continuous map between balls with a unique inverse set $X = f^{-1}(y)$, $y \in \mathcal{B}^d$ which is contained in the interior of B^d. Then X is cellular.*

Note that we do not assume that f maps boundary to boundary.

Proof. We first observe that $y \in \mathcal{B}^d$ is an interior point and that we can find an $\epsilon > 0$ such that the standard ball $B_\epsilon(y) \subset \mathcal{B}^d$ around y is contained in the image of f.

Exercise 2.6. Convince yourself that this is true. (Hint: Invariance of domain)

Next we choose some homeomorphism $s_\epsilon\colon \mathcal{B}^d \to \mathcal{B}^d$ of the target ball which restricts to the identity on the smaller ball $B_{\epsilon/2}(y)$ and squeezes the rest of $\mathcal{B}^d$ into $B_\epsilon(y)$. (Such a homeomorphism can be obtained, for example, by constructing an isotopy that moves y to 0 with which we then conjugate a suitable radial contraction.) Using this we now define a map $\sigma_\epsilon\colon B^d_s \to B^d_s$ from the source ball to itself by

$$\sigma_\epsilon(x) = \begin{cases} x & \text{if } x \in X \\ f^{-1} \circ s_\epsilon \circ f(x) & \text{if } x \notin X. \end{cases}$$

Note that σ_ϵ is well defined because f restricts to a injection $B^d \setminus X \to \mathcal{B}^d \setminus \{y\}$ and, by construction, s_ϵ does not map $f(x)$ to y. Moreover, one can show:

Exercise 2.7. Verify that σ_ϵ is injective, continuous and a homeomorphism onto its image.

The proof is finished by choosing a sequence $\epsilon = \epsilon_1 > \epsilon_2 > \cdots > 0$ which converges to zero and the observation that the balls $B_i = \sigma_{\epsilon_i}(B^d) \subset B^d$ exhibit X as a cellular set. □

The next result introduces the central idea of *shrinking* in the context of cellular sets.

Lemma 2.8 (Shrinking cellular sets)**.** *Let $X \subset B_d$ be a cellular set. For any $\epsilon > 0$ there exists a homeomorphism $h^X_\epsilon\colon B^d \to B^d$ such that*

(i) h^X_ϵ is the identity outside a ϵ-neighborhood of X.

(ii) The diameter of $h^X_\epsilon(X)$ is less then ϵ.

Proof. Since X is cellular we can find a ball around X all of whose points have distance at most ϵ to X. Given such a ball, we can construct h^X_ϵ by a similar "radial squeeze" argument as in the previous proof. □

Going one step further, we can not only shrink cellular sets but in fact crush them.

Lemma 2.9. *If $X \subset B^d$ is cellular, then the quotient B^d/X is homeomorphic to B^d.*

Proof. We choose a sequence $\epsilon_1 > \epsilon_2 > \cdots > 0$ which converges to zero and define a map

$$g^X = \lim \left(\cdots \circ h^{h^X_{\epsilon_1}(X)}_{\epsilon_2} \circ h^X_{\epsilon_1} \right)\colon B^d \to B^d$$

with h^X_ϵ given as in Lemma 2.8.

Exercise 2.10. Convince yourself that this limit exists in the space $C(B^d, B^d)$ of continuous self maps of B equipped with the sup-norm.

If $\pi\colon B^d \to B^d/X$ denotes the quotient map, then it is easy to see that the expression $\pi\circ g^{-1}$, which is a priori only a *relation*, actually defines a map. Moreover:

Exercise 2.11. $\pi \circ (g^X)^{-1}\colon B^d \to B^d/X$ is a homeomorphism.

□

Remark 2.12. Some remarks about the topology of quotients are in place. First of all, we will always equip quotient spaces with the *quotient topology* which means that the open sets in the quotient are exactly those sets whose preimages are open. Since all these lectures live in the world of compact metric spaces, it is important to note that it is not completely obvious how to obtain metrics on quotient spaces. What keeps us safe is the *Urysohn metrization theorem* which states that compact, second countable Hausdorff spaces are metrizable. Compactness and second countability are never an issue since these properties are preserved by dividing out closed sets, so all we have to check is the Hausdorff property which will be obvious is most cases we will encounter.

We want to point out two rather obvious properties of the map g^X which nevertheless have interesting consequences. On the one hand, it is easy to see that g^X maps X to a single point while it is injective in the complement of X. This gives another characterization of cellular sets.

Corollary 2.13. *A subset $X \subset B^d$ is cellular if and only if there is a map $f\colon B^d \to \mathcal{B}^d$ as in Lemma 2.5 which has X as its unique inverse set. (In fact, one can assume that $\mathcal{B}^d = B^d$, that f is surjective and that it restricts to the identity on a neighborhood of the boundary.)*

On the other hand, g^X is defined as the limit of homeomorphism. Maps with this property are important enough to have a name.

Definition 2.14. A continuous map $f\colon X \to Y$ between complete metric spaces X and Y is called *approximable by homeomorphisms* or *ABH* if it can be written as the limit of homeomorphisms in the sup-norm.

Hence, from the above consideration we can deduce:

Corollary 2.15. *If $f\colon B^d \to B^d$ is the identity on the boundary and has a unique inverse set, then f is ABH.*

Remark 2.16. A more precise statement of Lemma 2.9 is that the projection $\pi\colon B^d \to B^d/X$ is ABH.

Proposition 2.17. *Let $f\colon B^d \to B^d$ be a map which is the identity on the boundary and has finitely many inverse sets $X_1, \dots, X_N$. Then:*

1. *Each X_i is cellular.*
2. *f is ABH.*
3. *The quotient $B^d/\{X_1, \dots, X_N\}$ is homeomorphic to B^d.*

Proof. We only treat the case $N = 2$, the rest is an easy induction. As in the proof of Lemma 2.5 we consider a conjugation of the form $f^{-1} \circ s_1 \circ f$ where s_1 is a squeeze for X_1 but this time we don't get a homeomorphism because of X_2. Instead, we obtain a map which has X_2 as its unique inverse set. From this we see that X_2 is cellular and can thus be collapsed. Morover, using Corollary 2.15 we can fix the above map to obtain a homeomorphism with which we can continue with the arguments in the proof of Lemma 2.5 eventually showing that X_1 is also cellular. Finally, the fact that f is ABH can easily be deduced from the local nature of the construction of g^X above. □

2.2 Brown's proof of the Schoenflies theorem

After this lengthy discussion we come back to the Schoenflies theorem (Theorem 1.6) which is almost turned into a one-line consequence by Proposition 2.17. For convenience we restate the Schoenflies theorem in a slightly different but equivalent form.

Theorem 2.18 (Brown [Bro60])**.** *Let $i\colon S^{d-1} \hookrightarrow S^d$ be an embedding which admits a bicollar. Then the closure of each component of $S^d \setminus i(S^{d-1})$ is homeomorphic to B^d.*

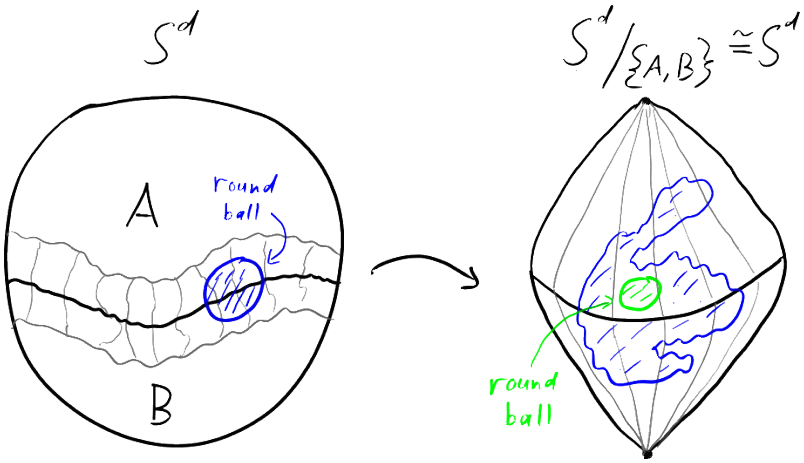

Figure 8: The setup of Brown's proof.

Proof. We extend i to an embedding $I\colon S^{d-1} \times [-1,1] \hookrightarrow S^d$ and denote by $A, B \subset S^d$ the closures of the components of the complement of the image of I. Observe that the quotient $S^d/\{A,B\}$ is obviously homeomorphic to S^d since I essentially identifies it with the suspension of S^{d-1} which is homeomorphic to S^d (see Figure 8). We can thus write down the composition

$$S^d \xrightarrow{\pi} S^d/\{A,B\} \xrightarrow{\cong} S^d$$

which is a map with exactly two inverse sets, namely A and B. In order to apply Proposition 2.17 we have to reduce the situation to a map between balls. This is achieved by excising small, standard balls from the source and target spheres such that the ball in the source (blue in Figure 8) is contained in the image of I and the one in the target (green in Figure 8) is contained in the interior of the image of the one in the source. □

2.3 The Bing shrinking criterion

The Bing shrinking criterion is a natural generalization of Lemma 2.8 where we showed how to shrink cellular sets. The idea of shrinking goes back to a paper of Bing in 1952 [Bin52] but was only formalized by Bob Edward's in his ICM talk in 1978 [Edw80] where he gave a very succinct statement of a shrinking criterion which had previously been absent in the literature.

Theorem 2.19 (Bing shrinking criterion à la Edwards 1978 [Edw80])**.** *Let $f\colon X \to Y$ be a map between complete metric spaces. Then f is ABH if and only if for any $\epsilon > 0$ there is a homeomorphism $h\colon X \to X$ such that*

(i) $\forall x \in X\colon \operatorname{dist}_Y\big(f(x), f \circ h(x)\big) < \epsilon$ *and*

(ii) $\forall y \in Y\colon \operatorname{diam}_X\big((f \circ h)^{-1}(y)\big) < \epsilon$.

The first condition roughly means that h is close to the identity as measure in the target space Y and the second condition controls the size of preimage sets. This is very similar to what we have seen in the process of shrinking cellular sets. The upshot of the theorem is that finding a coherent way of shrinking the preimage sets is equivalent to approximating by homeomorphisms.

Proof. The one direction is very easy. If we have a sequence of approximating homeomorphisms $h_n\colon X \to Y$, then the compositions of the form $h_n^{-1} \circ h_{n+k_n}$ will satisfy (i) and (ii) for a given $\epsilon > 0$ as long as n, k_n is large enough.

The other, more interesting direction can be proved by elementary methods but we will sketch a "Bourbaki style" proof due to Edwards. Consider the space $C(X, Y)$ with the sup-norm topology. This is well known to be a complete metric space. According to Edwards we consider the set

$$\{f \circ h \,|\, h\colon X \to X \text{ homeomorphism}\} \subset C(X, Y)$$

and denote by E its closure. Then E is also a metric space and, in particular, satisfies the *Baire category theorem* which states that the countable intersection of open and dense sets is still dense. For $\epsilon > 0$ we let E_ϵ be the subset of E of all maps whose inverse sets have diameter strictly less than ϵ. This is clearly an open set and the conditions (i) and (ii) eventually imply that E_ϵ is also dense in E. By the Bair category theorem the set $E_0 = \cap_{\epsilon>0} E_\epsilon$ is dense in E, in particular, it is none-empty. But E_0 clearly consists of homeomorphisms because the inverse sets have to be points. □

The relation to cellurarity is given by the following easy exercise.

Exercise 2.20. If X, Y are compact metric spaces and $f\colon X \to Y$ is ABH, then all point preimages $f^{-1}(y)$ are cellular.

Remark 2.21. So far we have discussed the situation where we take a ball and a couple of subsets and we ask whether we can crush these sets to points and still get something homeomorphic to a ball. The general question in decomposition space theory is a little wilder. Usually we have some manifold and there may be infinitely many things to crush in it, possibly even uncountably many. To answer the question whether the quotient is homeomorphic to the original space there are two main tools. One of them is the Bing shrinking criterion with which we can try to shrink everything simultaneously in a controlled way. However, we will later see examples which indicate that this is a highly non-trivial problem. The problem is that, when we have infinitely many inverse sets, these might be linked in the sense that whenever we shrink some of them, some others will be stretched out, leading to a subtle and beautiful story which things can or cannot be shrunk.

In this discussion the Alexander's horned sphere makes another prominent appearance and, in fact, it was main the focus of Bing's paper [Bin52]. Bing's motivation was the following. In the 1930s Wilder had constructed an interesting space and had asked whether it was homeomorphic to the 3-sphere. He considered the exterior of Alexander's horned ball and took its double. Wilder's interest was the fact that the doubled object has an obvious involution which merely exchanges the two halves. However, if this space turned out to be homeomorphic to S^3, then this would give a very interesting involution on the 3-sphere whose fixed point set is a very wild 2-sphere. As a consequence, it would be a topological involution which is not conjugate to a smooth involution. While he could gather some evidence that his space was the 3-sphere, Wilder was unable to produce a conclusive proof and his question remained unanswered until Bing's paper.

3 Decomposition space theory and shrinking: examples

3.1 Some decomposition space theory

We begin by setting up some basic terminology from *decomposition space theory*. An extensive account is given in Daverman's book [Dav86] although the terminology used therein differs slightly from ours.

Definition 3.1. A *decomposition* of a space X is a collection $\mathcal{D} = \{\Delta_i\}_{i\in I}$ of pairwise disjoint, closed subsets $\Delta_i \subset X$, the *decomposition elements*, indexed by a (possibly uncountable) index set I.

Given a decomposition $\mathcal{D}$ of X, the *quotient space* or *decomposition space* of $\mathcal{D}$ is the space $X/\mathcal{D}$ obtained by crushing each set $\Delta \in \mathcal{D}$ to a point[1] and endow it with the quotient topology as in Remark 2.12. We generically denote quotient maps by $\pi\colon X \to X/\mathcal{D}$.

Remark 3.2. You may notice that our notion of decomposition is a slight abuse of language. Strictly speaking, a decomposition should be a partition of the whole space into pairwise disjoint sets. However, any decomposition as in Definition 3.1 can be completed to an honest decomposition by adding singletons to the decomposition for each point which was not contained in any decomposition element. Clearly, these singletons do not change the decomposition space or the quotient map so that they can essentially be ignored. Equivalently we can think of it as an equivalence relation with closed equivalence classes.

We will usually start with X being a compact, second countable, Hausdorff space (and thus metrizable by Urysohn's theorem) and we need a condition to guarantee that the $X/\mathcal{D}$ stays within this nice class of spaces. As mentioned earlier, the only problem is the Hausdorff property.

Definition 3.3. Let X be a space with a decomposition $\mathcal{D}$. Given any subset $S \subset X$ we define its *($\mathcal{D}$-)saturation* as

$$\pi \in v(\pi(X)) = (S \setminus \cup_{\Delta\in\mathcal{D}}\Delta) \cup (\cup_{\Delta\subset S}\Delta)$$

and say that S is *($\mathcal{D}$-)saturated* if $S = \pi^{-1}(\pi(S))$. The saturation is the smallest, saturated subset of X that contains S. We can also consider the largest saturated subset of X, defined by

$$S^* := X \setminus \pi^{-1}\pi(X \setminus S).$$

In other words, a subset is saturated if it is the union of decomposition elements and points outside decomposition elements.

Definition 3.4. A decomposition $\mathcal{D} =$ of X is *upper semi-continuous* if each $\Delta \in \mathcal{D}$ has a saturated neighborhood system or, equivalently, if $U \subset X$ is an open subset, then U^* is also open.

Figure 9 illustrates some typical upper semi-continuous behavior of a decomposition and a failure thereof.

Exercise 3.5. Show that the two conditions in Definition 3.4 are in fact equivalent.

Exercise 3.6. Let $\mathcal{D}$ be an upper semi-continuous decomposition of X. Show that, if X is second countable, then so is $X/\mathcal{D}$. Show the same for the Hausdorff property

[1] Note that $X/\mathcal{D}$ is different from $X/(\amalg_i\Delta_i)$ where all the Δ_i are crushed to a single point!

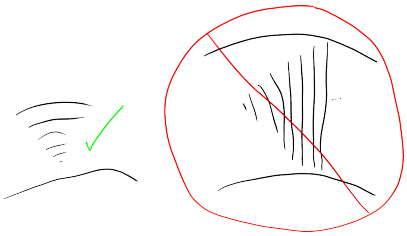

Figure 9: Upper semi-continuity and its failure

The latter exercise implies that, if we consider upper semi-continuous decompositions of compact metric spaces, then we never have to leave this nice class of spaces. However, there is usually no canonical metric on the quotient. It's tempting to try to "see" a metric on the quotient without going through any metrization theorems but it's usually not that easy.

Figure 10: The "middle third" construction of the Cantor set.

Example 3.7. An interesting 1-dimensional decomposition is to take the "middle third" construction of the Cantor set in the unit interval (see Figure 10) and to think of the closed middle third regions as the elements of the decomposition. It turns out that the quotient is again homeomorphic to the interval and one might try to measure length on the quotient by imagining being a taxi cab driving through the interval and turning the meter off inside decomposition elements. But the inconvenient thing is that the Cantor set has measure zero, so the naive taxi cab idea doesn't work.

Now that we have singled out the appropriate class of spaces and decompositions for our purposes, we introduce the important concept of *shrinkability*. With the Bing shrinking criterion (Theorem 2.19) in mind we make the following working definition.

Definition 3.8 (Shrinkability, working definition)**.** An upper semi-continuous decomposition $\mathcal{D}$ of a compact metric space X is *shrinkable* if the quotient map $\pi\colon X \to X/\mathcal{D}$ is ABH.

This definition certainly hides the actual shrinking but it avoids the (ultimately inessential) ambiguity of choosing a metric on the decomposition space on the other end of Theorem 2.19. We will usually appeal to the following shrinking criterion which easily follows from Theorem 2.19.

Corollary 3.9. *Let $\mathcal{D}$ be an upper semi-continuous decomposition of a compact metric space X. Assume that for any $\epsilon > 0$ there exists a homeomorphism $h\colon X \to X$ such that*

(i) h is supported in an ϵ-neighborhood of the decomposition elements and

(ii) for each $\Delta \in \mathcal{D}$ we have $\operatorname{diam}(h(\Delta)) < \epsilon$.

Then $\mathcal{D}$ is shrinkable.

Remark 3.10. In its most general form, shrinkability can be defined for an arbitrary decomposition $\mathcal{D}$ of an arbitrary space X by requiring that for any saturated open cover $\mathcal{U}$ and any arbitrary open cover $\mathcal{V}$ of X there exists a homeomorphism $h\colon X \to X$ such that

(i) $\forall x \in X\ \exists U \in \mathcal{U}\colon x, h(x) \in U$ and

(ii) $\forall \Delta \in \mathcal{D}\ \exists V \in \mathcal{V}\colon h(\Delta) \in V$.

What happens to the old assumptions, like the quotient is metrizable etc.

3.2 Applying the Shrinking criteria to shrink an "X".

Maybe its really just a remark or an example.

Example 3.11. Let $A = \{(x, \pm x) | -\frac{1}{2} \leq x \leq \frac{1}{2}\}$ and let $\mathcal{D} = \{A\}$ be the decomposition of $X := B_1(0) \subset \mathbb{R}^2$. We already verified that $\pi : X \to X/\mathcal{D}$ is ABH, but it will be illuminating to verify the conditions of the Shrinking principle. Let us verify the conditions appearing in the most general form in remark 3.10.

So let $\mathcal{U}$ be any saturated cover of X and let $\mathcal{V}$ be any open cover of X. We now have to produce a homeomorphism with certain properties. By saturation we can find a open set $U \in \mathcal{U}$ that contains A. We will define h in such a way that $\text{supp}(h) \subset U$. Thus we get

$$\forall x \in X\ \exists U \in \mathcal{U}\colon x, h(x) \in U.$$

The statement is trivial for $x \notin \text{supp}(h)$. Otherwise x and $h(x)$ both lie in U. Pick some point $x \in X$ and an open set $V \in \mathcal{V}$ containing x. Now choose a homeomorphism of U fixing its boundary that maps A into a small ball around x that is still contained in $V \cap U$. This will ensure the second shrinking condition. The picture looks like this: A bit fishy

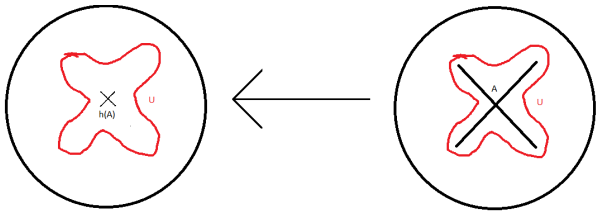

Figure 11: The homeomorphism that shrinks the X.

but I hope its OK.

3.3 Three descriptions of the Alexander gored ball

We now come back to Bing's discussion of the Alexander horned sphere, more precisely, its exterior as shown in Figure 1. By turning the latter picture inside out we obtain a ball where the horns poke into the inside. Following a suggestion of Bob Edwards we call this creature the *Alexander gored ball*, denoted by $\mathcal{A}$. We will give three descriptions of $\mathcal{A}$.

3.3.1 The usual picture: an intersection of balls

The first picture is the above mentioned inside out version of Figure 1. Starting with the standard 3-ball, we drill two pairs of holes in it creating two almost-tunnels which are "linked" as in Figure 12 and repeat this construction indefinitely as indicated.

Remark 3.12. Note that this construction is easily modified to show that $\mathcal{A}$ is a cellular subset of B^3.

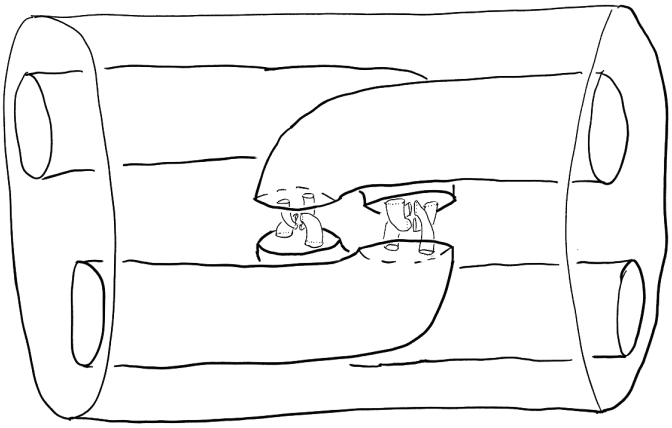

Figure 12: $\mathcal{A}$ as a countable intersection of 3-balls.

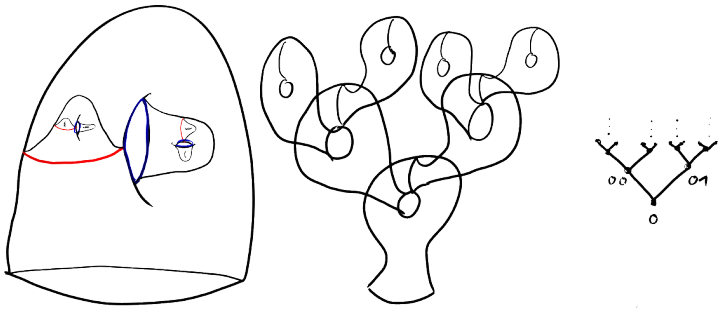

Figure 13: $\mathcal{A}$ as a grope.

3.3.2 The grope picture

There's an equally productive picture of $\mathcal{A}$ as an infinite union of thickened, punctured tori with some limit points added. The construction goes as follows. We denote by T_0 the 2-torus with an open disk removed and let $\boldsymbol{T} = T_0 \times [0,1]$. We also fix a meridian-longitude pair of curves $\mu, \lambda \subset T_0$. We start with a single copy $\boldsymbol{T}_0$ of $\boldsymbol{T}$ and attach two extra copies $\boldsymbol{T}_{00}$ and $\boldsymbol{T}_{01}$ along $\mu_0 \times \{0\}$ and $\lambda_0 \times \{1\}$, respectively, where meridian and longitude are indexed according to the corresponding copy of $\boldsymbol{T}$ (note that there's a canonical framing swept under the rug). Next, we attach four more copies $\boldsymbol{T}_{000}$, $\boldsymbol{T}_{001}$, $\boldsymbol{T}_{010}$ and $\boldsymbol{T}_{011}$ along $\mu_{00} \times \{0\}$, $\lambda_{00} \times \{1\}$, $\mu_{01} \times \{0\}$ and $\lambda_{01} \times \{1\}$ and so on. The result is an infinite union of copies of $\boldsymbol{T}$ indexed by a tree as indicated in Figure 13. This process can be done carefully so that the resulting space is embedded in 3-space and which forces the longitudes and meridian to get smaller and smaller in the successive stages such that they will ultimately converge to points in the limit. It is clear from the construction that these limit points form a Cantor set in 3-space; indeed, they correspond to the limit points of the tree in Figure 13 which, in turn, correspond to infinite dyadic expansions.

We claim that the infinite union of tori together with these limit points is homeomorphic to $\mathcal{A}$. To see this we first give a complicated description of B^3. Figure 14 shows a picture of $B^2 \times I \cong B^3$ which can be interpreted as relative handle decomposition built on B^2 with a canceling 1- and 2-handle pair (the neighborhoods of the yellow arcs). In the intermediate level we see a copy of T_0 with a longitude-meridian pair given by the belt circle of the 1-handle and the attaching circle of the 2-handle each of which naturally bounds a disk; we call these disks *caps* for T_0, anticipating some future language. We now take this picture of $B^2 \times I$ and replace the neighborhood of each yellow arc, which is

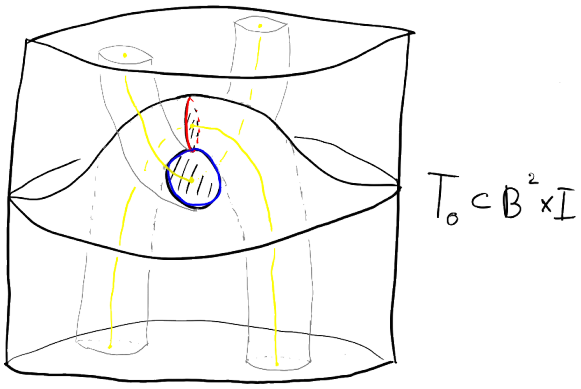

Figure 14: A "capped torus" thickened in 3-space

clearly homeomorphic to $B^2 \times I$, with a copy of the entire picture and repeat this process indefinitely. Note that, with each step the caps will appear smaller and smaller and, again, limit to a Cantor set in B^3. Moreover, through each of these limit points there will be precisely one yellow arc with endpoints on either the top or the bottom of $B^2 \times I$ giving rise to a Cantor set worth of arcs.

The relation between the two constructions of the gored ball now becomes obvious. On the one hand, we can modify the construction slightly to the extend that, in each step we drill out the neighborhoods of the yellow arcs (parametrized by $B^2 \times [-1, 1]$, say), but instead of gluing the model along the whole of $S^1 \times [-1, 1]$ we only glue along $S^1 \times [-\epsilon, \epsilon]$ for some small $\epsilon \in (0, 1)$. This modified construction matches precisely with Figure 12. On the other hand, it is easy to see that, if we remove the neighborhood of the yellow arcs from $B^2 \times I$ in Figure 14, then we are left a copy of $\boldsymbol{T} = T_0 \times I$. Removing the neighborhoods of all yellow arcs in each step of the construction exhibits the infinite union of tori in Figure 13 embedded in B^3 and what's missing from the gored ball is exactly the limit Cantor set of the longitude meridian pairs.

Remark 3.13. The "union of (capped) tori"-construction is a first example of a *(capped) grope*. More general versions of this constructions (where the torus can be replaced with a different orientable surface with one boundary component in each step and the thickening takes place in 4-space) will play a central role in the 4-dimensional arguments. Forgetting the embedding into 3-space in our toy example, we can think of the grope as a 2-complex made by assembling a countable collection of punctured tori as in the middle of Figure 13. This kind of picture, although not accurate in three dimensions, will appear frequently in the 4-dimensional context.

Remark 3.14. I figured this out by hand. Hopefully it is correct. If there is a better argument, we should give it. Let $\partial\mathcal{A}$ be the boundary of the Alexander gored-ball. If we add a collar to it, ie. consider the mapping cylinder of the inclusion of the boundary we get a 3-ball. But the mapping cylinder construction does not change the homotopy type. Thus $\mathcal{A}$ is simply connected. Maybe we should place a reference to the collar statement here (IF there is none Schoenflies will also do the job.

3.3.3 The gored ball as a decomposition space

Finally, we will exhibit $\mathcal{A}$ as a decomposition space $B^3/\mathcal{D}$ where the decomposition $\mathcal{D}$ of B^3 is given by the Cantor set of yellow arcs in our complicated picture of $B^3 \cong B^2 \times I$ from the previous sectionref. Moreover, these yellow arcs will exhibit some iterated clasping as in Figure 15.

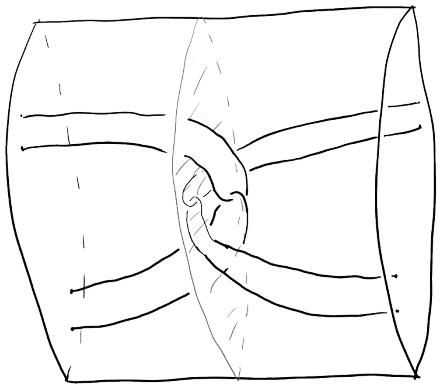

Figure 15: The decomposition of B^3 giving rise to $\mathcal{A}$.

To see that the quotient space of $\mathcal{D}$ is homeomorphic to $\mathcal{A}$ we take a closer look at the first description. There we had written $\mathcal{A} = \cap_{k=0}^{\infty} B_k$ as a countable intersection of 3-balls B_k such that $B_0 = B^3$ and $B_{k+1} \subset B_k$. The important observation is that, in each step, B_{k+1} can be obtained from B_k by performing an ambient isotopy of 3-space, in particular, we have homeomorphisms "retractions" instead of "homeomorphisms"?Otherwise I do not see some of the statements... $h_k \colon B_k \to B_{k+1}$. Taking the limit we obtain a map

$$h_\infty := \lim_k h_k \colon B^3 \to \cap_k B_k = \mathcal{A}$$

whose union of inverse sets consist of all points that are moved by h_k for infinitely many k and it is easy to see that the h_k can be chosen such that these points agree with the yellow arcs in $\mathcal{D}$. $\mathcal{D}$ is given by the preimages of points of h_∞. Thus $B^3/\mathcal{D} \xrightarrow{\cong} \mathcal{A}$ is a bijection which is, in fact, a homeomorphism given that h_∞ is continuous. Let us have a look at the decomposition induced by h_∞. We can further collapse everything that between the gaps in the tori in the n-th stage we get a map $B^3 \to \mathcal{A} \to \mathcal{A}/\sim_n$. The induced decomposition on B^3 consists of 2^n cylinders linked as in ref to a picture. If we pass to the limit we have to take the intersections of those sequences of cylinders and we end up with the decomposition given by the Cantor set of yellow arcs from the previous section.ref. Especially note that by compactness $\mathcal{A} = \lim_{\leftarrow} \mathcal{A}/\sim_n$.

Exercise 3.15. Show that $h_\infty \colon B^3 \to \mathcal{A}$ is continuous.

Remark 3.16. This construction of $\mathcal{A}$ brings up an interesting question about the Bing shrinking criterion. We have described $\mathcal{A}$ as the result of crushing certain arcs in B^3 to points and this crushing could be done by homeomorphisms of 3-space and it can be done so as not to move points far in the quotient. So one might think that crushing this decomposition should not change the topology of B^3. However, the point is that the Bing shrinking criterion requires homeomorphisms of B^3 and not of the ambient space. It only tells us that the topology of 3-space does not change when $\mathcal{D}$ is crushed to points. In fact, for fundamental group reasons the topology of B^3 has to change which tells us that $\mathcal{D}$ cannot be shrunk. I understand this as: The interior of the Alexander gored ball has nontrivial fundamental group, while the interior of a Ball has trivial fundamental group. If they were homeomorphic, the interior would be mapped to the interior (argument!). So they can not be homeomorphic.

3.4 The Bing decomposition: the first shrink ever

In the following we will see the first decomposition that was ever shrunk and how it was shrunk. Interestingly enough, it was quite a non-trivial shrink.

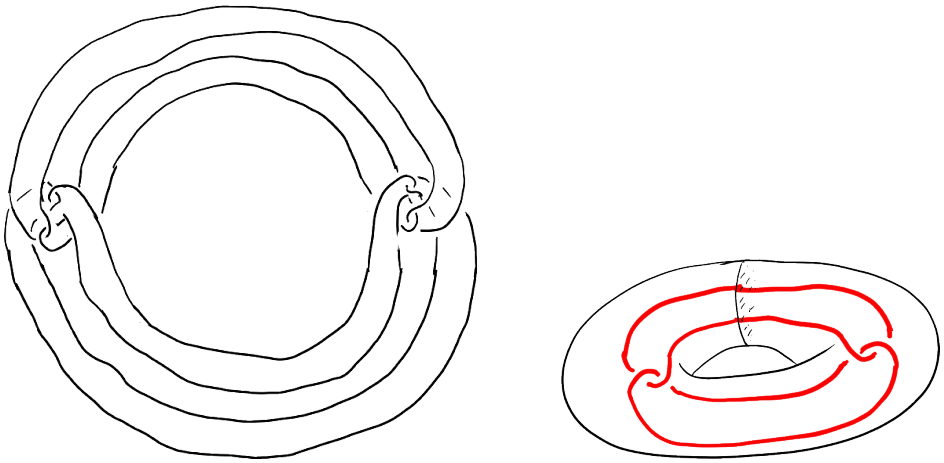

Figure 16: The second stage of the Bing decomposition (left) and its defining pattern (right).

We take the double $D\mathcal{A}$ of the Alexander gored ball and also double the corresponding decomposition $\mathcal{D}$ of B^3 to obtain a decomposition $\mathcal{B} = D\mathcal{D}$ of S^3 known as the *Bing decomposition*. The picture of the Bing decomposition is what nowadays would be called the infinitely iterated untwisted *Bing double* of the unknot in S^3 (the left of Figure 16 shows second iteration). More precisely, the Bing decomposition is the countable intersection of nested solid tori where the nesting pattern is shown in the right of Figure 16.

Remark 3.17. When we draw a picture of a decomposition what we really draw is usually only a *defining sequence*, that is, we describe a system of closed sets nested in each other and the decomposition element are the components of the intersection. In many cases it is enough to indicate a nesting pattern as we did above for the Bing decomposition.

Theorem 3.18 (Bing, 1952 [Bin52])**.** *The Bing decomposition is shrinkable. In particular, the quotient map* $D\pi\colon S^3 \to D\mathcal{A}$ *is ABH.*

As mentioned earlier, this answered the question of Wilder whether the obvious involution on $D\mathcal{A}$ was an exotic involution on S^3 instead of just an involution on some pathological metric space.

So how do we shrink this thing? Recall that the decomposition elements are the countable intersection of nested solid tori where each torus contains two successors which form a neighborhood of the Bing double of the core of the original torus. Note that the n-th stage of this construction adds 2^n solid tori and in each stage the tori get thinner and thinner while their "length"[2] roughly remains the same. Now, given some $\epsilon > 0$ we have to come up with a homeomorphism of S^3 which shrinks each decomposition element to size less than ϵ and whose support has distance less than ϵ from the decomposition elements. The basic idea is as follows: We focus on a stage far enough in the construction, call it n_ϵ, where the 2^{n_ϵ} tori are thinner than ϵ and in each of these tori we produce an isotopy that shrinks the decomposition elements. Since all tori within a given stage are isometric it is enough to describe such an isotopy on a single torus.

To construct such an isotopy, the first thing to note is that the normal directions in the torus will not cause any problem because we can choose the torus as thin as we like. The only problem is the linear extent and in doesn't really matter what coordinate system we use to make that small. Bing's idea was to lay the torus out along the real line, to just measure diameter in terms of that direction and to make the tori of the subsequent

[2]More precisely: the length of the core curves.

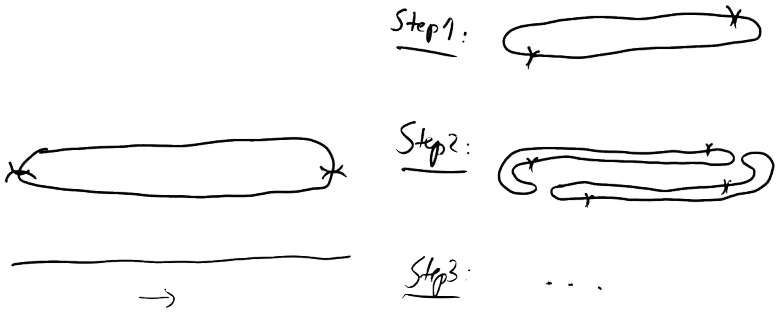

Figure 17: Bing's construction.

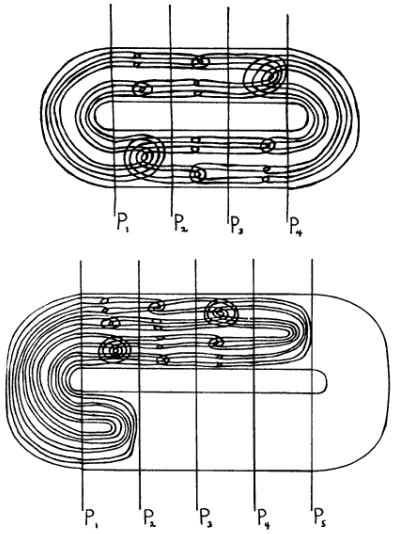

Figure 18: Bing's construction.

stages have small diameter. This can be achieved by successively rotating the clasps in the subsequent stages as indicated in Figure 17.

Remark 3.19. I think the following argument is clearer: Let us apply the shrinking criterion from remark 3.10. Given any saturated open cover $\mathcal{U}$ of B^3 and any open cover $\mathcal{V}$ of B^3. By compactness we can assume without loss of generality that $\mathcal{U}$ is finite. Since $\mathcal{A} \cong \lim_{\leftarrow} B^3/\sim_n$ there is some N such that $\mathcal{U}$ arises as a pullback of a cover of $B^3/\sim_N$. So if we manage to define a self-homeomorphism of B^3 whose support is contained in the 2^N decomposition elements of $\sim_N$, it would fulfill the first shrinking condition.

A decomposition element of $\sim_N$ is a solid torus. Now we have to find a homeomorphism of the torus relative boundary that moves each decomposition element of $D\mathcal{D}$ into a open set of $\mathcal{V}$. By compactness $\mathcal{V}$ has a positive Lebesque number. Thus it would also suffice to move it into some ε-Ball. We will even move the larger decomposition elements of $\sim_M$ for some $M \gg N$ into such balls. The idea is to cut the torus into $M - N$ equally sized pieces and arrange the decomposition elements from the M-th stage in such a way that each decomposition element is contained in at most two of them. Furthermore we can isotope everything as close to the meridian as needed. This will then ensure the second shrinking condition if we pick M large enough. Figure 18 is taken from Bings '52 paper. It shows exactly how to arrange the tori. hope there is no copyright problem.

Remark 3.20. Why the obvious rotation doesn't seem to work at first sight but does

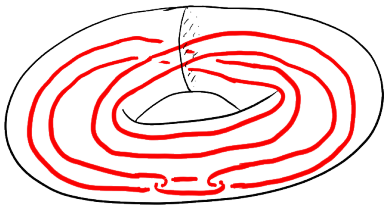

Figure 19: A defining pattern for $\mathcal{B}_2$

eventually. (Coming soon...)

An interesting question in point set topology, similar in spirit to Wilder's original question, is whether the Bing involution on S^3 is topologically conjugate to a Lipschitz homeomorphism (with respect to the round metric). What makes this interesting is that it has to do with dihedral group symmetry. The basic element in the shrinking process above is to rotate within sub-solid-tori in a big solid torus and this rotation creates a tremendous stretching, because the tori are very thin and we have to rotate rather long distances around them. Moreover, each rotation can be made clockwise or counterclockwise and this choice seems to be reversed by the Bing involution. So to say that the involution is Lipschitz means that the top and the bottom copy of $\mathcal{A}$ have roughly the same shape. But if they have the same shape, then the cavities between the rotated layers in the tori should be mirror images of each other which seems very unrealistic. Unfortunately, it is not clear how to make this rigorous because the tori can have very bad shapes and cannot be assumed to be round.

This very specific question motivates a more abstract question which we state as a conjecture.

Conjecture 3.21. *Any finite, bi-Lipschitz group action on a compact 3-manifolds is conjugate to a smooth action.*

3.5 Something that cannot be shrunk

I didn't get why punctured Meridean discs are the right notion. Until now we have seen both simple and complicated things that shrank and later in these lectures we're going through extreme efforts to show that certain other things also shrink. But not everything shrinks as the following example, also due to Bing, shows.

We consider the decomposition $\mathcal{B}_2$ of S^3 defined by a similar defining sequence as the original Bing decomposition. Again, the decomposition consists of a Cantor set worth of continua which are defined as a nested intersection of solid tori and the solid tori are nested in such a way that, at each stage, two of them are place inside one in the previous stage. The only difference is in how the two are placed and, basically, the "2" in $\mathcal{B}_2$ means that they go around twice instead of once (see Figure 19).

In order to see that $\mathcal{B}_2$ doesn't shrink, we call the two nested tori in the defining pattern P and Q and consider two meridional disks A and B in the ambient solid torus. The idea is to show that some decomposition element has to intersect both A and B in the first stage, no matter what happens in the subsequent stages. More precisely, we will show that in each stage n at least one of the 2^n tori has to intersect A and B. If that's true, then the decomposition can't be shrunk.

We take a 2-fold cover of this picture and take lifts of P, Q, A and B which we continue to denote by the same letters for convenience. Although each of them has two lifts, it will be enough to consider only one of them for P and Q.

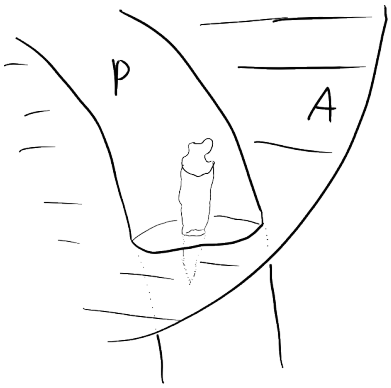

Figure 20: A "substantial" intersection.

Lemma 3.22. *In the lifted picture, either P or Q has "substantial" intersection with A and B*

The precise meaning of "substantial" is as follows. Ideally, the intersections should be in meridian disks for P and Q but this is too much to hope for, so we have to come up with a slightly weaker notion. The right notion turns out to be intersections in *punctured* meridian disks, that is, meridian disks punctured by loops that are trivial in the boundary of P or Q (see Figure 20).

Proof. We look at the intersections $\partial P \cap A$, $\partial P \cap B$, $\partial Q \cap A$ and $\partial Q \cap B$, each will be a collection of circles. Since these circles lie in planar disks, are unknotted and have framing zero in space, each of them must be either a longitude, a meridian or trivial in the boundary of P or Q. Moreover, all these possibilities can occur and we have to think about them.

First, suppose there is some longitudinal intersection in $\partial P \cap A$, say. We claim that either $\partial Q \cap A$ or $\partial Q \cap B$ contains no longitude. The reason for this is that such an intersection would not be consistent with the linking in the picture. Observe that the cores or any longitudes of P and Q together with either boundary of an A or B disk form a copy of the Borromean rings which are known to be a non-trivial link as detected by the Milnor invariant $\bar{\mu}_{123}$, for example. But if Q had a longitudinal intersection with either A or B, then the link would have to be trivial. Moreover, we claim that Q must intersect all lifts of A and B in punctured meridian disks for if either of them contained only trivial intersections, then standard arguments in 3-manifold topology would allow us to remove all intersections and make Q disjoint from that lift and the link would have to be trivial or at least have trivial $\bar{\mu}_{123}$. So each lift must contain at least one meridian and an innermost one will then bound a punctured meridian disk.

Now, if there is no longitude in the intersections, then we focus on P and Q one at a time. For example, if P has no substantial intersections (and thus only trivial intersections) with both lifts of A, then we can deform it into the complement of those lifts. Similarly, if Q has no substantial intersection with either both lifts of A or B, then we can deform the whole link into either half or three quarters of the solid torus and in neither case can this create a non-trivial $\bar{\mu}_{123}$. □

Based on this lemma we can run an inductive argument. If in some stage there is a P or Q which has substantial intersections with a lift of A or B, then within it we see a P and a Q and one of those has to have a substantial intersection with A and B. Thus we get a nested sequence of solid tori which all have intersections with A and B. Their intersection is a decomposition element of $\mathcal{B}_2$ intersecting A and B. We have shown

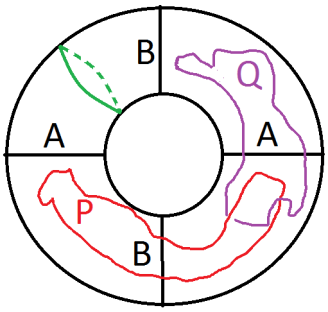

Figure 21: One of P or Q intersects both A and B, otherwise adding a meridean of the Big Torus won't give the Borromean rings.

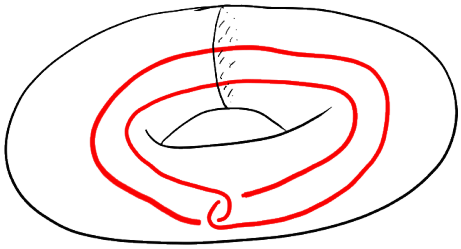

Figure 22: The nesting pattern for the Whitehead decomposition.

that such a thing always exists no matter how we exactly choose to embed the 2-Bing Decomposition. Especially there is always one which is not contained in some ε-Ball if $\varepsilon < d(A, B)$. Thus $\mathcal{B}_2$ cannot be shrunk.

3.6 The Whitehead decomposition

Another prominent example is the *Whitehead decomposition* $\mathcal{W}$ of S^3. Just as the two other examples it can be described as an infinite intersection of nested solid tori with nesting pattern as in Figure 22. In other words, in each stage a solid torus is embedded into its predecessor as a neighborhood of a *Whitehead double* of the core. This decomposition is clearly not shrinkable because its elements are not even cellular. But there's a very interesting story when the situation is moved into four dimension by crossing with a line which will be discussed in the next chapter.

Remark 3.23. Actually, one should be a little more precise. In order to explain the nesting pattern we should not only describe the core of the nested solid torus but also a framing number which determines how the core is thickened. Although this affects how subsequent stages are embedded, the shrinking properties of the decomposition will actually be independent of the framings. So for the point set topology we don't have to pay attention to the framings. But in the context of smooth constructions it will be important that the framing number is zero, that is, that we take *untwisted* doubles.

Remark 3.24. From the construction it is clear that the Whitehead decomposition has only a single element, also known as the *Whitehead continuum*, whereas the Bing decomposition had a Cantor set worth of elements. But in practice, this distinction is fleeting because there will be multiplicities. For example, the nesting patterns might involve several copies of Whitehead or Bing doubles in each step. The meaning of multiple Bing double is easy to understand.

Exercise 3.25. Repeat the "union of tori" construction of the gored ball with a genus g surface Σ with one boundary component: fix a standard basis of curves for $H_1(\Sigma)$, start

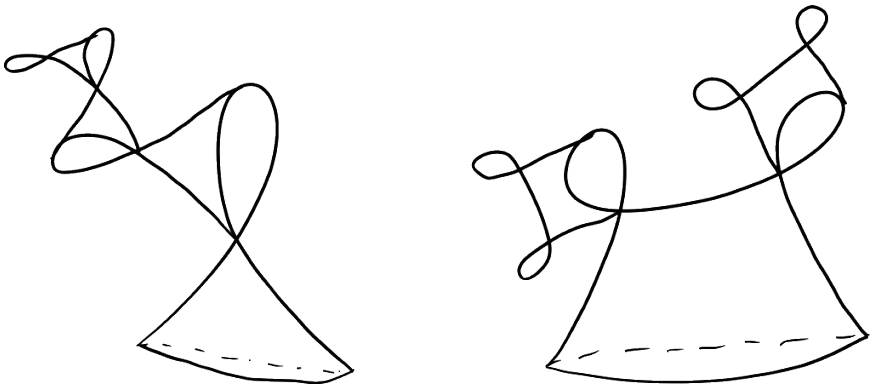

Figure 23: Two Casson handles. More about this later...

with a copy of $\Sigma \times [0,1]$, successively attach further copies of $\Sigma \times [0,1]$ along the basis curves such that everything embeds in 3-space and, finally, add the limit set of the sequence of basis curves and take the double. Show that the corresponding decomposition of S^3 has a nesting pattern where g parallel Bing doubles of the core are embedded in a solid torus.

Similarly, we will see that multiple Whitehead doubles are related to some kind of 4-dimensional diagrams (Figure 23) which we will learn all about. The left picture, where there is no branching, corresponds to a single Whitehead double while the right hand side would have two Whitehead doubles which would also lead to a Cantor set worth of decomposition elements.

I also tried to apply the most general shrinking criterion to the Whitehead decomposition cross the real line. However Without compactness It is not true that a saturated open cover comes from a finite stage and so it is getting a bit tricky. The idea in Bings paper to consider crossing with S^1 first, where we have compactness, and then pass to the cover seems to fix this but it feels so tricky.

4 Decomposition space theory and shrinking: more examples

In the last section we focused on the idea of shrinking cellular decomposition, that is, decompositions whose elements are cellular sets (Definition 2.1). The natural question is to what extend is the converse true. More precisely, suppose we have a cellular decomposition, is it shrinkable?

In Proposition 2.17 we have seen that the answer is yes for finite decompositions. So the first real problem occurs when there are infinitely many cellular sets and we saw two examples of this case, one where the answer was yes ($\mathcal{B}$) and one where the answer was no ($\mathcal{B}_2$). So cellularity alone is not enough. Note that both examples have a further property in common. Namely, we can arrange that the decompositions only have a countable number of elements and further that for any $\epsilon > 0$ there are only finitely many elements that have diameter larger than ϵ. The latter condition is called *null*. More abstractly:

Definition 4.1. A collection of subsets $\{T_i\}_{i \in I}$ of a metric space X is called *null* if for any $\epsilon > 0$ there are only finitely many $i \in I$ such that $\operatorname{diam}(T_i) > \epsilon$.

An instant consequence of nullity is that the collection of sets must be countable; we simply have to consider a countable sequence of ϵ's converging to zero.

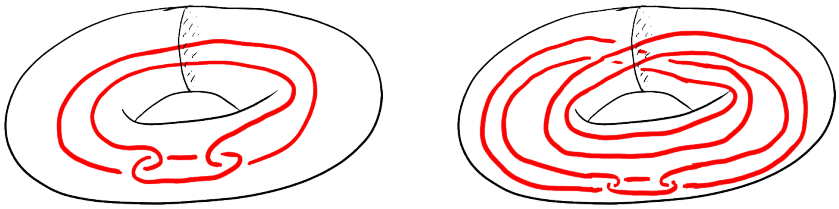

Figure 24: Models for defining sequences for $\mathcal{B}$ and $\mathcal{B}_2$.

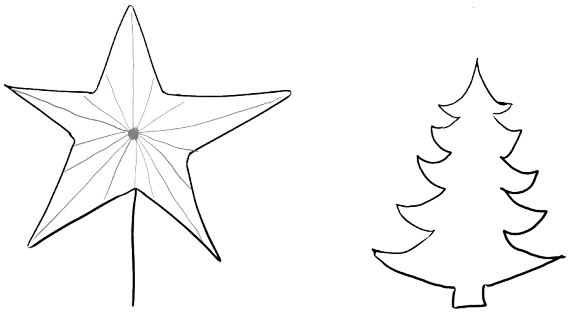

Figure 25: A starlike set (left) and a starlike-equivalent set (right),

To realize $\mathcal{B}$ and $\mathcal{B}_2$ as null (and thus countable) we can model the defining sequences each asymmetrically with one torus being longer than the other (see Figure 24). So the dyadic pattern has a long branch and a short branch and the decomposition elements only have non-zero size when we take the short branch only finitely many times and, if we always take the small torus to have $\frac{1}{10}$ the diameter of the previous one, then the diameter of this decomposition element is less than $\frac{1}{10}$ to the power of the number of short branches that we took.

Remark 4.2. Note that the homeomorphism type of the decomposition elements is not well defined. In fact, it depends on the defining sequence. Using the symmetric defining sequence of $\mathcal{B}$ we found that each of the uncountably many (!) decomposition elements was an arc. But in the asymmetric picture, all decomposition elements that take the short branch infinitely many times must have diameter zero and are thus points. However, it turns out that the topology of the quotient is well defined.

To sum up, we should be disappointed that even null, cellular decompositions do not shrink. In fact, later we will see that the proof of the Poincaré conjecture requires us to shrink such a decomposition, so we must look stronger properties than celluratity.

4.1 Starlike-equivalent sets and shrinking

Consider a subset $S \subset \mathbb{R}^d$ of Euclidean space. We say that S is *starlike* if it has an "origin" $0_S \in S$ and is a union of closed rays emanating from this origin. More generally, we call a subset $S \subset X$ of an arbitrary space *starlike-equivalent* if a neighborhood of S embeds in Euclidean space such that S is mapped onto a starlike set.

Exercise 4.3. Let $S \subset \mathbb{R}^d$ be a starlike set. We define its *radius function* as the map $\rho_S \colon S^{d-1} \to [0, \infty)$ given by $\rho_S(\xi) = \max\{t \geq 0 \,|\, 0_S + t\xi \in S\}$. Show that S is closed if and only if its radius function is upper semi-continuous.

Obviously, starlike sets are contractible. Moreover, it is easy to see that closed, starlike sets are cellular. In fact, they are a little more than that: not only can they be approximated by arbitrary balls but by starlike balls which just amounts to approximating the radius function by a continuous function.

Exercise 4.4. If $\rho\colon S^{d-1} \to (0,\infty)$ is a continuous function, then the starlike set given by $\{t\xi \mid t \leq \rho(\xi)\} \subset \mathbb{R}^d$ is homeomorphic to a ball.

This extra bit of regularity that starlike-equivalent sets have over cellular sets turns out to be strong enough to guarantee shrinkability.

Theorem 4.5 (Bean [Bea67])**.** *Any null, starlike-equivalent decomposition of $\mathbb{R}^d$ is shrinkable.*

Most of the work is in proving the following lemma.

Lemma 4.6. *Let $T \subset B^d$ be starlike and let $\{T_i\}$ be a null collection of closed sets disjoint from T. Then for any $\delta > 0$ there is a radial homeomorphism $k\colon B^d \to B^d$ which is the identity on the boundary and satisfies*

(i) the diameter of $k(T)$ is less than δ and

(ii) either $k(T_i)$ has diameter less than δ or each point $x \in T_i$ the distance of t and $k(t)$ is less than δ.

In other words, the lemma tells us that we can shrink T without doing too much damage to the other T_i. However, it does not say, for example, that none of the T_i gets stretched bigger than it was before. Even if something had diameter less than $\delta/1000$, say, all we can say is that it will stay smaller than δ.

Proof of Theorem 4.5. We fix some $\epsilon > 0$ and consider all the stars which are larger than ϵ. By nullity there are only finitely many of those and we can thus find coordinates in which they all appear starlike. Keeping the modulus of continuity of the coordinate transformation in the back of our head, we simply have to apply the lemma in the new coordinates with $\delta > 0$ determined by the modulus of continuity. □

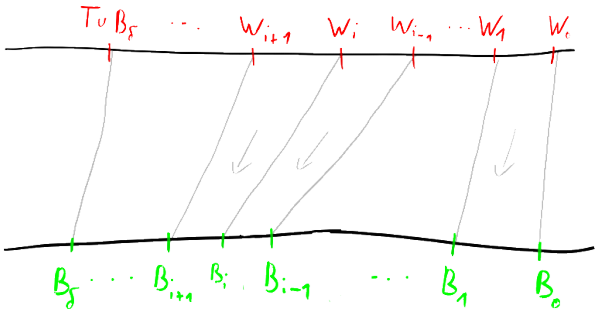

Figure 26: Defining k on a ray.

Proof of Lemma 4.6. We only indicate the construction of k and refer to [FQ90, Secion 4.5] for a detailed proof.[3] For convenience, we assume that the origin of T is the actual origin of B^d.

We start by choosing a nice neighborhood system of the star T, that is, we write $T = \cap_{i=0}^{\infty} V_i$, $V_{i+1} \subset \mathrm{int} V_i$, where the V_i are starlike balls with the following properties:

- V_0 meets only those T_i with diameter less than $\delta/2$.
- Each T_i meets the frontier of at most one V_j ("no spanning").

[3] A full proof was actually presented in the lecture but the written account in [FQ90] seems hard to beat.

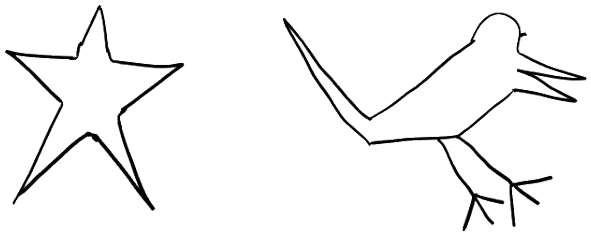

Figure 27: A star and a bird.

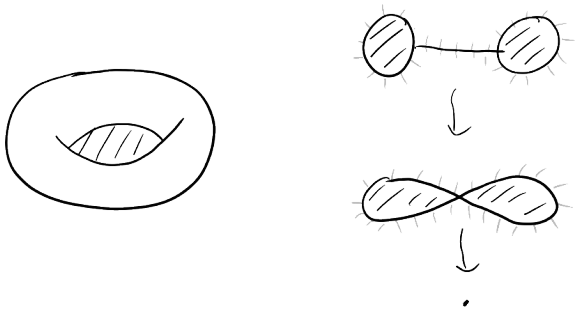

Figure 28: A red blood cell ($S^1 \times B^3 \cup B^2$) from [Fre82]

.

This can be achieved by the null condition and upper semi-continuity. Next, we define B_i to be a sequence of round balls of radii r_i around the origin of T such that the $r_0 = 1$ (in other words, $B_0 = B^d$) and the radii decrease as slowly as $0 < r_i - r_{i+1} < \frac{\delta}{8}$ and converge to δ. As a final step in the setup we let $W_i = V_i \cup B_i$.

We then define a map $k\colon B^d \to B^d$ by requiring that, for each ray R emanating from the origin, k maps the segment $R \cap (W_i \setminus W_{i+1})$ affinely onto $R \cap (B_i \setminus B_{i+1})$. This is illustrated in Figure 26.

The rest of the proof is a tedious, but straightforward case by case study in which it is actually necessary to go down to $\delta/8$ in certain estimates. □

Remark 4.7. The fact that the lemma is true is probably not too surprising, but it is somewhat remarkable that there does not seems to be a soft, qualitative proof. Although the Bing school is probably as far from analysis as one gets in mathematics, one actually has to put pencil to paper and make a calculation involving a $\delta/8$-argument.

Remark 4.8. A useful generalization of Bean's theorem is due to Mike Starbird and one of his student [Reference?]. Instead of stars one can consider birds (Figure 27) and ask: what is the difference between a star and a bird? While a star is starlike, meaning that a single radial crush reduces it to a point, a bird is *recursively starlike* or *birdlike* which means that a finite number of starlike crushes are enough to turn the bird into a point. Going through the arguments above, it becomes clear that they generalize to birdlike decompositions and it turns out that this is exactly what we need in the proof of the Poincaré conjecture; we will need to shrink 2-stage birds instead of stars. In [Fre82] there are things called "red blood cells" (Figure 28) which have to be crushed. These are sets of the form $S^1 \times B^3 \cup B^2$ where∂B^2 goes to $S^1 \times \{p\}$ where $p \in \partial B^3$. If such a set is embedded in a standard way in Euclidean space then it has birdlike equivalent structure. Roughly, it becomes starlike after crushing the central B^2 but the precise argument involves keeping track of some normal directions.

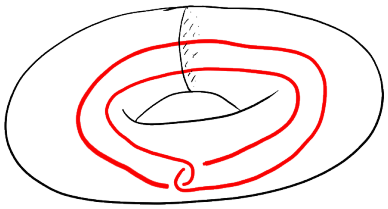

Figure 29: The defining pattern for the Whitehead decomposition.

4.2 A slam dunk for the Bing shrinking criterion

Recall that the Whitehead decomposition $\mathcal{W}$ was constructed as the intersection of nested solid tori where the basic embedding pattern was as shown in Figure 29. It's quite easy to see that the elements of the Whitehead decomposition are not cellular because it is impossible to embed a ball around the embedded torus in the big torus. It is also known that its complement is not simply connected at infinity. So the Whitehead decomposition is definitely not shrinkable. Surprisingly, if we cross with $\mathbb{R}$ and consider the uncountable decomposition

$$\mathcal{W}_{\mathbb{R}} = \{W \times \{t\} | W \in \mathcal{W}, t \in \mathbb{R}\}$$

of $S^3 \times \mathbb{R}$, then this becomes shrinkable!

Remark 4.9. This observation leads to the notion of *manifold factor*: while $S^3/\mathcal{W}$ is not a manifold (this also follows from local fundamental group considerations), the Bing shrinking criterion shows that the product $S^3/\mathcal{W} \times \mathbb{R} \cong (S^3 \times \mathbb{R})/\mathcal{W}_{\mathbb{R}}$ is homeomorphic to $S^3 \times \mathbb{R}$.

The fact that $\mathcal{W}_{\mathbb{R}}$ is shrinkable was first proved by Andrews and Rubin in 1965 [AR65] although the argument seems to have been known to Shapiro several years earlier who probably mentioned it to Bing. We will present the same argument that Bob Edwards decided to explain on a napkin during some southern California topology meeting around 1977. At that time it had been known that the Whitehead link and Whitehead doubles were intimately connected with Casson handles and the fact that the Whitehead decomposition was nearly a manifold was very encouraging for the attempt to prove the Poincaré conjecture since it indicated that the extra direction that is available in four dimension might make some of the wildness disappear.

Theorem 4.10. *The decomposition $\mathcal{W}_{\mathbb{R}}$ of $S^3 \times \mathbb{R}$ is shrinkable.*

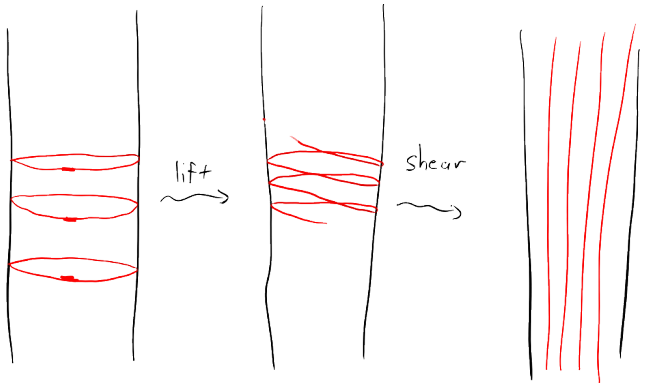

Figure 30: Shrinking $\mathcal{W}_{\mathbb{R}}$.

We will only present a sketch of the proof. A more detailed account is given in Kirby's lecture notes [Kir89, p.87], for example.

Proof. Schematically, going into a very deep stage of the Whitehead decomposition has the effect of squeezing down the radial coordinate in the outer solid torus of that stage and the stage appears as a "circle with and arc inside" whose ends slightly overlap. Crossed with the real line this picture sits in every level.

We know that we can do nothing to shrink the "arc" inside the "circle" but using the fourth dimension we can shift the embeddings in a spiral fashion so that there is a holonomy, meaning that going once around the big torus raises the extra direction by an arbitrarily small amount (see Figure 30). If we re-embed the subsequent stages in that way, the tori don't link themselves but a different copy and the totality of tori in the next stage appear as spirals. So instead of a line worth of circles we are left with a circle worth of spirals.

But now we can shear the picture to straighten the spirals and the interval segments of which they are made are now very short vertical segments. So every one of the subsequent tori has now been shifted and sheared so that it is concentrated mostly in the vertical direction in which it is very short. Looking back at what we have done so far, we realize that we have met the requirements of the Bing shrinking criteria because we did not have to begin in the outer stage. We can start in an arbitrarily deep stage, which takes care of the support condition, and by shifting we can make the subsequent stages arbitrarily small. □

Remark 4.11. The proof of the Poincaré conjecture which we will present follows more closely the approach of [FQ90] and will not directly use the above theorem but it did play a central role in the original proof [Fre82].

4.3 Mixing Bing and Whitehead

So far we have considered decompositions of S^3 obtained by iterating either Bing or Whitehead doubling. We can also mix the two in the sense that, in each stage, we can either use the Bing or the Whitehead double to pass to the next one. Roughly, it turns out that, if we put in enough Bing, Bing always wins over Whitehead and the decomposition will be shrinkable.

We have by now become used to the idea that, in the end, Bing doubling somehow makes things shorter while Whitehead doubling doubles the length. So if we build a mixed Bing-Whitehead decomposition, we should think that the Bing doubles are helping us while the Whitehead doubles are hurting us.

Precise results in this direction were worked out by Starbird and Ancel [AS89] in the late '80s. One very concise result addresses decompositions of the form

$$\mathcal{W}\,\mathcal{B}^{b_1}\,\mathcal{W}\,\mathcal{B}^{b_2}\,\mathcal{W}\,\mathcal{B}^{b_3}\,\ldots \tag{4.1}$$

which means that in the first stage we start with a Whitehead double followed by Bing doubling in the next b_2 stages and so on.

Theorem 4.12. *The decomposition defined a sequence as in* (4.1) *is shrinkable if and only if the series* $\sum_i \frac{b_i}{2^i}$ *diverges.*

The proof is a tour-de-force in matching up the two techniques that were highlighted in Section 3. The first technique was Bing's rotation trick to show that something does shrink and the other was to track intersections with certain meridional disk to show that something doesn't.

While the precise bound is probably not very intuitive, it should be clear that the decomposition shrinks if the sequence of Bing doubles grows sufficiently fast. Although

each Whitehead double sets us back in terms of shrinking, we can make up for it with enough layers of Bing.

Interestingly enough, Theorem 4.12 is exactly what will come out of the four manifold topology.

5 The ball to ball theorem

It is time to discuss another main ingredient in the proof of the Poincaré conjecture: the *ball to ball theorem*. The formulation we will give is taken from [FQ90, p.80] but the proof will be closer to the original one given in [Fre82] where we actually prove a sphere to sphere version. As pointed out by Bob Edwards, there is another writeup by Fredric Ancel [Anc84]. To put the theorem into context, recall that we have seen a decomposition that was cellular and null but still did *not* shrink. The ball to ball theorem is a tool for shrinking such decompositions when the extra information is available that the quotient is a manifold. In the basic case, the quotient is a ball.

Theorem 5.1 (Ball to ball Theorem)**.** *Let $f\colon B^4 \to B^4$ be a surjective map such that*

- (a) *the collection of inverse sets is null,*
- (b) *the singular image of f is nowhere dense*[4] *and*
- (c) *for a closed set $E \subset B^4$ containing ∂B^4 the map $f^{-1}(E) \xrightarrow{f} E$ is a homeomorphism.*

Then f can be approximated by homeomorphisms that agree with f on $f^{-1}(E)$.

Here, the *singular image* of f, henceforth denoted by $\mathrm{sing}(f)$, is the set of points in the target whose preimages are not singletons.

Some remarks about this theorem are in place. First, the restriction to dimension four is completely irrelevant, the proof actually works an all dimensions. Moreover, there is a much more general result of Siebenmann which states that, under weaker assumptions than in Theorem 5.1, any map between manifolds of dimension five or higher can be approximated by homeomorphisms. This was actually known before Theorem 5.1 which would have been an easy special case in high dimensions. So, it was only the 4-dimensional case that required a special argument.

Second, there is a general principle called *majorant shrinking* due to Bob Edwards which was developed in the context of proving the local contractibility of the space of homeomorphisms. It addresses the question of approximating a given map by homeomorphisms which already is a homeomorphism on the preimage of a closed set. If one understands the annulus conjecture, the torus trick and related material towards the local contractibility of the space of homeomorphisms of a manifold, then the hypothesis (c) in Theorem 5.1 is completely redundant. However, this involves working with non-compact spaces, leading to a rather elaborate theory. This was actually central in the original arguments in [Fre82] but it is not used in [FQ90].

It is also worth noting that the hypothesis (c) implies that f is proper and of degree one. So, the assumption on f to be surjective is not really needed, becoming a consequence of (c).

5.1 The main idea of the proof

Before going into the details we will outline the main idea of the proof. First, to avoid confusion, we relabel the source and the target balls to X and Y, that is, we put $X =$

[4] Recall that a subset is *nowhere dense* if its closure has empty interior.

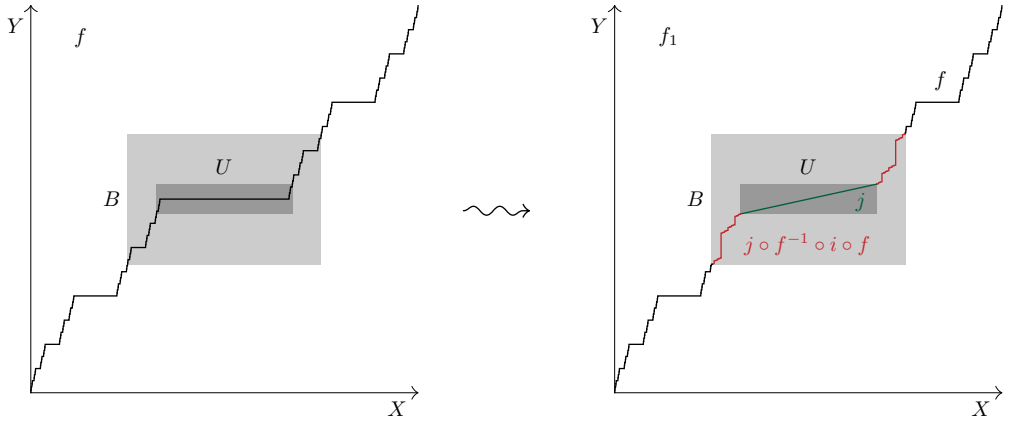

Figure 31: The modification of the Cantor function.

$Y = B^4$ and consider $f\colon X \to Y$. Note that f fails to be a homeomorphism exactly when there are inverse sets and, obviously, the ones with largest diameter are the most offensive. Since we are assuming that the collection of inverse sets is null, there are at most finitely many largest inverse sets and we can work on each separately.

The idea is to look at a small neighborhood of such a largest inverse set $f^{-1}(y)$ in X, to implant it photographically in a tiny ball U around its image point $y \in Y$ and then to taper the original f into this little photograph by similar tricks as in Brown's proof of the Schoenflies theorem. What this step accomplishes is to get rid of one largest inverse set, but it turns out that there is some price to pay: although we start with a function what we will end up with is only a relation. Thinking in terms of the graph of the function, we have traded a large horizontal spot for some vertical steps.

A good example to keep in mind is the graph of the Cantor function (Figure 31) which has a large horizontal spot in the middle. What is going to happen is that a neighborhood of this horizontal spot is changed by a homeomorphism which tilts the horizontal spot but introduces some vertical cliffs. Moreover, we can control the tilting such that the vertical spots are as short as we want. Of course, the Cantor function can be approximated by homeomorphisms without such complications, but in dimension four is not so simple.

Eventually, the theorem will follow from an iteration of this idea once we have recast it in the language of relations.

Now we will put the above ideas into precise formulas, to illustrate the very first step of the proof. For simplicity we assume that a largest inverse set of f maps to $0 \in Y$. We take two concentric round balls $U \subset B \subset Y$ around $0 \in Y$, where U has very small radius (for example, we can take $U = B_\delta(0)$ and $B = B_{2\delta}(0)$ for some small $\delta > 0$) and define an "inverse squeeze" homeomorphism

$$i\colon B \xrightarrow{\cong} Y$$

which is the identity on U and sends $B - U$ onto $Y - U$ (for example by taking a radial expansion, but later we will need more flexibility). We note that the composition $i^{-1} \circ f$ is a homeomorphism near ∂X, so it can be extended to a homeomorphism

$$j\colon X \xrightarrow{\cong} B$$

(this extension always exists, we can take the cone for instance). Finally, we define

$f_1 \colon X \to Y$ by

$$f_1 = \begin{cases} f & \text{on } X - f^{-1}(B) \\ j & \text{on } f^{-1}(\operatorname{Int} U) \\ j \circ (f^{-1} \circ i \circ f) & \text{on } f^{-1}(B - \operatorname{Int} U). \end{cases} \tag{5.1}$$

Exercise 5.2. Check that f_1 is a closed *relation*.

Now, why is f_1 not a function? The reason are the points $y \in B - U \subset Y$ such that $i(y)$ lies in the singular image of f while y itself does not. In that case, $f^{-1}(y)$ must be a single point $x \in f^{-1}(B - \operatorname{Int} U) \subset X$ and going through the definition it is easy to see that $f_1(x)$ is, in fact, a subset of Y with more than one element. So, f_1 is only a relation. But note that $f_1(x)$ is by definition contained in B which we could choose arbitrarily small. So, f_1 is close to being a function in some sense. Before we continue we recall some elementary facts about relations.

5.2 Relations

Recall that a *relation* from X to Y is just a subset $R \subset X \times Y$. As indicated, we like to think of a relation as a multivalued function $X \xrightarrow{R} Y$ which assigns to $x \in X$ the subset

$$R(x) = \{y \in Y \mid (x, y) \in R\} \subset Y.$$

Functions can be identified with their graphs, and so, by abusing terminology, we consider functions as special relations. Clearly, a relation $R : X \to Y$ is a function if and only if $R(x)$ is a singleton for all $x \in X$. So, the set of functions naturally embeds in the set of relations.

In analogy with functions, we define the composition of relations $X \xrightarrow{R} Y \xrightarrow{S} Z$ as

$$S \circ R = \{(x, z) \in X \times Z \mid \exists\, y \in Y \colon (x, y) \in R, (y, z) \in S\} \subset X \times Z.$$

Also, any relation $X \xrightarrow{R} Y$ has an inverse given by

$$R^{-1} = \{(y, x) \in Y \times X \mid (x, y) \in R\} \subset Y \times X.$$

Obviously, we have $(S \circ R)^{-1} = R^{-1} \circ S^{-1}$ and it is easy to see that these definitions reduce to the corresponding ones for functions.

Next, we want to bring topology into the picture, as usual in the context of compact metric spaces. First of all, it is an easy exercise in point set topology that for compact metric spaces X and Y a function $f \colon X \to Y$ is continuous if and only if its graph is closed in $X \times Y$ (in fact, compact Hausdorff is enough). So, the appropriate generalization of continuous functions are closed relations. Clearly, the failure of a relation $R \colon X \to Y$ to be a function is measured by the quantity

$$\operatorname{vd}(R) \stackrel{\text{def}}{=} \max_{x \in X} \operatorname{diam}_Y(R(x))$$

which we call the *vertical defect* of R. We also define the *horizontal defect* by

$$\operatorname{hd}(R) \stackrel{\text{def}}{=} \max_{y \in Y} \operatorname{diam}_X(R^{-1}(y)) = \operatorname{vd}(R^{-1})$$

which is the obstruction for R^{-1} to be a function. In particular, a closed relation R is a homeomorphism if and only if

(i) $R(x) \neq \emptyset \neq R^{-1}(y)$ for all $x \in X$ and for all $y \in Y$ and

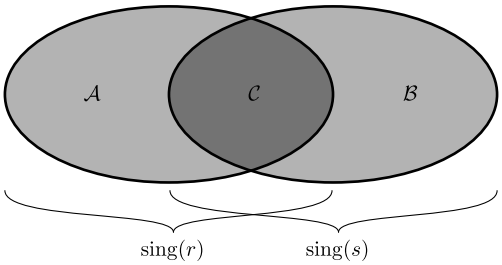

Figure 32: The sets $\mathcal{A}$, $\mathcal{B}$ and $\mathcal{C}$.

(ii) $\mathrm{hd}(R) = \mathrm{vd}(R) = 0$.

As a final piece of notation we define the *singular image* of a relation R by

$$\mathrm{sing}(R) = \left\{ y \in Y \,\middle|\, \#\, R^{-1}(y) > 1 \right\}.$$

So far our strategy has been to stay within the world of functions and to approximate f by homeomorphisms by reducing the horizontal defect. However, we could also go into the world of closed relations and try to reduce both the horizontal and vertical defects and this is exactly how we will prove Theorem 5.1.

5.3 Iterating the main idea: admissible diagrams

As mentioned before, the idea is to iterate the construction of f_1 out of f and, in order to do this, we have to extend the construction from functions to relations where we now have to worry about the singular images of both the relation and its inverse. A simple way of doing this (which was suggested by Ric Ancel and Jim Cannon) is to use a third ball $Z = B^4$ to keep track of where the singular sets lie. The formalism involves commutative diagrams of closed relations of the form

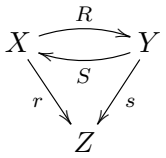

denoted altogether by $\mathfrak{A} = (R, S; r, s)$, where r and s are surjective functions, and $X = Y = Z = B^4$ are balls. Such a diagram $\mathfrak{A}$ is called *admissible* if

(a) $S = R^{-1}$;

(b) the collections of inverse sets of r and s are null;

(c) the singular images $\mathrm{sing}(r)$ and $\mathrm{sing}(s)$ are nowhere dense in Z;

(d) R and r are homeomorphisms over a neighborhood E of ∂B^4;

(e) the sets $\mathcal{A} = \mathrm{sing}(r) - \mathrm{sing}(s)$, $\mathcal{B} = \mathrm{sing}(s) - \mathrm{sing}(r)$ and $\mathcal{C} = \mathrm{sing}(r) \cap \mathrm{sing}(s)$ (see Figure 32) are *mutually separated*, that is, each is disjoint from the closures of the others, and

(f) R restricts to a homeomorphism $R\colon r^{-1}(\mathcal{C}) \xrightarrow{\cong} s^{-1}(\mathcal{C})$.

Note that an admissible diagram is determined by the (admissible) pair (R, r).

Exercise 5.3. Check that $s(\mathrm{sing}(R)) = \mathcal{A}$ and $r(\mathrm{sing}(S)) = \mathcal{B}$.

The starting data for our inductive scheme is the diagram

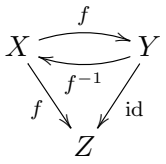

which is clearly admissible. So, when we start s is the identity so that $\mathcal{B}$ and $\mathcal{C}$ are empty and we only have $\mathcal{A}$. But when we do the first step and pass to f_1 we erase some singular image of f by implanting the photograph and we create singular image of the inverse relation which means that $\mathcal{B}$ and $\mathcal{C}$ come alive. Thereafter, we will have to deal with non-empty $\mathcal{A}$, $\mathcal{B}$ and $\mathcal{C}$. Roughly, $\mathcal{C}$ is where we have already solved the problem in the sense that, even though there is some singular image, we have arranged the map above them to be a homeomorphism.

Lemma 5.4. *Let $\mathfrak{A} = (R, S; r, s)$ be an admissible diagram. For any neighborhood $\mathcal{N}(R) \subset X \times Y$ of R and for any $\epsilon > 0$ there is an admissible diagram $\mathfrak{A}' = (R', S'; r', s')$ with $r' = r$, $R'_{|E} = R_{|E}$, $R' \subset \mathcal{N}(R)$ and $\mathrm{hd}(R') < \epsilon$.*

In other words, there is a relation which is arbitrarily close to R whose horizontal spots have arbitrarily small size and we can also control the vertical defect.

In the proof of the lemma we use a notion of *general position* which is very different from the usual one in manifold theory. We state it as an exercise.

Exercise 5.5. Let X be a compact manifold and let $C \subset X$ be countable and $N \subset X$ be nowhere dense. Then for all $\epsilon > 0$ there exists a homeomorphism h of X which is ϵ-close to the identity and is supported in an arbitrary neighborhood of C, such that $h(C) \cap N = \emptyset$.

Proof of Lemma 5.4. As the first step, by following the construction of f_1 above, we consider two small round balls U and B centered at a point $a \in \mathcal{A}$ such that

(i) $r^{-1}(a)$ has maximal diameter,

(ii) $U \subset B \subset Z - (\mathrm{Cl}(\mathrm{sing}(s) \cup E) \subset Z$ (this is possible because $\mathcal{A}$ is separated from $\mathrm{sing}(s) = \mathcal{B} \cup \mathcal{C}$) and

(iii) $\partial U \cap \mathrm{sing}(r) = \emptyset$ (possible because $\mathrm{sing}(r)$ is countable).

Then, s is non-singular over B, and so $s_| : s^{-1}(B) \to B \cong B^4$ is a homeomorphism. Let $i : B \to Z$ be suitable homeomorphism such that $i_{|U} = \mathrm{id}_U$. By Exercise 5.5 we can assume that $\mathrm{sing}(r) \cap \partial U = i(\mathrm{sing}(r)) \cap (\mathrm{sing}(r) - U) = \emptyset$. Now, choose a homeomorphism $j : X \to s^{-1}(B) \subset Y$ such that $j = s^{-1} \circ i^{-1} \circ r$ on ∂X.

The relation R' can be constructed by iteratively applying the following formula finitely many times

$$R' = \begin{cases} R & \text{on } X - r^{-1}(\mathrm{Int}(B)) \\ j & \text{on } r^{-1}(\mathrm{Int}(U)) \\ j \circ (r^{-1} \circ i \circ r) & \text{on } r^{-1}(\mathrm{Int}(B) - \mathrm{Int}(U)). \end{cases}$$

This is almost the same as the formula (5.1) for f_1, the only thing that is slightly different is the definition of j. Again, it is easy to check that R' is well defined. To complete the new admissible diagram we simply take $r' = r$ and for s' we are forced to choose

$$s' = \begin{cases} s & \text{on } Y - s^{-1}(B) \\ i^{-1} \circ r \circ j^{-1} & \text{on } s^{-1}(B) \end{cases}$$

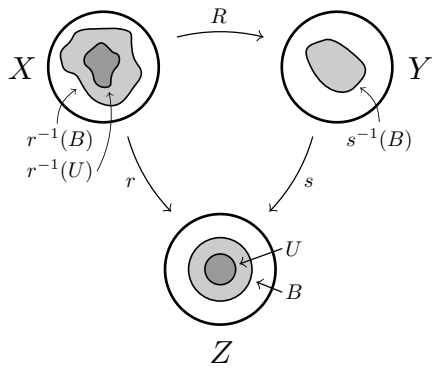

Figure 33: The admissible diagram.

as can be shown by a simple computation (hint: first compute $(s')^{-1} = R' \circ r^{-1}$).

It remains to check the mutual separation of $\mathcal{A}'$, $\mathcal{B}'$ and $\mathcal{C}'$. We have $\mathrm{sing}(s') = \mathrm{sing}(s) \cup i^{-1}(\mathrm{sing}(r))$, and so

$$\mathcal{A}' = \mathcal{A} - U, \quad \mathcal{B}' = \mathcal{B} \cup (i^{-1}(\mathrm{sing}(r)) - U) \quad \text{and} \quad \mathcal{C}' = \mathcal{C} \cup (\mathcal{A} \cap U).$$

So, $R' : r^{-1}(\mathcal{C}') \to (s')^{-1}(\mathcal{C}')$ is a homeomorphism because over $\mathcal{C}$ it coincides with the old R, and over $\mathcal{A} \cap U$ we have $R' = j$.

Now the proof is almost done. By choosing B small enough we can guarantee that R' is contained in $\mathcal{N}(\mathcal{R})$ and the photographic implanting trick using j wipes out one large horizontal spot of R (by Exercise 5.3). Since the collection of inverse sets of r is null, by repeating the construction finitely many times we can eliminate the inverse sets of R' of diameter bigger than ϵ. □

5.4 Proof of the ball to ball theorem

The final step of the proof was not addressed in detail in the lectures. We follow the basic idea from Ancel's paper [Anc84].

We start with our function $f : B^4 \to B^4$. Let us choose a closed neighborhood $\mathcal{N}(f) \subset B^4 \times B^4$. Our goal is to construct a homeomorphism $h : B^4 \to B^4$ which is close to f, meaning that $h \subset \mathcal{N}(f)$ (we are still considering functions as subsets of $B^4 \times B^4$).

The idea is to construct in $\mathcal{N}(f)$ a sequence $(R_n)_{n\in\mathbb{N}}$ of closed relations of decreasing horizontal and vertical defects, and take the limit. However, Lemma 5.4 only allows us to make the horizontal defect arbitrarily small, while the vertical defect can increase just a little bit, being controlled by the given neighborhood of the original relation. So in order to gain more control on the vertical defect, we will construct R_n from $R_{n-1}^{-1} = S_{n-1}$, by using the lemma. In this way, we can reduce, alternately, both the horizontal and the vertical defects. Moreover, we prefer to obtain the homeomorphism h as the intersection of a telescopic sequence of compact sets in $\mathcal{N}(f)$, instead of considering the limit of a sequence of relations.

Now we give the formal construction. For a subset $A \subset X$ of a metric space (X, d) we denote by $\mathcal{N}_\epsilon(A)$ the ϵ-neighborhood of A in X. Let $(\epsilon_n)_{n\in\mathbb{N}}$ be a suitably chosen positive sequence converging to zero. By induction we define a sequence of admissible diagrams $\mathfrak{A}_n = (R_n, S_n; r_n, s_n)$ such that $\mathfrak{A}_0 = (f, f^{-1}; f, \mathrm{id})$ and, for $n \geq 0$, $\mathfrak{A}_{n+1}$ is obtained from $\mathfrak{A}_n^{-1} = (S_n, R_n; s_n, r_n)$ by Lemma 5.4 under the assumption that $R_{n+1} \subset \mathrm{Int}(\mathcal{N}_{\epsilon_n}(S_n))$ and $\mathrm{hd}(R_{n+1}) < \epsilon_n$. Here S_n and $\mathcal{N}_{\epsilon_n}(S_n)$ play the role of R and $\mathcal{N}(R)$ in the lemma. Note that, by construction we have $R_{n|E} = \mathrm{id}_E$.

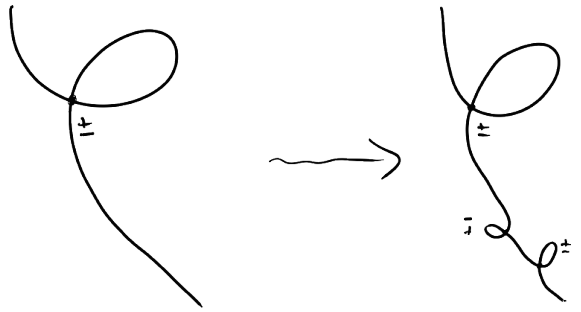

Figure 34: Adjusting the algebraic self-intersection number.

Moreover, ϵ_n is chosen so that $\mathcal{N}_{\epsilon_n}(S_n) \subset \mathrm{Int}(\mathcal{N}_{\epsilon_{n-1}}(R_{n-1}))$, and $\lim_{n\to\infty} \epsilon_n = 0$, starting from a sufficiently small ϵ_0 satisfying $\mathcal{N}_{\epsilon_0}(f) \subset \mathrm{Int}(\mathcal{N}(f))$. So, $\mathrm{vd}(R_{n+1}) < \epsilon_{n-1} + 2\epsilon_n$. It follows that, roughly speaking, R_n converges to a homeomorphism h for even n, and to h^{-1} for odd n. To formalize this, we consider the relation $\mathcal{H}_n = \mathcal{N}_{\epsilon_{2n}}(R_{2n})$. We have $\mathcal{H}_{n+1} \subset \mathcal{H}_n \subset \mathcal{N}(f)$ for all n, $\mathrm{hd}(\mathcal{H}_n) < \epsilon_{2n-1} + 2\epsilon_{2n}$, and $\mathrm{vd}(\mathcal{H}_n) < \epsilon_{2n-2} + 2\epsilon_{2n-1} + 2\epsilon_{2n}$.

Finally, we put

$$h = \bigcap_{n=0}^{\infty} \mathcal{H}_n \subset B^4 \times B^4$$

and it is now obvious that $h : B^4 \to B^4$ is a homeomorphism such that $h_{|E} = \mathrm{id}_E$. This concludes the proof of the ball-to ball theorem.

Part II
Casson handles

6 From the Whitney trick to Casson handles

6.1 The Whitney trick in dimension 4

After all this work in compact metric spaces, we now step into the smooth world. An important geometric construction in smooth manifold is the *Whitney trick* which was introduced by Whitney [Whi44] in order to prove that any n-dimensional smooth manifolds, $n \geq 3$, embeds in the Euclidean space $\mathbb{R}^{2n}$ of twice the dimension, which is one better than what we get for free(=by general position). However, this result is of little consequence compared to the method used to prove it.

Remark 6.1. Conspicuously, Whitney's proof does not work for $n = 2$ although, by example, the fact that any surface embeds in $\mathbb{R}^4$ is still true since it holds for the real projective plane.

Whitney looked at the manifold M^m as it is mapped into $\mathbb{R}^{2n}$ and he realized that by general position there are only transverse double points to think about to which one can assign signs and he also realized the algebraic sum of these points can be controlled by putting in small kinks (see Figure 34). In particular, one can make it zero. In the case of algebraically zero self intersection he was led to a local picture as in Figure 35 where there are two sheets of the manifold (two different manifolds would work, too) with two intersection points of opposite signs. To improve the situation to an embedding he noticed that the must be a disc W as in the picutre (which he probably didn't call W) and that

Figure 35: The Whitney trick in the plane.

Figure 36: The Hopf link near a transverse intersection.

it looks like it should be possible to push one sheet over the other along the disk to cancel the two intersection points.

While this looks pretty good in the plane, how should it work in high dimensions? Some aspects of the picture are conserved when passing to higher dimension, for example, the intersection points stay 0-dimensional (since the dimensions of the two intersecting sheets add up to the dimension of the ambient space) and the disk W is going stay 2-dimensional. The idea is to find two arcs connecting the two points, one in each sheet, which will make up two halfs of the boundary of W. In addition, some normal data is necessary in order to do the push without introducing new intersections. Something that's favorable high dimensions ($n \geq 3$) is that 2-dimensional objects are generically disjoint from everything $< n-2$-dimensional, so we don't have to worry about making (the interior of) W embedded and disjoint from the image of the manifold; in contrast, in four dimensions (n=2) W will intersect itself and the manifold. Another advantage is that the space of $(n-1)$-planes in $\mathbb{R}^{2n-2}$, whose fundamental group controls the ambiguity in normal data, is simply connected for $n \geq 3$ while for $n = 2$ the fundamental group is $\mathbb{Z}$. However, since we are ultimately interested in 4-manifolds we have to make a careful analysis of the 4-dimensional situation.

A local model for a transverse intersection of surfaces in 4-manifolds are the planes $\{z = 0\}$ and $\{w = 0\}$ in $\mathbb{C}^2$. If we look at a small 3-sphere around the origin, then it is an extremely important observation that the two planes intersect the 3-sphere in a Hopf link (see Figure 36). Let's build up to the Whitney trick from this starting point. Suppose that we have two intersection points of opposite sign. That means we should have two Hopf links in two separate 3-spheres (Figure 37). This picture comes from thinking of neighborhoods of the points and asking what's going on the boundary, but for the Whitney trick we have to look a little more globally at a neighborhood of the circle made up from the two arcs connecting the points. Assuming that the ambient 4-manifold is simply connected, the neighborhood of such a circle is $S^1 \times B^3$ and on its boundary $S^1 \times S^2$ it turns out that we see a Bing double of $S^1 \times \{\textit{south pole}\}$ in the solid torus $S^1 \times \textit{southern hemisphere} \subset S^1 \times S^2$. Note that the opposite signs of the two intersection points account for the fact that we see a link with linking number zero, if signs agreed, then we would get linking number plur

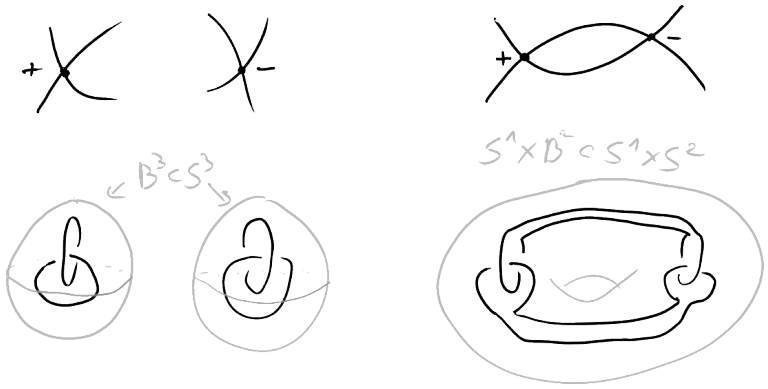

Figure 37: From two Hopf links to a Bing double

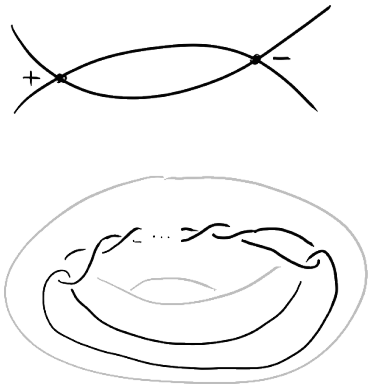

Figure 38: The wrong framing produces twisted Bing doubles.

or minus two.

Figure 37 is also great for understanding the "normal data" mentioned above which is nothing but a choice of framing for the circle. Note that we have drawn an untwisted Bing double and the reason for this is that we have implicitly chosen the correct framing. A different framing will give a twisted Bing double as in Figure 38. In any case, this picture really only lives int the copy of $S^1 \times S^2$ embedded in the our ambient 4-manifold and not in a 3-sphere. But if there's an embedded Whitney disk W bounded by the circle and we attach it to the picture, then we create a bordism from $S^1 \times S^2$ to a 3-sphere inside the 4-manifold. In other words, then W provides a core for surgery which takes this $S^1 \times S^2$ to a 3-sphere and it's highly relevant what link we end up with in this 3-sphere. Because if we end up with the unlink, then we can easily see how to separate the two surfaces; we can think of each circle as representing a hole in a surface which needs to be repaired and if we can fill these holes with disjoint disks then we obtain new surfaces without intersection points and it's not hard to see that they are isotopic to the original surfaces.

6.2 4-manifolds in the early 1970s: surgery and h-cobordism

The 1950s and 1960s saw the development of surgery theory and the h-cobordism theorem which allowed to translate classification problems for manifolds of dimension five and higher completely into questions in homotopy theory and algebra. In the beginning of the 1970s surgery theory had become very mature; at the frontier were things like equivariant or controlled surgery which were very technical subjects. On the other hand, almost nothing was known in dimension four. The main reason was the failure of the Whitney trick and the goal of this section is to pin down how this failure prevents us from using

surgery and the h-cobordism theorem.

Surgery theory addresses the existence problem whether we can find a manifold within some previously identified homotopy type. (This might take place in the smooth, PL, topological or any other category.) The h-cobordism theorem is related to the corresponding uniqueness problem. When we have found two manifolds M_1 and M_2 of dimension d, say, in the same homotopy type and we want to find an isomorphism between them. The strategy, which was developed by Smale, is to first find some cobordism N of dimension $d+1$ between the two and then try to find the simplest possible one. Preferably this simplest N should be in the same homotopy type as the M_i, in other words, the inclusions $M_i \hookrightarrow N$ should be homotopy equivalences, and in this case N is called an h-cobordism. In a favorable situation, for example, if all fundamental groups are trivial and the dimensions are high enough, then Smale would conclude that N is a product and, in particular, M_1 and M_2 are isomorphic. But in the end, it turns out that the existence and uniqueness side involve essentially the same methods because in the h-cobordism story the main problem is to take turn some cobordism into and h-cobordism using surgery.

In dimension four, Milnor had investigated the simply connected homotopy types of closed manifolds or, more abstractly, *Poincaré duality spaces* which are certain cell complexes that obey the algebraic condition that manifolds obey in terms of the duality between homology and cohomology. Milnor was able to classify the (homotopy types of) 4-dimensional Poincaré duality spaces that are simply connected and it turned out that they are in one-to-one correspondence with (equivalence classes of) of $\mathbb{Z}$-unimodular quadratic forms or, in less fancy terms, symmetric integer matrices with determinant plus or minus one up to similarity. So in 1973, the existence and uniqueness questions in dimension four that people were thinking about were which of these forms are realized by smooth (or equivalently PL) manifolds and whether two homotopy equivalent 4-manifolds are h-cobordant and thus diffeomorphic (or PL homeomorphic). It turns out that these two questions are very similar.

An interesting example of a simply connected 4-manifold known as the *K3 surface* is given by a quartic $K = \{W^4+X^4+Y^4+Z^4 = 0\}$ in $\mathbb{C}\mathrm{P}^3$. It was known that its quadratic form is isomorphic to the matrix

$$E_8 \oplus E_8 \oplus H \oplus H \oplus H$$

where E_8 is the famous even, 8-by-8 integer matrix known as the Cartan matrix of the exceptional Lie algebra and $H = \left(\begin{smallmatrix} 0 & 1 \\ 1 & 0 \end{smallmatrix}\right)$ is a so-called *hyperbolic pair* which corresponds to the intersection form of $S^2 \times S^2$. Now, we know that there is a Poicaré duality space corresponding to $E_8 \oplus E_8$ and there is the obvious projection

$$E_8 \oplus E_8 \oplus H \oplus H \oplus H \xrightarrow{\mathrm{pr}} E_8 \oplus E_8.$$

The question was whether one could realize this projection geometrically. More precisely, is it possible to do surgery on K with the effect of removing the hyperbolic pairs from the intersection form? We know by now that this won't work in the smooth category as a consequence of Donaldson theory. One might wonder why we didn't just take one copy of E_8, but it was already known by Rokhlin's theorem that the intersection form of a smooth, spin 4-manifold must have signature divisible by 16. It turns out that one copy of E_8 does occur for a topological 4-manifold which is a concrete instantiation of something called the Kriby-Siebenmann invariant which we'll get to later on. So since back in 1973 we knew Rokhlin's theorem and we were always trying to work in the smooth category (and only desperation forced us out of it) we're going to try to make a smooth $E_8 \oplus E_8$-manifold out of the K3 surface K.

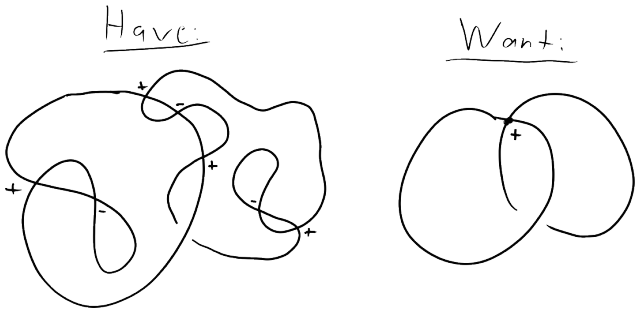

Figure 39: Trying to surger out a hyperbolic pair.

So what's the picture for doing this? We know from the Hurewicz theorem that the hyperbolic pairs in the homology of K are represented by maps $S^2 \to K$ which we can take as smooth and in general position. One hyperbolic pair is shown schematically on the left of Figure 39. In general, there will be excess intersections, after all we only know the algebraic intersection numbers. If we could use the Whitney trick to remove the extra intersections to get to the picture on the right then we could do surgery on either of the embedded spheres, that is, we could cut out a neighborhood diffeomorphic to $S^2 \times B^2$ of one sphere and replace it with $B^3 \times S^1$, with the effect of removing the hyperbolic pair from the intersection form. (The other sphere is also important since it makes sure that the surgery does not change the fundamental group.)

Remark 6.2. All this is completely analogous to dimension two. If we have a surface which has an extra genus that we don't want, then we identify a dual pair of simple closed curves, cut out an annular neighborhood of one of them and fill in the two resulting boundary components with disks.

Next, let's try to prove the h-cobordism theorem in dimension four. Given an h-cobordism N^5 between two simply connected 4-manifolds M_1 and M_2, we look at a handle decomposition of N^5 and try to simplify it as much as possible. The handle decomposition induces a chain complex computing $H_*(N, M_1) = 0$ which can be simplified algebraically such that there are only 3-chains and 2-chains and the boundary map is an isomorphism represented by the identity matrix in suitable bases. The whole idea of the proof is to match the geometry with the algebra of the chain complex. We can easily remove handles of index 0 and 5 and with just a little more work, since everything is simply connected, we remove handles of index 1 and 4. What is left are only handles of index 2 and 3 and the level in between the 2- and 3-handles is another 4-manifold $M_{2/3}$ which is obtained from either M_1 or M_2 by a sequence of surgeries on embedded circles. But since the manifolds are simply connected all circles are null-homotopic and in dimension 4 homotopy implies isotopy, so the surgeries happen on tirvial, standard circles and it's an easy exercise that this results in $S^2 \times S^2$ summands. It follows that we have diffeomorphisms

$$M_{2/3} \cong \begin{cases} M_1 \# k(S^2 \times S^2) \\ M_2 \# k(S^2 \times S^2) \end{cases}$$

where k is the number of 2- (or 3)-handles. The spheres we see in $M_{2/3}$ are the k belt spheres of the 2-handles and the k attaching spheres of the 3-handles and each of them has a dual sphere which intersects it in a single point. So the situation is very clean separately, but the problem is that the belt spheres and attaching spheres together don't look so nice. However, the algebra forces that for each belt sphere there is an algebraically

[5]More precisely, we take a relative handle decomposition of N built on M_1.

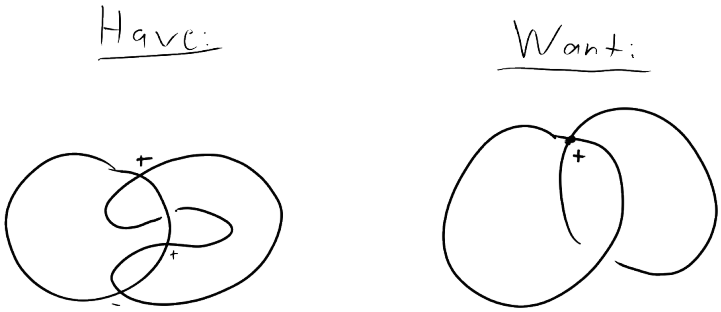

Figure 40: Algebraically dual spheres in the middle level of an h-cobordism.

dual attaching sphere. So the picture is very similar to the one we encountered when we tried to surger out hyperbolic pairs (see).

This time we have a pair of embedded spheres which are algebraically dual and if we can get rid off all extra intersection points, then we can also cancel the remaining handles of index 2 and 3, hence N must be the trivial cobordism.

6.3 Finding dual spheres

The solution to finding Whitney disks is virtually the same for surgery and the h-cobordism problems and the first two steps toward the solution were taken by Andrew Casson in 1974 [Cas86]. Let us put Casson's ideas into a broad bruch before going into the details.

The first idea is that the solving local problem is impossible but there is global information that might help. So what is the local problem? Since the 1950s Fox and Milnor had developed the idea of *slice knots*, that is, knots in S^3 which bound a smooth or locally flat disks in B^4. Slice knots arise, for example, as cross sections of knotted 2-spheres in 4-space. By now, a tremendous amount is known about the obstruction theory for slice knots. For example, Peter Teichner and his collaborators [COT03, COT04] have pushed this very far and before Casson and Gordon [CG78] had developed some higher order obstructions. But even in 1973 it was known that there were obstructions, for example, the Seifert matrix has to obtain a certain form for a knot to be slice. This is discouraging for out attempts to remove self-intersections of immersed disks in 4-manifolds because any knot bounds an immersed disk in B^4 for non-slice knots it's impossible to remove the intersection points. But Casson realized that there was global information that could be exploited, namely the fact that the spheres in the surgery and h-cobordism problem come in dual pairs.

The second idea is that there is a trade-off the fundamental group of the complement, which is bad, and intersections which, in some sense, are also bad. This can be explained in the local model of a transverse double point (see Figure 36 on page 39). We already saw that the intersecting planes appear as a Hopf link in the boundary of a small ball around the intersection. Another interesting gadget that appears in this picture is the *Clifford torus* $\left\{(z,w)\in\mathbb{C}^2 \,\middle|\, |z|=|w|=\frac{1}{\sqrt{2}}\right\}$ which is the common boundary of tubular neighborhoods of the two components of the Hopf link. This Clifford torus exemplifies the relation between intersection points and the fundamental group of the complement because the complement of the intersecting planes actually deformation retracts onto the Clifford torus and thus has free Abelian fundamental group of rank two (generated by linking circles of the planes). In contrast, the complement of two disjoint planes in $\mathbb{C}^2$ has free fundamental group of rank two, so the intersection point must account for a relation in the fundamental group. This is just the most microscopic instance of a concept that we'll be working with all the time.

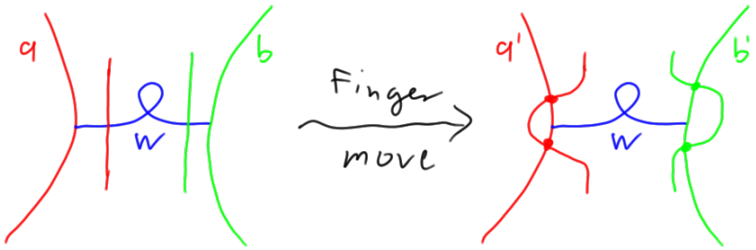

Figure 41: Trading intersections for self-intersections.

So how are Casson's ideas used to make progress on the surgery and h-cobordism problems? In both problems we have an algebraically dual pair of spheres $a, b \subset M$ in a 4-manifold M and we'd like to remove algebraically canceling pairs of (self-)intersection points by finding Whitney disks. For simplicity, we take M simply connected most of the time. For starters, we're going to try to fix up the fundamental group of the complement. We'd like to arrange that $\pi_1(M \setminus (a \cup b))$ is also trivial; more generally, if M is not simply connected, we'd like the map $\pi_1(M \setminus (a \cup b)) \to \pi_1(M)$ to be an isomorphism. In that case we call the pair a, b π_1-*negligible*. The simple reason is that a Whitney move, for example, on b across a Whitney disk that intersects a, will not help us in reducing the number of intersection points. So if a, b are π_1-negligible, then at least we have a chance to find useful Whitney disks although, even if we can achieve π_1-negligibility, the Whitney disks will still cross themselves and we still have work to do. But this is just a first step in what will turn out to be an infinite construction and before we proceed with the construction we want to keep firm control over the fundamental group.

The key thing in arranging something to be π_1-negligible is to make all linking circles null-homotopic in the complement as can be seen immediately by van Kampen's theorem. Geometrically, such a null-homotopy would create an immersed disk in the complement which, together with the meridian disk bounding the linking circle, gives a sphere which intersects the original object in one point. So π_1-negligibility is basically equivalent to the existence of what we call *geometric duals*, that is, spheres that meet the important pieces in one point.

Remark 6.3. In [FQ90] the terminology *transverse spheres* is used for geometric duals with self-intersection zero which is sometimes useful. In these lectures we will also never run into geometric duals with nontrivial self-intersection although they can arise in certain situations.

In the surgery situation we need geometric duals $\hat{a}$ and $\hat{b}$ for spheres a and b which form a hyperbolic pair in the intersection form of M, in particular, a and b are algebraically dual. The idea is to modify a and b simultaneously by regular homotopies until they become geometrically dual. We take some framed, immersed Whitney disk W for a pair of algebraically canceling intersection points between a and b which will meet both a and b in general. The first step is to push a and b off W as indicated in Figure 41 by so-called *finger moves* resulting spheres a' and b' intersecting each other just as a and b but they don't meet W and have more self-intersections than the original spheres. Next we do a Whitney trick across W on either a' or b' and we get new spheres that are regularly homotopic to a and b, have two fewer intersection point but possibly more self-intersections each. Repeating this process finitely many times we eventually obtain a geometrically dual pair $\hat{a}$ and $\hat{b}$.

In the h-cobordism problem the setup was slightly different. Here a and b are not only algebraically dual but each is embedded and comes with a geometric dual $\hat{a}$ and $\hat{b}$, respectively. These dual spheres already tell us that a and b are π_1-negligible individually

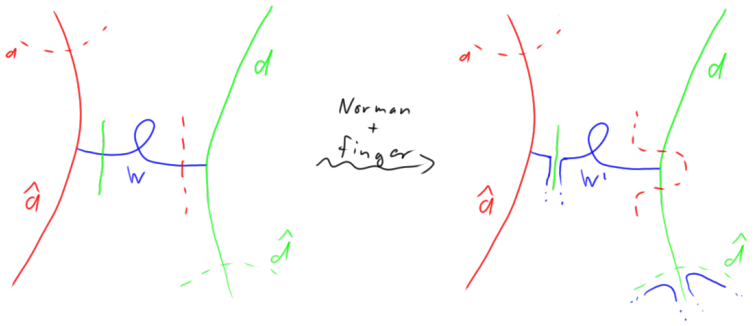

Figure 42: Dual spheres for the h-cobordism problem.

but they might not be simultaneously, the problem is that $\hat{a}$ might intersect b, for example. Our task is to arrange $\hat{a}$ to be disjoint from b with the additional difficulty of that we're only allowed to move a and b by isotopies (instead of regular homotopies) in order to keep them embedded. The first step is to make the intersection number $\hat{a} \cdot b$ zero which is easily achieved by "adding" copies of a to $\hat{a}$, that is, connect summing a and $\hat{a}$ inside M along a suitable arc. This is also known as the *Norman trick*. Next we take some framed, immersed Whitney W disk for intersections between $\hat{a}$ and b and, as in the surgery case, the idea is to cleanse W from bad things and then do the Whitney trick on $\hat{a}$. However, we have to pay close attention to a and b in the process. If we did the Whitney trick right away we'd be running danger of creating new intersections with whatever W intersects which a priori might be either of a, b, $\hat{a}$ and $\hat{b}$. But we don't care about intersections of $\hat{a}$ with $\hat{b}$ or itself so that the only problems are caused by intersections of W with a or b. We can remedy the b intersection by Norman tricks adding copies of $\hat{b}$ to W so that the new W has only problematic intersections with a which, in turn, can be removed by isotoping a off W by finger moves in the direction of b. This will possibly make the new Whitney disk more singular (if $\hat{b}$ meets W) and create new a, b-intersections and but that's okay. Now that the Whitney disk is clean, a singular Whitney trick on $\hat{a}$ produces a (most likely immersed) geometric dual for the isotoped version of a.

Remark 6.4. You probably noticed that finger moves are exactly the inverses of Whitney tricks. It is ironic that the first step in order to do Whitney tricks is to do their inverses, we somehow have to make the situation worse before we can start to make it better.

As mentioned, this is only the first step in Casson's construction. The following lemma, which can be proved using similar tricks as above, leads the way to the further steps.

Lemma 6.5. *Let M be a simply connected 4-manifold and let $\alpha\colon (D^2, \partial D^2) \to (M, \partial M)$ be a properly immersed disk such that there exists a 2-cycle β with $\alpha \cdot \beta = 1$ (homologically). Then α is regularly homotopic (rel ∂) to a π_1-negligible $\alpha'\colon (D^2, \partial D^2) \to (M, \partial M)$.*

Exercise 6.6. Prove Lemma 6.5.

6.4 Casson handles and Kirby calculus

We have figured out that for both the surgery and the h-cobordism problem we can assume that there's a pair of algebraically dual spheres whose union is π_1-negligible and we can start throwing Whitney disks for unwanted intersection points into their complement. That's still not perfect because the disks will cross themselves but Casson noticed that the process can be iterated. Indeed, any Whitney disk meets the Clifford tori of its intersection points exactly once and thus we can use Lemma 6.5 to arrange the Whitney disks to be

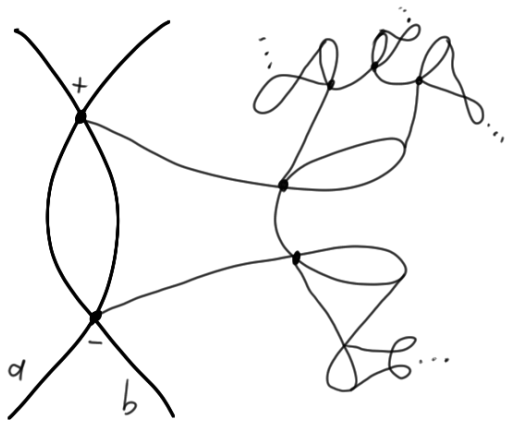

Figure 43: Building a Casson handle.

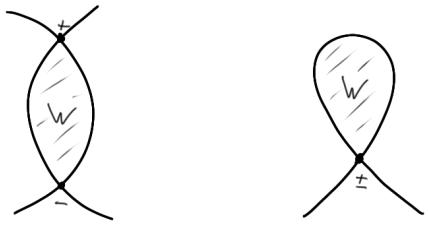

Figure 44: Two-sided (left) and one-sided (right) Whitney disks.

disjoint and π_1-negligible in the complement of a and b so that we can map a second collection of Whitney disks into the complement of a, b and the union of the first collection of Whitney disks and so on (see Figure 43). This leads to an infinite process for building a 2-dimensional spine which, in the end, turns out to be contractible (it is not homeomorphic to the disk in any obvious way, though). Indeed, we're building some infinite, non-compact 2-complex going into the 4-manifold which has lots of free fundamental group at every stage but at each stage that free fundamental group is annihilated by the immersed disks of the next stage so the direct limit will be a contractible space. So we can build this thing that's somehow "like a disk" and it bounds the Whitney circle. This is the first conceptual core of the idea of what Casson called *flexible handles* and what everyone else calls *Casson handles*.

Remark 6.7. Note that the Whitney disks in the higher stages of Figure 43 don't really look like the ones we know in that they only involve one intersection point each (see also Figure 44). Such *one-sided* Whitney disks were also discussed in Whitney's paper [Whi44] and there is a corresponding Whitney trick just as in the two-sided case. The difference is that, in the case of self-intersections, the two-sided trick produces regular homotopies while the one-sided version only gives homotopies. (For intersections of two different surfaces the two-sided trick actually produces isotopies of one of the surfaces.) To keep the pictures as simple as possible we only draw one-sided Whitney disks in higher stages. For two-sided Whitney circles we've seen earlier that the two intersecting sheets appear on the boundary of a tubular neighborhood as a Bing double. Similarly, in the one-sided case we see a Whitehead double (Figure 45) which might be twisted if we choose the wrong framing. (Note that this is intimately related to our discussion in Remark 3.23.)

As the term "handle" indicates, there's still something missing from our discussion: we've just focused on the 2-dimensional spine and we have to find a away to thicken

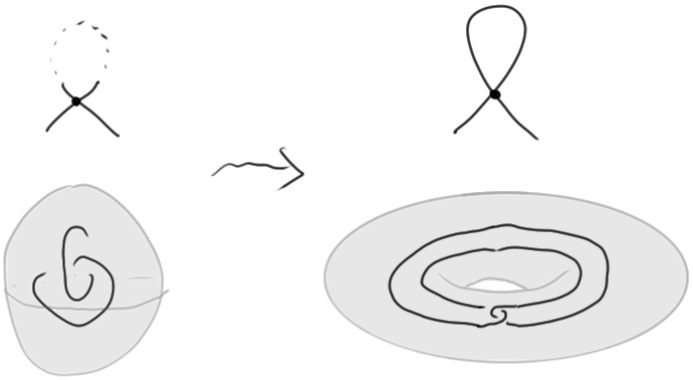

Figure 45: Self-intersections and Whitehead doubles.

the construction a little bit in order to get a good 4-dimensional neighborhood. This is related to the framing issued mentioned before and disasters lurk if we don't carefully select framing conditions for all the Whitney disks. But it turns out that this is not a big issue in the end. We will define the framing conditions idiosyncratically in terms of the so-called *Kirby calculus*. There is an equivalent way of understanding this in terms of 3-manifold topology which fits perfectly with our discussion of Bing and Whitehead doubling and decomposition space theory. It turns out that one of the most important things in the infinite construction is what the frontier looks like, which is a 3-manifold. Different framings can actually produce different frontiers and we can understand if we got the framings right in terms of the 3-manifold topology of the frontier. We'll say more about this later.

6.4.1 Kinky handles and Kirby calculus

We want to understand how to thicken immersed Whitney disks, so we have to know what a neighborhood of a disk crossing itself in a 4-manifold look like. By standard results in differential topology, a generic immersion of B^2 can be extended (uniquely up to isotopy) to an immersion of $B^2 \times B^2$ – in other words, a 4-dimensional 2-handle[6] – which factors through an embedding of a self-plumbing of $B^2 \times B^2$ into the 4-manifold (see Figure 46). (Recall that self-plumbing means to identify two interior sub-disks and glue them together interchanging horizontal and vertical coordinates.[7]) Note that the plumbings don't affect the solid torus $\partial_- = S^1 \times D^2$ – the *attaching region* of the 2-handle – which is indicated in blue; self-plumbed 2-handles are commonly called *kinky handles* and ∂_- serves as their attaching region. In summary, the correct notion of a thickened (or framed) immersed Whitney disk is an embedding of a kinky handle and any Whitney disk has a canonical thickening, that is, whenever we can find a Whitney disk we can also find a kinky handle and vice versa.

Exercise 6.8. Show that $B^2 \times B^2$ becomes homeomorphic to $S^1 \times B^3$ after one self-plumbing.

To see how we get to Figure 45, we should take the sphere that contains the Hopf link around the crossing and surger it to itself by cutting out a 3-ball on each component and

[6] Some terminology: the disks $B^2 \times \{0\}$ and $\{0\} \times B^2$ are called *core* and *cocore*, their boundaries $S^1 \times \{0\}$ and $\{0\} \times S^1$ are the *attaching circle* and *belt circle* and $\partial_- = S^1 \times B^2$ is called the *attaching region*. (For some reason, $B^2 \times S^1$ doesn't seem to have a standard although the term *belt region* suggests itself.)

[7] More precisely, we take disjoint embeddings $\phi, \psi \colon D^2 \to \mathrm{int} D^2$ and identify $\phi(D^2) \times D^2$ with $\psi(D^2) \times D^2$ via $(\phi(x), y) \sim (\psi(y), x)$.

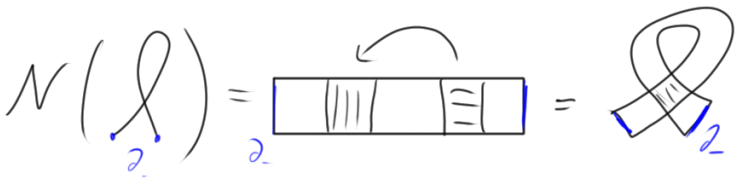

Figure 46: Self-plumbing $B^2 \times B^2$. (Imagine the extra dimensions!)

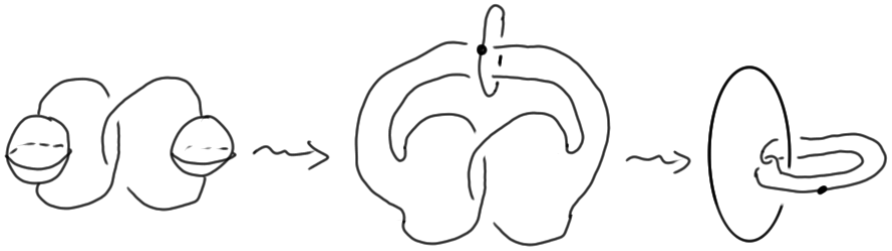

Figure 47: Kirby diagrams of a single (negative) self-plumbing of $D^2 \times D^2$.

declaring that their boundary 2-spheres are identified by reflection (Figure 47, left). That gives a Whitehead double embedded in $S^1 \times S^2$ and its 0-framed neighborhood is just the attaching region ∂_- of the corresponding kinky handle.

The pictures in Figure 47 actually show the full glory of the 4-dimensional situation. In fact, we should think of the whole situation as a 4-ball around the intersection point to which a 4-dimensional 1-handle is attached and its attaching region are the two balls in the left picture. So we simply have to imagine a 4-dimensional 1-handle connecting these balls. Schematically, this is shown in Figure 48 and there's another notation which is part of the Kirby calculus to represent links in simple 3-manifolds such as $S^1 \times S^2$. In that notation we record the fundamental group generator of $S^1 \times S^2$ dually by drawing a circle that links both strands in the middle of Figure 47 and putting a dot on it. The meaning of this notation is that anytime we see an unlink with dots on it in S^3, we should think of removing the standard slices in B^4 beneath the dotted components as indicated in the right of Figure 48. If we just have one dotted component, then the complement of the standard slice is homeomorphic to a meridian of the dotted circle times a 3-ball, so it is sort of the Alexander dual space of $S^1 \times B^3$. Moreover, by general position we can always arrange links in the boundary of the Alexander dual picture to be actually out on the boundary of B^4. So a general link in $S^1 \times S^2$ can then be drawn as a link in S^3 which

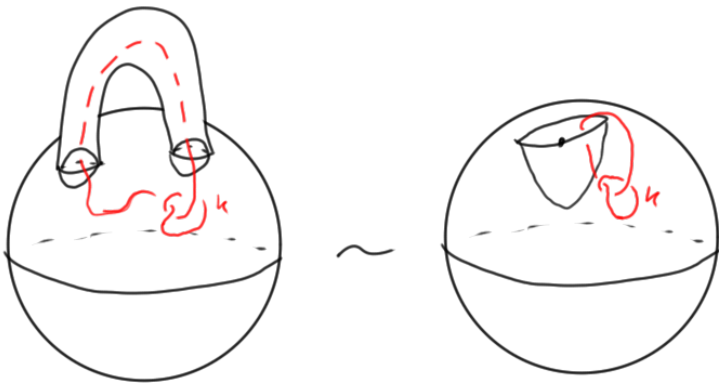

Figure 48: How to read Kirby diagrams.

might link the dotted unknot.

The other thing we have to know about Kirby calculus is that whenever we see a link component that doesn't have a dot on it, then that means that a 4-dimensional 2-handle has been attached to the 4-ball (instead of dug out in the case with dots) and then it better have a number next to it in order to determine a framing by adding that number of twists to the canonical framing of the knot in S^3.[8]

6.4.2 The definition of Casson handles

We can finally describe what Casson handles actually look like in the simply connected context. The process of building Casson handles in a π_1-negligible situation is then as follows:

- Locate Whitney disks for unwanted intersections. *(Lather.)*
- Make them π_1-negligible and thicken to kinky handles. *(Rinse.)*
- Repeat this process for the new π_1-negligible situation. *(Repeat.)*

Note that each thickening process induces a canonical framing on the corresponding Whitney circle and we have to use precisely this framing to attach the kinky handles in each stage. This infinite process replaces each original Whitney disk with a contractible 4-dimensional gadget called a *Casson handle*, generically denoted by CH, and inside CH we find the attaching region ∂_- of the kinky handle in the first stage which now serves as attaching region for CH. In other words, a Casson handle $(\mathrm{CH}, \partial_-)$ has been attached to each original Whitney circle. After scraping off all frontier of CH except for ∂_- we obtain an *open Casson handle* which we denote by $\mathring{\mathrm{CH}}$. Our main goal is to prove the following theorem.

Theorem 6.9. *The pair* $(\mathring{\mathrm{CH}}, \partial_-)$ *is homeomorphic to* $(B^2 \times \mathbb{R}^2, S^1 \times \mathbb{R}^2)$.

Once we know this result we can make surgery and h-cobordism work in the simply connected context in dimension four because everything we wished to have done with Whitney disks we can now do with Casson handles.

In order to draw Kirby diagrams of Casson handles, the first thing we do is to make the pattern in the middle of Figure 47 more symmetrical by passing to the right picture using the symmetry of the Whitehead link so that the attaching region ∂_- of the kinky handle appears as an unknot and the dotted circle has the clasp on it. Next we note that the diagram generalizes immediately to kinky handles with several self-plumbings, we simply have to add several dotted circles to (untwisted) Whitehead doubles of meridians of the attaching circle. For the inductive process we have to located the attaching regions for the higher stages of kinky handles and it is easy to see that, in each stage, the kinky handles are attached to meridians of the dotted circles of the previous stage and the framing condition is that we have to use the zero framing of these meridians. Figure 49 shows the first three stages of the simplest Casson handle where each Whitney disk has only one self-intersection and Figure 50 shows an example with more complicated branching of self-intersections.

[8] Note that there's $\mathbb{Z}$ worth of choices for the framing coming from $\pi_1(SO(2))$.

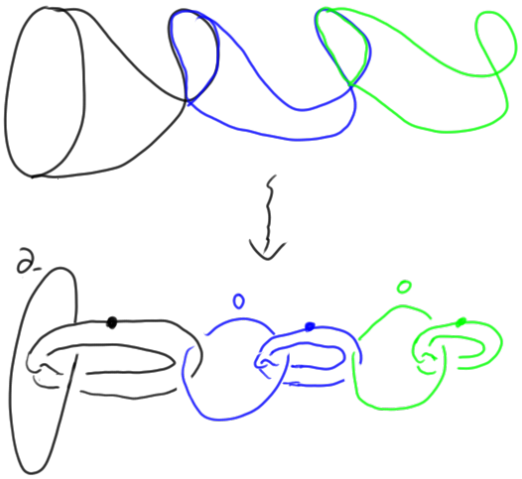

Figure 49: The first three stages of the simplest Casson handle.

Figure 50: A more complicated Casson handle.

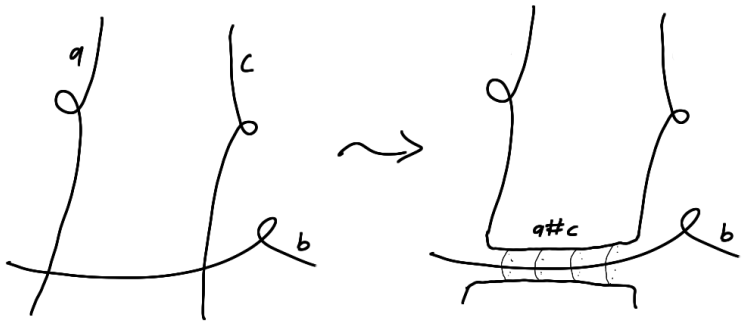

Figure 51: Piping.

Figure 52: Piping to improve double point loops.

7 Exploring Casson handles

7.1 Picture Camp

Welcome to Picture Camp! We're going to draw a lot of pictures and get familiar with them. The first set of pictures are kind of schematics – although they can be made rigorous by regarding them as cross section of 4-dimensional picture – where arcs represent bits of surfaces.

Piping. We might have a configuration of bits of surfaces a, b and c as in the left of Figure 51 where a and c both intersect b in one point. (Note that it wouldn't make a difference if the self intersection of b were in the middle because we're looking at 2-dimensional sheets.) Then we can add a tube along some arc on b to unite the sheets of a and c – that is, we take an ambient connected sum of a and c – so that the result has no intersection with b. This is called *piping.*

Here's an example of how we will use piping. Suppose we have an immersed disk attached to some lower stage stuff and it has a dual sphere which might have self-intersections, too. Ans suppose we know that the loops in the dual associated with its self-intersection points are trivial in the fundamental group while the double point loops in the disks are essential. Then we can pipe the dual onto the disk and what we get is still a disk. But we gain something because we see that the new disk has trivial double point loops.

Pushing down. Another picture which we call *pushing down* is shown in Figure 53. Lots of our constructions have a surface coming into another surface sort of forming a T-junction (for example, when we glue in Whitney disks). What we see is that one point of intersection between a and b is traded for two points of intersection of opposite sign

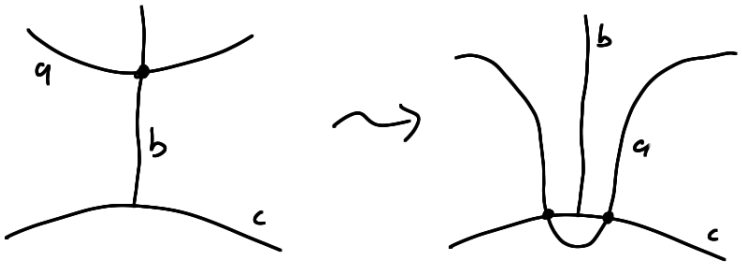

Figure 53: Pushing down.

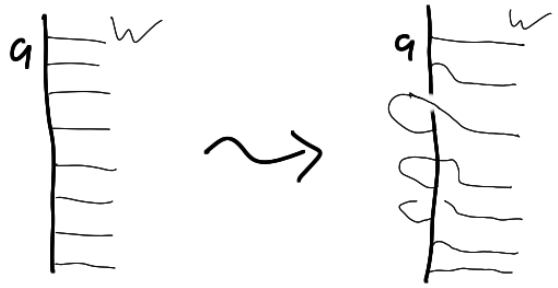

Figure 54: Spinning.

between a and c.

Spinning. The last of the schematic pictures is called *spinning* which we have already used to adjust framings of Whitney disks at the expense of creating intersections. Suppose we have one edge of a surface a and another thing W coming in. Then spinning means that we change the normal picture by first pushing the arcs behind and then bring the back arc through to create an intersection point at some moment and then after creating that intersection point the arc stays on top and we push it back to the original position.

The Whitehead link. Next we point out some symmetric links that we have to deal with. We've already encountered the *Whitehead link* (Figure 55) as the beginning of a Casson handle. Recall that in Kirby calculus it represents a neighborhood of a disk with a single self-intersection. The symmetry allows us to draw either component as a trivial unknot. (Technically, this link appears in two forms depending on the sign of the claps, but this seems to be irrelevant for the decomposition space theory.)

There's a quite useful generalization of this symmetry. Let $\mathrm{Wh}_{j,k}(H)$ be the link obtained from the Hopf link H by taking the untwisted Whitehead double of the first and the second component j and k times, respectively. Note that the Whitehead link is either $\mathrm{Wh}_{0,1}(H)$ or $\mathrm{Wh}_{1,0}(H)$ and the symmetry says that these two are isotopic.

Figure 55: Symmetry of the Whitehead link.

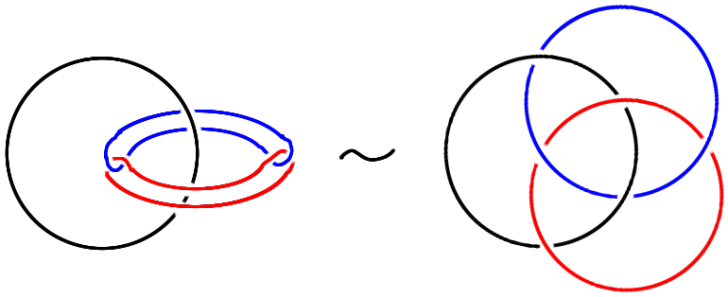

Figure 56: A symmetry of the Borromean rings

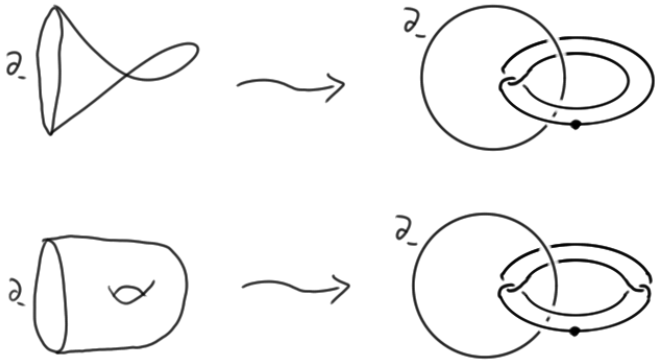

Figure 57: From immersed disks and surfaces to Whitehead and Bing doubles.

Exercise 7.1. Show that $\mathrm{Wh}_{j,k}(H)$ and $\mathrm{Wh}_{j',k'}(H)$ are isotopic if and only if $j+k = j'+k'$.

The Borromean rings. Another link arose when we studied the double of the Alexander gored ball. There we encountered a link in a solid torus and referred to it as the Bing double of the core circle. But it's often convenient to represent the solid torus dually by drawing the core of its complement in the 3-sphere (which is also a solid torus) and if we do that we get the *Borromean rings* which have a threefold symmetry as indicated in Figure 56.

While we're drawing the Borromean rings, there's also a 4-dimensional picture associated with them. If we put dots on two components, then we claim that we see a Kirby diagram of a thickened punctured torus $T_0 \times B^2$ where the third component with the 0-framing represents $\partial_- = \partial T_0 \times B^2$ (see Figure 57). To see this, note that T_0 deformation retracts onto a wedge of circles and as an abstract manifold $T_0 \times B^2$ can't be anything else than $S^1 \times B^3 \natural S^1 \times B^3$. In Kirby calculus this is represented by a dotted 2-component and the two circles appear as meridians of the dotted circles. Furthermore, the core of ∂_- should be representable as a curve in the complement of the dotted circles and it has to represent the commutator of the meridians in the fundamental group. And since this is a very simple picture it must be the simplest possible such curve and therefore it's the third component of the Borromean rings.

If that proof doesn't satisfy you entirely, here's a more math style derivation. When we analyzed the Alexander gored ball we sat that $T_0 \times I$ can be obtained from $B^2 \times I$ by drilling out two 3-dimensional 1-handles. Now, if we cross with another I-factor to get $T_0 \times B^2$, then we simply have to cross the 3-dimensional picture with I and on the boundary we see what's shown in Figure 58.

Figure 58: The Borromean rings and $T_0 \times B^2$.

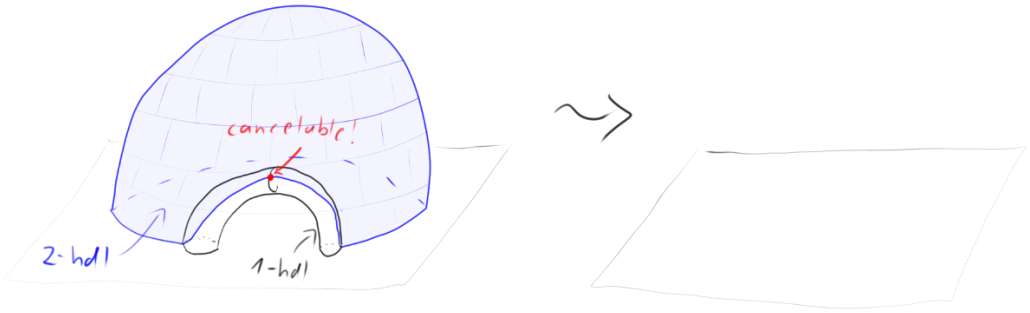

Figure 59: An igloo melting back into the arctic.

Some more Kirby calculus. Some of the basic ingredients in manifold topology is manipulating Morse functions and the most basic manipulation is to cancel critical points of adjacent indices when they're geometrically in a configuration where they can be canceled; the way Smale would have said this is that the descending manifold of the index $k+1$ critical point meets the ascending manifold of the index k point transversely in one point. The paradigm picture for this is the igloo melting back into the arctic (see Figure 59) where a 3-dimensional 1-handle (the archway) and 2-handle (the roof) are canceled. The cancellation criterion is satisfied since the roof edge passes over the archway exactly once and the cancellation proceeds by melting the igloo back down into the ice.

So how does this look in Kirby calculus? In the case of index 1 and 2 (which is all we'll need) there'll be a dotted circle representing a 1-handle and the attaching circle of the canceling 2-handle linking the dotted circle geometrically once (see Figure 60). Canceling them means that they disappear from the picture but we can't just erase them, we have

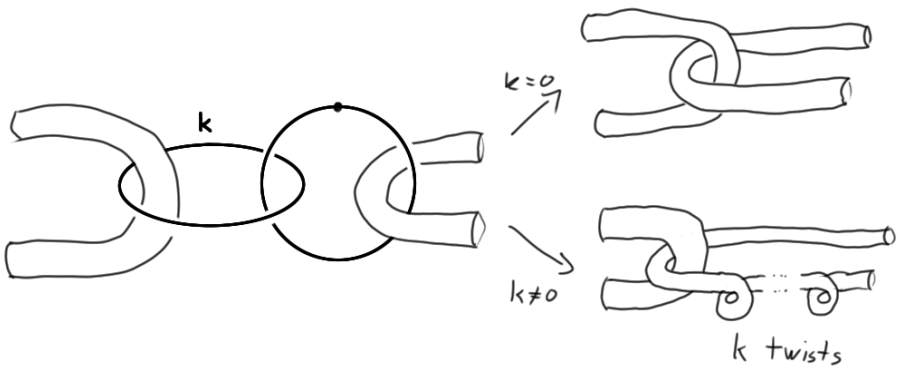

Figure 60: Cancellation of 1- and 2-handles in Kirby calculus.

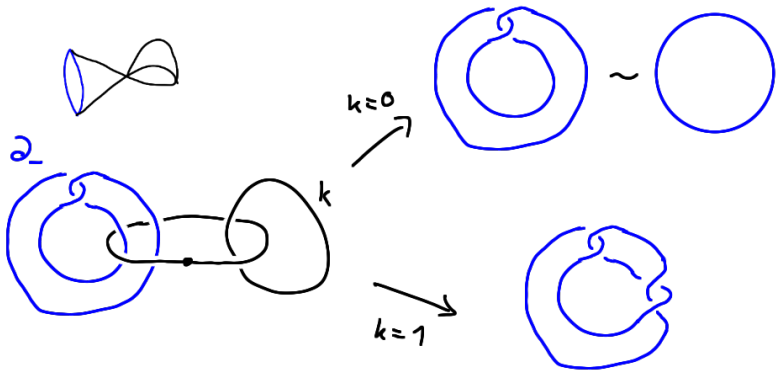

Figure 61: Cancellation in a simple Casson tower.

to pay attention to other things that might pass through (indicated by the tubes). If nothing passes through the dotted circle, then erasing works fine, but if something passes through, then the we have to modify the tubes as in Figure 60. Note that the framing of the two handle doesn't matter for the cancellation criterion but it does affect the way the cancellation appears in the diagram.

Actually, in the diagrams for Casson towers and handles all the framings will be zero if we do it correctly, so we never have to do the calculation with a nonzero twist. In order to fully appreciate why we need zeros let's look at a simple example and see what happened if there was a non-zero twist.

Example 7.2. We consider a 2-stage Casson tower with one disk in each stage such that the first stage has one self-intersection, the second is embedded and its framing produces framing coefficient k in the Kirby diagram (see Figure 61). By construction, the 2-handle of the second stage cancels the 1-handle of the first stage and in order to make the cancellation more transparent we have used the symmetry of the Whitehead link to draw the 1-handle as an unknot and the attaching region ∂_- as a Whitehead double. According to the rules, when we cancel we have to twist what goes through the 1-handle side k-times, in this case that's ∂_-.

Suppose first that we were lucky and the 2-handle had zero framing. Then can simply erase the pair and we don't have to twist anything. What's left would be ∂_- represented by a zero framed unknot. But that's just the picture of a 2-handle

$$(B^2 \times B^2, S^1 \times B^2) \cong (B^4, \text{0-framed unknot}).$$

So this would be great it's perfectly consistent with the schematic picture (top left) because it says that the little kink in the first stage wasn't necessary after all.

However, if k wasn't zero but $k = 1$, say, then we'd have to put one full twist in ∂_- and we'd either get a trefoil or a figure eight knot (depending on the sign of the clasp). In any case, neither of them is slice and it doesn't look like there's a smoothly embedded core associated with this construction. So this is not an auspicious start for a 4-dimensional 2-handle and we've kind of gotten off on the wrong foot. This is one of the many places where it's necessary to keep zero framings propagating in Casson's construction.

Example 7.3. Now let's consider a general Casson tower with only zero framed 2-handles. Again, by construction, all 1-handles except for those in the last stage can be canceled with the 2-handles of the subsequent stages. What would that look like? To keep things simple let's first assume that each stage has only one disk with a single self-intersection; Figure 62 contains shows the case of two stages. Using the symmetry of the generalized Whitehead

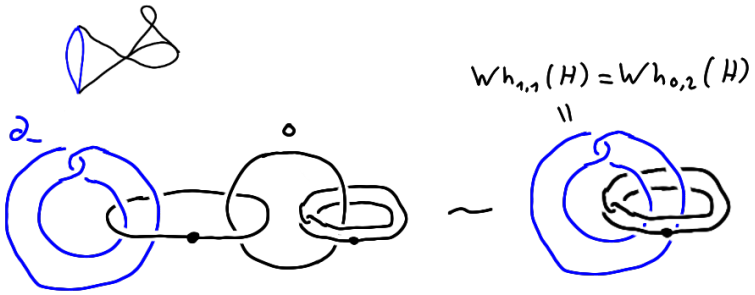

Figure 62: Cancellation in a more complicated Casson tower.

links (Exercise 7.1) it is easy to see that after canceling we see the link $\mathrm{Wh}_{0,n}(H)$ where n is the number of stages, that is, we see ∂_- as a trivial unknot and a 1-handle which appears as an iterated Whitehead double of a meridian.

From here on, it is probably obvious that the general case, with an arbitrary branching pattern in the stages of the tower, results in ∂_- as a trivial unknot together with ramified, iterated Whitehead doubles of a meridian.

Exercise 7.4. Use cancellation in Kirby calculus to show that

(a) as an absolute space, a Casson tower is diffeomorphic to $\natural^r S^1 \times B^3$ for some r.

(b) the interior of a Casson handle is diffeomorphic to $\mathbb{R}^4$.

Remark 7.5. As we keep Whitehead doubling links, in some sense they become more and more fragile with respect to 4-dimensional topology. It's not link the link would become the unlink or anything like that because each doubling gives an amalgamation with a free group in the link group but, for example, if we start with a link that has non-trivial Milnor invariants, then after we double a couple of times we get a boundary link whose Milnor invariants vanish, and if we double further, we get something called a *good boundary link* which, for all our knowledge, looks like it was smoothly slice. So it look like if we can double things repeatedly, we're making the link closer and closer to the trivial link. That philosophy is intimately related to the idea that it's good to go to higher and higher Casson towers. Somehow the fact that the boundary region of a Casson handle is tangled up with a more and more highly doubled 1-handle as we increase the tower should intuitively make us think that the 1-handle is influencing the attaching region less and less and it's looking more like an actual 2-handle.

7.2 The boundary of a Casson handle

A Casson handle CH is a non-compact 4-dimensional manifold improperly embedded in 4-space and its boundary has two pieces

$$\partial \mathrm{CH} = \partial_- \mathrm{CH} \cup_{T^2} \partial_+ \mathrm{CH}$$

where $\partial_-\mathrm{CH}$ is just a solid torus, the attaching region, and we want to explain what the more complicated piece $\partial_+\mathrm{CH}$ looks like. We assume that CH is given to us as a Kirby diagram living in S^3, which we consider as a union of two solid tori

$$S^3 \cong S^1 \times B^2 \cup_{T^2} B^2 \times S^1 \big(= \partial(B^2 \times B^2) \big) \tag{7.1}$$

where $\partial_-\mathrm{CH}$ shows up as $S^1 \times B^2$, and the idea is to keep track of what's happening to the other solid torus $B^2 \times S^1$ throughout the construction. It turns out that the Kirby diagram gives us a precise way of understanding this.

Remember that when we discussed the Alexander horned sphere as the boundary of the gored ball it was very helpful to focus on the portion of the boundary which was there permanently. In the construction of the gored ball as an infinite union (with some limit set thrown in), in each finite stage of the union there were always some annulus regions in the boundary that were there only temporarily, they weren't in the boundary anymore after we attached the next stage. Similarly, in one higher dimension, as we go out in the Casson handle attaching stages of kinky handles, the attaching regions of the kinky handles are only temporarily in the boundary; when we attach the k-th stage it has some solid tori in it which disappear from the boundary when we attach the $(k+1)$-th stage.

Let's see how this works in detail. For convenience we write $T_n \subset \mathrm{CH}$ for the Casson tower in the n-th stage and note that the boundary decomposes as $\partial T_n = \partial_- \mathrm{CH} \cup_{T^2} \partial_+ T_n$. Since $\partial_-\mathrm{CH}$ is not affected by going to higher stages it is enough to focus on the ∂_+-parts. At the very beginning, we just have $T_0 = B^4$ and $\partial_+ T_0$ is the solid torus $B^2 \times S^1$ from (7.1). In the first stage we attach 1-handles along dotted circles in $\partial_+ T_0$ which appear as untwisted Whitehead doubles of the core $\{0\} \times S^1$. Recall that the dotted circle notation for 1-handles means that a neighborhood of a standard slice for the dotted circle is to be removed from B^4. This has the following effect on the boundary.

Exercise 7.6. Show that carving out the standard slice underneath a dotted circle from B^4 changes the boundary by a zero framed surgery on the dotted circle.

So we obtain $\partial_+ T_1$ from $\partial_+ T_0$ by zero framed surgery on the dotted circles, that is, we remove a neighborhood of each dotted circle and replace it with a solid torus such that the longitudinal push off of the dotted circle bounds a disk. Thus $\partial_+ T_1$ has two parts, $\partial_+ T_0$ minus neighborhoods of the dotted circles and a collection of solid tori which are slightly more impossible to draw; the former is a cobordism from $T^2 = \partial(\partial_+ T_0)$ to tori around the Whitehead curves given by the dotted circles. The important observation is that the impossible to draw tori are isotopic to the attaching regions of the 2-handles in the second stage and will thus disappear when we pass to $\partial_+ T_2$, so we don't actually have to draw them. Moreover, the dotted circles of the second stage can be isotoped into the attaching regions of their corresponding 2-handles so that the cobordism part of $\partial_+ T_1$ remains untouched when passing to $\partial_+ T_2$, in fact, it will stay permanently in the boundary and gives the first piece of $\partial_+ \mathrm{CH}$.

With this understood, it's very easy to figure out how to keep going. In each stage we're supposed to put in the attaching regions of the 2-handles of the next stage, which would fill in all the holes in S^3 again, and then remove neighborhood of the dotted circles. In particular, if there were no extraneous 1-handles hanging off in the next stage, the attaching regions of the 2-handles would repair the damage in S^3 and then we'd see that $\partial_-\mathrm{CH}$ bounded a disk and we'd be done. But realistically, there will always be a proliferating number of 1-handles and that means that the next stage is not a solid torus but it's a solid torus minus some Whitehead curves sitting at its core. So $\partial_+\mathrm{CH}$ is a cobordism from a torus to a (perhaps iterated) Whitehead double, followed by another such cobordism and so on.

What we see is that $\partial_+\mathrm{CH}$ is something that we've already run into when we were studying decompositions. If there was no branching, it would just be the solid torus $B^2 \times S^1$ minus a standard Whitehead continuum and, if there was branching, it would be a solid torus minus a Cantor set worth of Whitehead continua which correspond to the endpoints of the tree which describes the branching pattern.

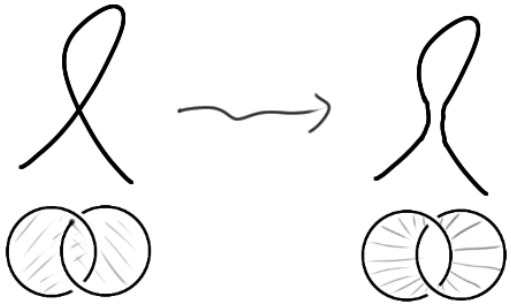

Figure 63: Resolving double points of surfaces.

7.3 An exercise in wishful thinking

Later we will develop some combinatorics involving a careful study of dual spheres that will enable us to achieve a lot of additional control over Casson's construction. But let's jump ahead a little bit and imagine that

(a) such control has been achieved and

(b) there was a variant of the construction that also involved surface stages

to see what this would say about the boundary.

Casson's original construction gives some non-compact thing which might fill up the whole manifold which Casson himself analyzed to a certain extent. In particular, he showed that an open neighborhood of the construction was proper homotopy equivalent to a standard handle, but that was a bit of a dead-end result, it wasn't possible to do much with that statement. But imagine that the construction was geometrically controlled – for example, like our construction of the Alexander gored ball where we went smaller and smaller in each step – and proceeded to a well defined limit. Then ∂_- would still be a solid torus but ∂_+ now would be the decomposition space of a ramified Whitehead decomposition instead of its complement. Indeed, the farther and farther out stages would get smaller and smaller which is exactly what would happen if we had taken that infinite intersection and crushed it to a point. So where we wanted to have a handle we at least see something with a manifold factor (remember Theorem 4.10?) as its frontier and if this were topologically collared, we'd see a solid torus cross an interval in there; everything would resolve and that would mean that we could put in a topological Whitney disk and we'd really be cooking but, of course, we have no way of knowing it's collared. But at least it looks like we're moving in the right direction.

Now, as long as we're imagining, suppose when we build this construction, instead of always using disks with double points, we were able to replace such a disk with an embedded surface. In fact, that's not such a far fetched thing because double points of surfaces can be resolved locally with the result of increasing the genus; in a ball around the double point we can simply replace the two intersecting sheets by the annulus connecting the two components of the Hopf link on the boundary (see Figure 63).

At the end of the day it turns out that, once we've found a Casson handle, then we can replace it with a construction that has any number of surface stages alternating in any fashion we like with any number of disk stages. For convenience we'll still call such a modified construction a Casson handle although Casson didn't talk about surfaces.

Now suppose we can do the modified construction in a controlled way; that's going to be a winning combination. Instead of just getting successive layers of disks we could intersperse an arbitrary number of surface stages whenever we like and at the end everything would be getting smaller and smaller and converge to a Cantor set. But from what we have learned in picture camp we know that the frontier of such a construction

would be the decomposition space of a mixed Bing-Whitehead decomposition; each disk stage gives a Whitehead double while surface stages result in Bing doubling (Figure 57). Now, remember that we had this result of Starbird and Ancel (Theorem 4.12) which tells us exactly when such decompositions shrink. Roughly, we need lots of Bing doubles to compensate for a few Whitehead doubles, in other words, we need lots of surface stages to make up for each disk stage. To sum up, we can expect

$$\partial_+ = (B^2 \times S^1) \setminus \mathcal{D}_{\mathcal{W}/\mathcal{B}} \quad \text{without control and}$$
$$\partial_+ = (B^2 \times S^1)/\mathcal{D}_{\mathcal{W}/\mathcal{B}} \quad \text{with control.}$$

In particular, if there are enough surface stages in the controlled case, then $\mathcal{D}_{\mathcal{W}/\mathcal{B}}$ is shrinkable and get $\partial_+ \cong B^2 \times S^1$ so that the frontier of this infinite construction looks exactly like the boundary of a 2-handle! That's considerable progress because if we think of goal as trying to produce a 2-handle where we wish to find a Whitney disk, at this point the boundary of whatever we have found is find, except we don't know if it's collared.

Our strategy will be to produce not only one frontier but to fill this kind of Casson handle up with many frontiers, each of which is recognized to be the standard thing, and at the end of the day very little of the Casson handle will be left unexplored, so little that it can ultimately be related to the standard handle by the sphere-to-sphere theorem (Theorem 5.1).

Remark 7.7. One might wonder: why we don't take just surface stages? After all, this would always give shrinkable decompositions. The problem with this approach is that we will actually need some disk stages to achieve geometric control. In turns out that we really need to intersperse with some disks to keep local information about the fundamental group.

7.4 A glimpse at reimbedding and the Design

To give more motivation for the combinatorics to come we continue to plow ahead and take a look at what we like to call "the design". One of the conclusions of these combinatorics is the idea of *reimbedding* which roughly says that, if we have a sufficiently complicated finite construction, then we can produce arbitrarily larger finite constructions inside.

Theorem 7.8 (Reimbedding for Casson towers)**.** *Inside any Casson tower T^0_m of sufficiently large height m (that is, there are m stages of disks) there is another tower $T^1_n \subset T^0_m$ of arbitrary height n such that T^1_n and T^0_m have the same bottom stage.*

Remark 7.9. In [Fre82] we used the constant $m = 6$ which is not optimal. In fact, Gompf and Singh [GS84] lowered the bound to $m = 5$ which may or may not be optimal. But at the end of the day it doesn't really matter what the constant is as long as there is one.

Let's see what we can do with this. For example, we can take something of height 6 and locate something of height 13 inside which we consider as something with six stages, six further stages and one more stage on top (just to make sure that nothing is tangled up in the fundamental group). Then we do the same thing in the middle six stages and repeat this process ad infinitum as shown schematically in Figure 64.

This picture already shows how to obtain control. We can modify each step by using the top stages to show that the middle six stages are null-homotopic inside the original 6-stage tower. After all, as an absolute manifold the middle six stages are just a boundary sum of copies of $S^1 \times B^3$ (and thus have a 1-dimensional spine), the final layer then provides null-homotopies for each $S^1 \times \{0\}$ and in four dimension homotopy implies isotopy for 1-dimensional things. So this whole middle 6-stage tower can be moved into a little ball somewhere inside the original tower and only then we focus on its internal structure. By

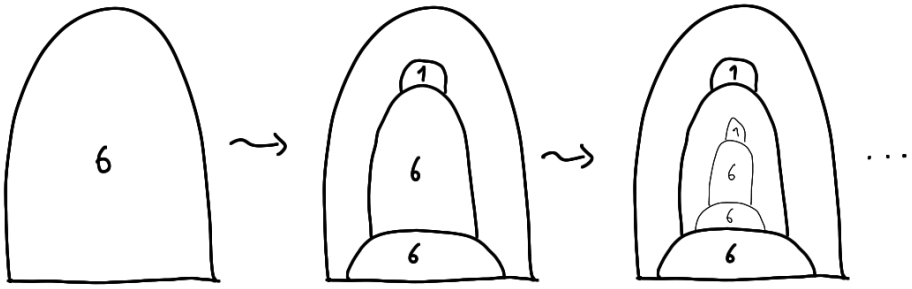

Figure 64: Reimbedding, first attempt: $13 = 6 + 6 + 1$

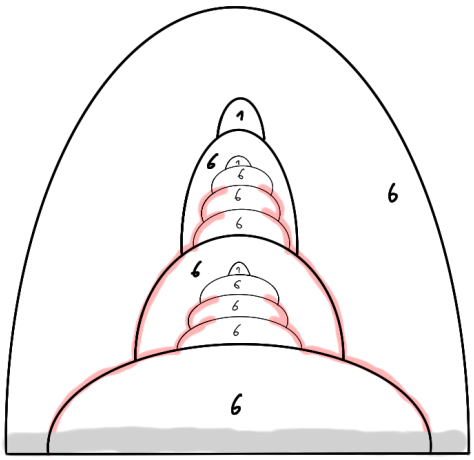

Figure 65: Reimbedding, second attempt: $19 = 6 + 6 + 6 + 1$ (aka *"the Design"*, part 1).

construction this modified process forces the towers to converge to points and if there was branching in the construction we'd see a Cantor set again.

This controlled construction gives us a single Casson handle and its frontier in the tower we started with – remember that our goal is to fill up most of this handle with, ultimately, a Cantor set worth of frontiers. In order do that we need another construction that bifurcates in another direction. This means that, every time we do this reimbedding, we want to have two choices, sort of an inner and an outer way to proceed. So we start over with a 6-stage tower but now we take a tower with $19 = 6 + 6 + 6 + 1$ stages inside. Now there are two middle 6-stage towers in each we find another 19-stage tower and so on. Then the frontier exhibits a dyadic branching pattern as indicated in Figure65 and it's easy to explicitly see what we're building: in the 3-dimensional context each piece would be $B^2 \times S^1$ minus a neighborhood of a ramified Whitehead link[9] and the thick red lines indicate that we take a small neighborhood so that each piece is of the form $(B^2 \times S^1 \backslash \nu L) \times I$ for some link L.

Now since these pieces are explicitly parametrized, we can take the standard 2-handle $B^2 \times B^2$ and start fitting them into it (see Figure 66). What we end up seeing is, first of all, the attaching region (shaded in grey), and then the red pieces will appear as indicated. In particular, they will get smaller and smaller and converge to some limit set (which may or may not be a Cantor set, this depends on whether we work with disks only or allow surfaces). What we have found is some common closed set in both the Casson handle and the standard handle which we call *the Design*.

[9]Remember that we're only using disks it this point, if we were also using surfaces, we'd see mixed Bing-Whitehead links.

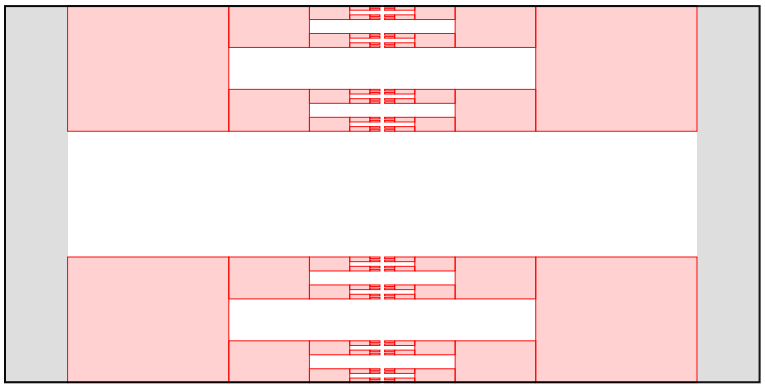

Figure 66: Filling up the standard 2-handle (aka *"the Design"*, part 2).

Remark 7.10. The path to the proof that we're going to explain – before we double back and give the original proof whose high point is a fantastic shrink due to Bob Edwards [Fre82, Chapter 8] – is to use surface stages because we can lean rather heavily on what we've already learned about shrinking decompositions that have adequate Bing components to them. The point of going through enough combinatorics to work with surface stages – a technology that was unavailable in 1981 – is that we can really arrange the limit set in the standard 2-handle to be a Cantor set.

The complement of the Design in both the exotic and standard situation is a countable number of regions and, although they're a tiny bit mysterious in the exotic guy, back in the standard handle all this is explicitly coordinate driven and they're just product solid tori. The proof will finish by studying a common quotient Q

$$\begin{array}{ccc} B^2 \times B^2 & & CH \\ & \overset{\cong}{\rightleftharpoons} & \\ & (\text{ABH})\ \alpha \searrow \quad \swarrow\ \beta\ (\text{ABH}) & \\ & Q & \end{array}$$

where α and β are decomposition maps ad the argument will be that we can first shrink the α-decomposition using the bird-like equivalent techniques so that α turns out to be ABH and that will tell us that Q is a ball. Then we have a map from CH to a ball and, although we don't know that CH is a ball, we'll understand that it is contained in a ball (in a similar way that the Alexander gored ball is contained in the standard 3-ball) and we can use the ball-to-ball theorem to deduce that β is also ABH so that CH must be homeomorphic to the standard handle.

8 Combinatorics day

We're first going to explain some of the original combinatorics in working in honest Casson handles [Fre82] and then go into more detail of the combinatorics with surface stages [FQ90]. The latter turns out to be much simpler and is really quite an improvement because.

8.1 Gropes and transverse spheres

We've already met a grope in Section 3.3.2 when we discussed the Alexander gored ball as a union of thickened, punctured tori. As far as we know, the term grope was introduced

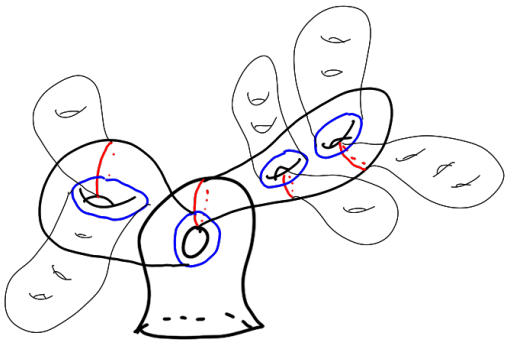

Figure 67: A grope as a 2-complex.

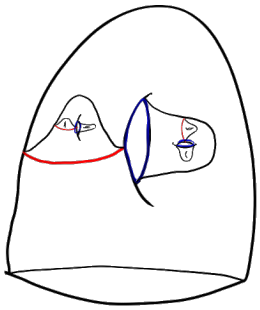

Figure 68: A 2-dimensional grope in 3-space.

by Jim Cannon and we're going to use the word to mean something that might be either 2-, 3- or 4-dimensional but the dimension should always be clear from the context.

Roughly, what a *2D grope* looks like is that we start with an oriented surface with one boundary component called the *base* or *1st stage*, take a symplectic basis[10] on the surface, attach other oriented surfaces with a single boundary component – the *2nd stage* – and repeat this process (see Figure 67). Note that each surface in the construction can have arbitrary genus but since the pictures get exponentially complicated anyway we're tempted to draw only genus one surfaces. Abstractly, a 2D grope is a 2-complex but we can embed it in 3-space by attaching half of the surfaces in each stage on the outside and the others to the inside as in Figure 68. In order to get a *3D grope* we simply take a thickening of this picture in 3-space. (That's fine for any finite stage but if we do an infinite construction and want a limiting object, then it's important that the stages shrink and limit to a Cantor set.) Finally, to get *4D gropes* we just take the 3-dimensional model and cross it with an interval. The 4D version is also equivalent to a handle picture in the spirit of the pictures for Casson towers. Basically, the pictures look almost the same, the only difference is that we see Bing doubles (one for each genus) instead of Whitehead doubles (Figure 69).

We generically denote gropes by G and call the boundary of the base surface the *attaching circle* and its thickening the *attaching region* $\partial_- G$ of the grope. Moreover, any 3D or 4D grope naturally contains a 2D grope as a deformation retract, this will be called the *body*.

Remark 8.1. Group theoretically gropes are related to the *commutator series* (or *derived series*) of the fundamental group because a grope displays its attaching circle as a com-

[10] A *symplectic basis* is a basis of H_1 consisting of simple closed curves $a_i, b_i \subset$ such that a_i and b_i intersect transversely in one point and there are no further intersections.

Figure 69: A Kirby diagram of a 4-dimensional grope.

Figure 70: A capped grope.

mutator in the first stage, then as a commutator of commutators and then a commutator of commutators of commutators and so on.

From now on we mostly focus on 4D gropes. Note that in our models in 4-space the top stage surfaces of a grope have a symplectic basis of curves which bound embedded disks (already visible in the 3D picture). If we add them to the picture, then we obtain an example of a *capped grope*. More generally, we call any immersed disk in 4-space which bounds a basis curve in a top stage surface and is otherwise disjoint from the body of the grope a *cap* and a *capped grope* G^c is a grope G together with caps for all basis curves in the top stage. Note that we allow arbitrary intersections and self-intersections among the caps.

Remark 8.2. As usual, there's a framing issue that we've swept under the rug. The basis curves have a natural framing in 4-space[11] and this framing must extend across the caps. In Kirby calculus language this means that we attach 0-framed kinky handles to meridians of the 1-handles in the top stage of a grope. However, since we allow the caps to intersect each other it is not completely straight forward to draw the pictures.

Exercise 8.3. Figure out how intersections among caps appear in the handle pictures.

Exercise 8.4. Show that a capped grope with embedded caps is diffeomorphic to a standard 2-handle (relative to their attaching regions).

We have a lot to learn about 1-stage capped gropes. A 1-stage capped grope is simply an oriented surface with a single boundary component with disks attached along a symplectic basis, Figure 71 shows the genus one case. Let's first look at the picture in three dimensions. If we have embedded caps as in the picture, then we can certainly use either one of them to turn the punctured torus into a disk by surgery. But there's another

[11] Up to orientations, they have a canonical framing inside the surface which canonically extends to a framing in 3-space and the latter is canonically framed in 4-space.

Figure 71: Symmetric surgery aka contraction.

Figure 72: Pushing things off the contraction.

interesting option when both disks are available which is called *symmetric surgery* or *contraction* [FQ90]: we remove cylinders around both curves but we think mod 2 and leave the square where the cylinders intersect in the space, and then we put in four disks (one pair for each cap) back in. The virtue of this construction is that it allows us to trade intersections with caps for self-intersections of whatever was intersecting the caps. Indeed, say something called X intersects the caps as in Figure 72, then the observation if that, after the contraction we can push one arc up and the other down. Note that this process of *pushing off the contraction* creates two self-intersections of X for each intersection with the caps.

Remark 8.5. Why is this an important technology? Recall that one of the key points in Casson's constructions was to clean things up by promoting homological duals to geometric duals which we called dual spheres. They are what makes these constructions run, they enable us to make higher stages in Casson towers and eventually to build Casson handles. It turns out that, if we understand it correctly, contraction is a very efficient machine for producing dual spheres. In fact, a test of how efficient it was has enabled Quinn to prove the annulus conjecture in dimension four [Qui82] (see also [Edw84]). He thought of the annulus conjecture as a controlled h-cobordism theorem and in order to do h-cobordism with geometric control you need ready access to dual spheres everywhere, you couldn't go looking for them far away.

In our original approach [Fre82] we were basically making dual spheres "by hand" and, although there was an algebraic presence of contraction picture in the background, we first learned about it from Bob Edwards at the 1982 Durham conference when Quinn had just announced his proof.

The technique of pushing off contractions has had a lot of influence in using gropes as a variant of Casson towers and that's the way the book [FQ90] is written; basically, wherever we could we used a capped surface instead of a disk which is much more convenient in terms of combinatorics. We're going to try to explain the bare bones of both, the old

and the new combinatorics. But before we want to give the most interesting corollary of the contraction trick which allows us to produce infinitely many disjoint duals in one fell swoop whereas with the only technology we had to find duals one at a time.

To see why this is useful, suppose we have a surface S intersected once by another surface T. If there is a dual sphere $\hat{S}$ for S we can pipe T and $\hat{S}$ to remove the intersection of T and S. That's good, but suppose we don't have just T but another surface T' and we want both T and T' disjoint from S. and we only have the one dual sphere $\hat{S}$. Of course, even if we have only one dual sphere $\hat{S}$ we can pipe both T and T' with parallel copies of $\hat{S}$ to achieve disjointness from S, but this is not entirely satisfactory because we add intersections of T and T' unless $\hat{S}$ happens to be embedded with trivial normal bundle. It would be much more convenient to have not only one dual but an arbitrary number of disjoint ones. So how do capped gropes and contraction solve this?

Lemma 8.6 (∞-Lemma)**.** *A (4D) capped grope G^c with immersed caps (disjoint from the body) contains arbitrarily many disjointly immersed disks with boundary parallel in $\partial_- G^c$.*

Proof. The proof is extremely simple. We first contract and then push the caps off the contraction. What we get is a new capped surface disjoint from the contraction and we simply repeat this process. □

Back to the situation described before the lemma, if we remove a disk D from $\hat{S}$ where it meets S, we're left with an immersed disk. Now, if we had a capped grope instead of the immersed disk, then we could cap off parallel copies of D with disks from the lemma and get infinitely many disjoint dual spheres and we can pipe arbitrarily many things off S without making them cross themselves!

8.2 Height raising and reimbedding for Casson towers

Let's see how we can raise height in Casson towers with the help of the ∞-Lemma 8.6. In the next section we'll talk about the more general towers interlacing surface and disk stages used in [FQ90]. The combinatorics for Casson towers is slightly messier and we could skip this part, but it's the way the original proof [Fre82] worked.

Suppose we're looking at a 4-stage Casson tower. Then there's a little computation in topology that tells you that the third stage has a transverse sphere.

Exercise 8.7. Prove this! (Hint: Lemma 4.1 in [Fre82])

This transverse sphere has two problem: it is immersed and crosses the fourth stage. What we'll do is to turn this sphere into a dual torus which has caps, and the caps cross themselves and the top stage. In the light of Lemma 8.6 this is an improvement since it's more powerful to have a dual capped surface than just a dual sphere. The way this works is that the Clifford tori of double points in the second stage and ...do something with it... By contracting this capped surface back to a sphere we can trade its intersections with the fourth stage for self-intersections in the fourth stage disks.

Then we use the Clifford tori in the third stage obtain a dual capped surface for the fourth stage.

The next thing is to use that we're in a higher tower so that all the double point loops in the fourth stage bound null-homotopies but these may cross the caps. Well, what can we do about that? We can make these null-homotopies cross themselves even more than they did to begin with and get them disjoint from an actual dual sphere.

Yada yada yada...

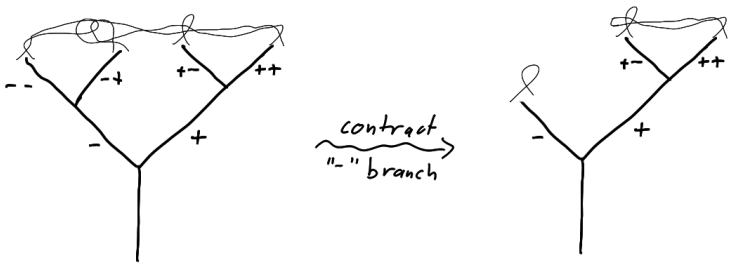

Figure 73: Shortening the left branch to clean up cap intersections.

(Sorry, didn't understand this stuff well enough to write something useful.)

So at the end of the day we see that within any 6-stage Casson tower we can find a 7-stage tower and then we can keep going and eventually prove the reimbedding theorem 7.8.

8.3 Height raising for gropes

We're over the most painful combinatorics and go to the good new days where we use capped gropes to height raise instead of all disk stages and we'll see that the combinatorics is much more pleasant. Here's the key result.

Lemma 8.8 (Height raising for capped gropes)**.** *Inside any 3-stage capped grope G_3^c there exists an n-stage capped grope $G_n^c \subset G_3^c$ with the same attaching region.*

Proof. When building the grope G_3^c we can divide each stage of surface into a left $(-)$ and right branch $(+)$ because of the symplectically dual basis. (In the picture in 3-space this would be the inside surfaces versus the outside.) On top we have the caps which are immersed and cross all through each other. Schematically, this is shown in the left picture in Figure 73.

The first thing we can do is to take the left branch and to sacrifice one of its bits of height in order to get all the intersections off. More precisely, we contract the third level of the left branch to push all intersections with the caps from the right branch off and we get the right side of Figure 73. The left branch of the second stage is then just a capped surface.

In the next step we use the shortened left branch to create a capped surfaces dual to the surfaces in the right branch of the second stage. To keep things simple we assume that everything has genus one; the general case is only notationally more complicated. Denote the base surface by Σ and let $\Sigma_\pm$ be the left $(-)$ and right $(+)$ branches of the second stage which are attached along a symplectic basis $C_\pm \subset \Sigma$. If we take the unit normal bundle of Σ and restrict it to C_-, then we get a torus T and it is easy to see that T intersects Σ_+ in one point. So we have found a homological dual to Σ_+ which is already a good sign but, of course, we want a higher quality dual. Note that T meets the left branch Σ_- in a circle (in fact, a parallel push off of C_-) so that we can remove a neighborhood of this circle from T and fill the resulting two boundary components with two parallel copies of the capped surface Σ_-^c. This "surgery" turns T into a capped surface and since the caps of Σ_- didn't interfere with the right branch we really get a dual capped surface for Σ_+.

At this point the right branch still has all three stages and caps on top. Now we use piping to convert all intersection among the right branch caps into intersections with Σ_+ (recall that the conversion ratio is 1:4) and for each of these intersections we throw in a disjoint copy of the dual capped surface for Σ_+. At the end of the day this turns each cap from the right branch into a capped surface. This recreates all kinds of intersections between right branch caps and left branch caps, so we're kind of back to where we started.

left	right
$1+2$	$1+2$
$1+1$	$1+3$
$1+3$	$1+2$
$1+2$	$1+4$
$1+5$	$1+3$
$1+4$	$1+7$
$\vdots$	$\vdots$

Figure 74: The heights of both branches progress in Fibonacci sequences. (The red numbers indicate on which branch we are working.)

But notice that the multiplicities have changed. The left branch now has height one over the base surface but the right branch has three stages on top of the base surface.

Now we simply reverse the roles. We do a contraction on the right branch to get the caps disjoint, create something dual to the left branch and pipe away. The important observation is that this time we not only get a dual capped surface but actually a dual 2-stage capped grope. So the height of the right branch goes down from 3 to 2, but the left branch grows taller from height 1 to 3. By iterating this process further and alternating between the left and right branch we see that the height of the branches evolves as in the table in Figure 74. At the end of the day, we can first raise the height of both branches asymmetrically and then use contraction to cut the heights down symmetrically. □

Remark 8.9. Having to work alternately on the left and the right side seems to be a general feature of using gropes. The reason is that, although we can use a copy of the left side to make a dual for the right side and vice versa, these dual are not disjoint, they intersect in two points. And that usually spoils more homogeneous arguments so that we have to go back and forth between the two sides.

Remark 8.10. Lemma 8.8 is kind of a baby reimbedding lemma. But what we'll actually have to work with gropes that have not only one but two layers of caps.

9 Geometric control and the Design

We start where Casson left us and do it with the new capped surface technology. We'll see how this leads to rather easy shrinking arguments. In the next chapter we will go back and revisit Edwards' original shrink.

9.1 Where Casson left us off

Recall that the original motivation for doing all this came from the surgery and h-cobordism programs for 4-manifolds which we continue to take simply connected for simplicity. Both programs led to the same kind of problem. We ended up in some (smooth, simply connected) 4-manifold M that contained possibly immersed spheres $a, b \subset M$ which were homologically dual and we somehow had to make them geometrically dual using the Whitney trick. Casson's early preparation made the complement $M \setminus (a \cup b)$ simply connected as well so that we could put in Whitney disks W into the complement spanning all Whitney circles for canceling intersection points. With a little bit of work we also made the further complement of $a \cup b \cup W$ simply connected by finding transverse spheres to W so that we could iterate this process to build Casson towers and eventually Casson handles.

Figure 75: Reimbedding and CEQFAS-towers.

This was the pre-grope technology. Let' see how the same situation plays out with gropes. With $a, b, W \subset M$ as above, notice that we have the Clifford torus for a transverse crossing of a and b sitting around; this is an algebraic dual to the disk W and its meridian and longitude are linking a and b, respectively. But we already fixed up that a and b have transverse spheres which means that this dual object to W actually is a capped surface. So what can we do with this? We can immediately start building a grope version of W by piping the double points of W into parallel copies of the base surface which turns W into an embedded surface with caps. And we can actually keep going and pass to a 2-stage capped grope. Indeed, all the intersection points of the caps can be pushed down to the base and then piped with further copies of the original dual. Then we can iterate that and produce a grope of arbitrary height with one layer of caps which are all disjoint from the body but the caps are crossing themselves. So this is really rapid progress compared to Casson towers.

Remark 9.1. Notice that we kind of shortcut the grope height raising which was a little more laborious. But in that situation we did not have the dual sitting around so we had to use the left and right branches to create each others duals.

Remark 9.2. The key open question in the topological category is actually whether capped gropes G_n^c of some height n with one layer of caps are already enough to finish the game, that is, whether this structure already contains an embedded flat disk. As we'll see, two layers of caps do the trick. Things like the A-B-slice problem or the conjecture that surgery and h-cobordism (or rather s-cobordism) work for free groups are all related to this central question.

9.2 Reimbedding in the grope world

Now we're going to use a second layer of caps to get a suitable analogue for the reimbedding theorem for Casson towers (Theorem 7.8). First we have to say what the analogue of Casson towers should be.

Definition 9.3. A *tower* with $k \in \mathbb{N} \cup \{\infty\}$ *stories* of *heights* $N \in \mathbb{N}^k$, is a 4-manifold pair $(\mathcal{T}_N, \partial_-)$ obtained from $(B^2 \times B^2, \partial_-)$ by adding N_1 layers of surface stages, followed by one layer of caps with only self-intersections, then another N_2 surface stages, another layer of disks and so on.

In notation we could write such a tower as a "composition"

$$\mathcal{T}_N = c \circ G_{N_k} \circ \cdots \circ c \circ G_{N_1}$$

where each G_{N_i} is a grope of height N_i and c indicates a layer of caps.

It's probably no surprise that we're mostly interested in the infinite case. For such an infinite tower $\mathcal{T}$ – which is a non-compact smooth 4-manifold – we denote its *end point compactification*[12] by $\widehat{\mathcal{T}}$ and call it a *compactified tower*. As in the case of Casson handles, the frontier of such a compatified tower $\widehat{\mathcal{T}}$ has two parts $\partial\widehat{\mathcal{T}} = \partial_-\widehat{\mathcal{T}} \cup_{T^2} \partial_+\widehat{\mathcal{T}}$ where $\partial_-\widehat{\mathcal{T}}$ naturally identified with $S^1 \times B^2$. The other part can be described as follows.

Lemma 9.4. *Let $\widehat{\mathcal{T}}$ be a compactified tower. Then $\partial_+\widehat{\mathcal{T}}$ is homeomorphic to $(B^2 \times S^1)/\mathcal{D}$ where $\mathcal{D}$ is a mixed Bing-Whitehead decomposition of $B^2 \times S^1$.*

This is good news since we know exactly which mixed Bing-Whitehead decompositions shrink. According to Theorem 4.12) this happens whenever the series $\sum_i \frac{N_i}{2^i}$ diverges where $(N_1, N_2, \dots)$ is the sequence of heights of a given tower $\mathcal{T}$. In that case we say that $\mathcal{T}$ has the *Ancel-Starbird property*. In particular, if $\mathcal{T}$ has the Ancel-Starbird property, then $\partial_+\widehat{\mathcal{T}}_N$ is homeomorphic to $B^2 \times S^1$.

Definition 9.5. An *open CEQFAS*[13]*-handle*, generically denoted by C··H, is an infinite tower such that

(i) C··H has the Ancel-Starbird property and

(ii) all stories of C··H have height at least three.

A *(compact) CEQFAS handle* $\widehat{\text{C··H}}$ is the end point compactification of an open CEQFAS handle.

The remainder of this chapter is devoted to the proof of the following theorem.

Theorem 9.6. *Any CEQFAS-handle $(\widehat{\text{C··H}}, \partial_-)$ is homeomorphic to the standard 2-handle $(B^2 \times B^2, \partial_-)$ as a pair.*

We will follow the strategy outlined in Chapter 7.4 and the first step is to establish appropriate reimbedding results.

Proposition 9.7 (Reimbedding for towers)**.** *Let G_3^c be a capped grope immersed in a 4–manifold M such that all double point loops of the caps are trivial in $\pi_1(M \setminus base)$. Then for any $N \in \mathbb{N}^k$, $k \in \mathbb{N} \cup \{\infty\}$, there is a tower $\mathcal{T}_N \subset G_3^c$ such that $\partial_-\mathcal{T}_N = \partial_- G_3^c$.*

In applications the base usually has a dual to it so the additional fundamental group concern is completely unwarranted. For example, we can prove surgery and h-cobordism without this hypothesis.

Proof. See Chapter 3.5 in [FQ90], more details to follow... □

Theorem 9.8 (Controlled reimbedding)**.** *With the same hypotheses as in Proposition 9.7, we can find a CEQFAS-handle $\widehat{\text{C··H}}$ inside G_3^c with $\partial_-\widehat{\text{C··H}} = \partial_- G_3^c$. Furthermore, we can choose $\widehat{\text{C··H}}$ such that everything above its second story is contained in an arbitrarily small ball inside G_3^c.*

"Proof" needs work!

Proof. Remember that in the context of Casson towers we repeatedly embedded $19 = 3 \cdot 6 + 1$-stage towers inside 6-stage towers. As a grope analogue of $19 = 3 \cdot 6 + 1$ we can use something like

$$c \circ G_{n^2}^{cc} \circ c \circ G_{n^2}^{cc} \circ G_r \subset G_n^{cc}$$

where $n \geq 3$ and $r \in \mathbb{N}$, that is, we use Theorem 9.7 to locate a towers of the form $C \circ G_{n^2}^{cc} \circ C \circ G_{n^2}^{cc} \circ G_r$ inside G_n^{cc}.

[12] Explain end point compactification

[13] CEQFAS=Casson-Edwards-Quinn-Freedman-Ancel-Starbird

Remark 9.9. Although Theorem 9.7 only gives single layers of caps, it's no problem that we're asking for multiple layers because we can always waste surface stages by contracting them to a layer of caps.

Then we proceed as before: Given G^{cc}_n we locate a tower of the form $C \circ G^{cc}_{n^2} \circ C \circ G^{cc}_{n^2} \circ G_r$ inside and achieve geometric control by using the extra layers of caps to move the $G^{cc}_{n^2}$-parts into small balls by an ambient isotopy of G^{cc}_n. Then we repeat this process inside each $G^{cc}_{n^2}$ and continue indefinitely.

□

9.3 The Design in CEQFAS handles

Remember that the Design is supposed to be a common closed subset of $\widehat{\mathrm{C}\cdot\cdot\mathrm{H}}$ and $B^2 \times B^2$. So how do we build the Design in the grope context? The key idea is to do an infinite construction using the controlled reimbedding theorem that produces an infinite collection of nested CEQFAS-handles inside a given one. In fact, we'll actually get a Cantor set worth of CEQFAS-handles as a result of inherent dyadic branching in the construction. We'll go through the construction twice, we first give a blueprint in order to convey the main ideas and then comes the fine print with all the technicalities.

But before going into the construction we set up some notation. By a *dyadic expansion* we mean a finite or infinite sequence $I = (i_1 i_2 \dots)$ of 0s and 2s, that is, an element of $\{0,2\}^k$ where $k \in \mathbb{N} \cup \infty$. The number k is called the *length* of I which we also denote by $|I|$. For finite k and possibly infinite l we have the juxtaposition operation

$$\{0,2\}^k \times \{0,2\}^l \to \{0,2\}^{k+l}, \quad (i_1 \dots i_k)(j_1 \dots j_l) \mapsto (i_1 \dots i_k j_1 \dots j_l)$$

and we use it to define a partial order of the set of all dyadic expansions by saying that J *contains* I, denoted by $I \subset J$, if $J = II'$ for some I'.

Note that the set of infinite dyadic expansion can be identified with the middle-third construction of the Cantor set $C_3 \subset [0,1]$ via the map

$$\{0,2\}^\infty \longrightarrow C_3, \quad I = (i_1 i_2 \dots) \mapsto \sum_{j=1}^{\infty} \frac{i_j}{3^j}.$$

It is easy to see that the expansions that eventually contain only 0s or 2s correspond to the lower and upper end points of the outer-third intervals that survive to some finite stage of the construction, respectively. At times we want to consider finite dyadic expansions as infinite ones and we do so by adding a tail of zeros or, in other words, by juxtaposing with $(00\dots)$.

9.3.1 The blueprint

Let $\widehat{\mathrm{C}\cdot\cdot\mathrm{H}}$ be a CEQFAS-handle. By definition all stories of $\widehat{\mathrm{C}\cdot\cdot\mathrm{H}}$ have height at least 3 which means that we can apply the controlled reimbedding theorem (Theorem 9.8) in any story and we will exploit this to devise an infinite construction whose first three steps of the construction are schematically indicated in Figure 76.

In the *first step* of our construction we take $\widehat{\mathrm{C}\cdot\cdot\mathrm{H}}$ and locate another CEQFAS handle in its *first story*. For reasons that will become apparent momentarily we call the new handle $\widehat{\mathrm{C}\cdot\cdot\mathrm{H}}_{(2)}$ and also relabel the original handle $\widehat{\mathrm{C}\cdot\cdot\mathrm{H}}$ as $\widehat{\mathrm{C}\cdot\cdot\mathrm{H}}_{(0)}$, that is, we label the CEQFAS handles we produce in the first step by dyadic expansions of *length one*.

Now assume that we have done k steps and we have found a collection of 2^k CEQFAS handles $\widehat{\mathrm{C}\cdot\cdot\mathrm{H}}_{(i_1\dots i_k)} \subset \widehat{\mathrm{C}\cdot\cdot\mathrm{H}}$, $(i_1 \dots i_k) \in \{0,2\}^k$, labeled by the dyadic expansions of

Figure 76: The first three steps in the preliminary construction of the design.

length k. Then the $(k+1)$-*st step* is to take each $\widehat{\mathrm{C}\cdot\cdot\mathrm{H}}_{(i_1\dots i_k)}$ and to locate new CEQFAS handles inside each capped grope of its $(k+1)$-*st story*. These handles naturally attach to the first k stories of $\widehat{\mathrm{C}\cdot\cdot\mathrm{H}}_{(i_1\dots i_k)}$ and we denote the union of these k first stories and the newly found handles by $\widehat{\mathrm{C}\cdot\cdot\mathrm{H}}_{(i_1\dots i_k 2)}$, which is a single CEQFAS handle. In addition, we let $\widehat{\mathrm{C}\cdot\cdot\mathrm{H}}_{(i_1\dots i_k 0)} = \widehat{\mathrm{C}\cdot\cdot\mathrm{H}}_{(i_1\dots i_k)}$ so that we end up with 2^{k+1} CEQFAS handles indexed by the dyadic expansions of length $k+1$.

As usual, we repeat this process indefinitely (with a certain amout of control, more about this later) and we end up with a collection of CEQFAS handles labeled by the infinite dyadic expansions $\{0,2\}^\infty$ or, alternatively, the middle third Cantor set C_3. So as promised we have found a Cantor set worth of handles inside $\widehat{\mathrm{C}\cdot\cdot\mathrm{H}}$ which itself corresponds to the expansion $(00\dots)$ or $0 \in C$.

So apart from producing a lot of CEQFAS handles, what is this construction good for? Let's forget about most parts of the handles and consider only their frontiers; the union

$$D = \bigcup_{r\in C_3} \partial_+ \widehat{\mathrm{C}\cdot\cdot\mathrm{H}}_r$$

is the first approximation of the Design. According to Lemma 9.4, each frontier $\partial_+\widehat{\mathrm{C}\cdot\cdot\mathrm{H}}_r$ is homeomorphic to $B^2\times S^1$ which means that we can find an embedding

$$B^2\times S^1\times C_3 \xrightarrow{\cong} D \subset \widehat{\mathrm{C}\cdot\cdot\mathrm{H}}$$

such that $B^2\times S^1\times\{0\}$ goes to $\partial_+\widehat{\mathrm{C}\cdot\cdot\mathrm{H}}$. On the other hand, we can also embed $B^2\times S^1\times C_3$ into the standard 2-handle via

$$B^2\times S^1\times C_3 \to B^2\times B^2, \quad \big(z, e^{i\theta}, r\big) \mapsto \big(z, (1-\tfrac{r}{3})e^{i\theta}\big),$$

so that we can consider D as a common closed subset of $\widehat{\mathrm{C}\cdot\cdot\mathrm{H}}$ and $B^2\times B^2$.

Remark 9.10. Note that D looks very close to a collar for $\partial_+\widehat{\mathrm{C}\cdot\cdot\mathrm{H}}$ in $\widehat{\mathrm{C}\cdot\cdot\mathrm{H}}$ as well as for $B^2\times S^1$ in $B^2\times B^2$. Further moral support that $\partial_+\widehat{\mathrm{C}\cdot\cdot\mathrm{H}}$ might be collared – which it would have to be if $\widehat{\mathrm{C}\cdot\cdot\mathrm{H}}$ were a manifold – comes from our previous observation that the closure of the complement of C_3 in $[0,1]$ gives a shrinkable decomposition (Remark 3.7).

So what can we do with D? Naively, we could try to shrink the decompositions of $\widehat{\mathrm{C}\cdot\cdot\mathrm{H}}$ and $B^2\times B^2$ given by the closures of the components of the complement of D but, as it turns out, in order to successfully shrink things we have to enlarge D a little bit. This enlarged version of D is the actual Design $\boldsymbol{D}$. Roughly, $\boldsymbol{D}\subset\widehat{\mathrm{C}\cdot\cdot\mathrm{H}}$ is going to be the union of neighborhoods $\nu\partial_+\widehat{\mathrm{C}\cdot\cdot\mathrm{H}}_r$ over all $r\in C_3\cap[0,\frac{1}{3}]$. However, in order to actually make this work we have to do the whole construction a little more carefully. So we start over again.

9.3.2 The fine print

We first have to take a small detour and discuss collars in towers. For that purpose consider an arbitrary infinite tower $\mathcal{T}$. Before passing to the end point compactification $\mathcal{T}$ is a non-compact, smooth 4-manifold and thus its boundary, in particular $\partial_+\mathcal{T}$ has a collar, that is, we can find an embedding $c\colon \partial_+\mathcal{T}\times[0,1]\hookrightarrow\mathcal{T}$ which maps $\partial_+\mathcal{T}\times\{0\}$ to $\partial_+\mathcal{T}$. Unfortunately, we can't just take any collar for our construction, we need some extra properties. We denote the stories of $\mathcal{T}$ by S_n and let $\partial_n^+\mathcal{T}=\partial_+\mathcal{T}\cap S_n$. Then we require that c maps $\partial_n^+\mathcal{T}\times[0,1]$ into S_n and $(\partial_+\mathcal{T}\cap\partial_-\mathcal{T})\times[0,1]$ into $\partial_-\mathcal{T}$.

Exercise 9.11. Convince yourself that we can always find such a collar!

From now on we will always assume that our collars have this property.

Now let's do the reimbedding construction again with a little more precision. Along the way we will define certain *puzzle pieces* that will eventually make up the Design. As before we start with a CEQFAS handle $\widehat{\mathrm{C}\cdot\cdot\mathrm{H}}$ and fix some metric on it. The first step begins with relabeling the handle to $\widehat{\mathrm{C}\cdot\cdot\mathrm{H}}_{(0)}$ and choosing a collar $c_{(0)}\colon \partial_+\mathrm{C}\cdot\cdot\mathrm{H}_{(0)}\times[0,1]\hookrightarrow\mathrm{C}\cdot\cdot\mathrm{H}_{(0)}$ as above. For convenience we introduce the short hand notation

$$\nu_{(0)}[s,t]=c_{(0)}\big(\partial_+\mathrm{C}\cdot\cdot\mathrm{H}_{(0)}\times[s,t]\big)$$

and we define the first puzzle piece $\boldsymbol{D}_{(0)}$ as the intersection of the first story of $\widehat{\mathrm{C}\cdot\cdot\mathrm{H}}_{(0)}$ with $\nu_{(0)}[0,1]$.

Next assume that we have done k steps and found CEQFAS handles $\widehat{\mathrm{C}\cdot\cdot\mathrm{H}}_I$, where $I\in\{0,2\}^k$ is a finite dyadic expansion of length k with $i_1=0$, together with collars

$$c_I\colon \partial_+\mathrm{C}\cdot\cdot\mathrm{H}_I\times[0,1]\longrightarrow\mathrm{C}\cdot\cdot\mathrm{H}_I.$$

For the $(k+1)$-st step we take the first $(k+1)$ stories from each handle $\widehat{\mathrm{C}\cdot\cdot\mathrm{H}}_I$ and truncate them by removing the part $\nu_I[0,\frac{2}{3})$ of the collar. The truncated $(k+1)$-st story consists of some number of capped gropes and inside each we can use Theorem 9.8 to locate a CEQFAS handle whose higher stories have diameter less than $\frac{1}{k}$ – this is the control we alluded to in the blueprint. After adding the truncated first k stories of $\widehat{\mathrm{C}\cdot\cdot\mathrm{H}}_I$, to which the newly found handles naturally attach, we obtain a single CEQFAS handle which we call $\widehat{\mathrm{C}\cdot\cdot\mathrm{H}}_{I(2)}$. Note that the first k stories of $\widehat{\mathrm{C}\cdot\cdot\mathrm{H}}_{I(2)}$ overlaps with the image of the collar c_I in $\nu_{(I)}[\frac{2}{3},1]$ and we construct a collar $c_{I(2)}$ for $\widehat{\mathrm{C}\cdot\cdot\mathrm{H}}_{I(2)}$ that is compatible with c_I in the sense that

$$c_{I(2)}(p,t)=c_I(p,\tfrac{2}{3}+\tfrac{1}{3}t)$$

for all $p\in\partial_+\widehat{\mathrm{C}\cdot\cdot\mathrm{H}}_{I(2)}$ the overlap. In addition, we rename $\widehat{\mathrm{C}\cdot\cdot\mathrm{H}}_I$ to $\widehat{\mathrm{C}\cdot\cdot\mathrm{H}}_{I(0)}$ and define a rescaled collar $c_{I(0)}(p,t)=c_I(p,\frac{1}{3}t)$. Finally, we define further puzzle pieces $\boldsymbol{D}_{I(i)}$, $i\in\{0,2\}$, as the intersection of the $(k+1)$-st story of $\widehat{\mathrm{C}\cdot\cdot\mathrm{H}}_{I(i)}$ with $\nu_{I(i)}[0,1]$.

As before we iterate this process infinitely many times. We immediately see that we obtain a countable collection of CEQFAS handles $\widehat{\mathrm{C}\cdot\cdot\mathrm{H}}_I\subset\widehat{\mathrm{C}\cdot\cdot\mathrm{H}}$, one for each *finite* dyadic expansions; all of them are equipped with collars c_I. As far as the handles are concerned, this list contains a lot of repetition since for all I we have

$$\widehat{\mathrm{C}\cdot\cdot\mathrm{H}}_I=\widehat{\mathrm{C}\cdot\cdot\mathrm{H}}_{I(0)}=\widehat{\mathrm{C}\cdot\cdot\mathrm{H}}_{I(00)}=\cdots.$$

However, note that the corresponding collars are different – they become thinner and thinner as we attach more and more zeros to I – and the puzzle pieces $\boldsymbol{D}_I,\boldsymbol{D}_{I(0)},\boldsymbol{D}_{I(00)},\ldots$ are derived from higher and higher stories of $\widehat{\mathrm{C}\cdot\cdot\mathrm{H}}_I$ (story $|I|$, $|I|+1$ and so on). So

what about the *infinite* dyadic expansions? After all, the blueprint promised a Cantor set worth of handles. For those expansions with an infinite tail of zeros, $r = I(00\dots)$ say, we simply take the "limit" of the finite case and let $\widehat{\mathrm{C}\cdot\cdot\mathrm{H}}_r = \widehat{\mathrm{C}\cdot\cdot\mathrm{H}}_I$. In this limit the collars $c_I, c_{I(0)}, \dots$ collapse onto $\partial_+\mathrm{C}\cdot\cdot\mathrm{H}_I$ so we don't equip $\widehat{\mathrm{C}\cdot\cdot\mathrm{H}}_r$ with a collar at all. Also, $\boldsymbol{D}_r$ should be derived from the infinite story of $\widehat{\mathrm{C}\cdot\cdot\mathrm{H}}_r$ and the best way to make sense of this is to define $\boldsymbol{D}_r$ as the end points of $\widehat{\mathrm{C}\cdot\cdot\mathrm{H}}_r$. For truly infinite expansions $r \in \{0,2\}^\infty$, whose tail contains infinitely many 2s, we also get handles $\widehat{\mathrm{C}\cdot\cdot\mathrm{H}}_r \subset \widehat{\mathrm{C}\cdot\cdot\mathrm{H}}$ but this is slightly less obvious. A priori, the construction only gives *open* handles $\mathrm{C}\cdot\cdot\mathrm{H}_r \subset \widehat{\mathrm{C}\cdot\cdot\mathrm{H}}$ but similar control arguments as in the proof of Theorem 9.8 show that the closure of $\mathrm{C}\cdot\cdot\mathrm{H}_r$ in $\widehat{\mathrm{C}\cdot\cdot\mathrm{H}}$ is homeomorphic to its end point compactification. Again, we don't need any collar and simply define $\boldsymbol{D}_r$ as the end points.

At this point we can finally define the Design $\boldsymbol{D} \subset \widehat{\mathrm{C}\cdot\cdot\mathrm{H}}$ as the union of our puzzle pieces $\boldsymbol{D}_I$ over all finite and infinite dyadic expansions starting with zero. If you like, you can think of the Design as a completed puzzle in $\widehat{\mathrm{C}\cdot\cdot\mathrm{H}}$. Since this is so important, here's the definition once more in symbols

$$\boldsymbol{D} = \bigcup_{k\in\mathbb{N}\cup\{\infty\}} \bigcup_{\substack{|I|=k,\\ i_1=0}} \boldsymbol{D}_I. \tag{9.1}$$

Remark 9.12. The way we have defined the Design looks slightly different than the blueprint suggested. But we can easily make the connection by considering the neighborhoods $\nu\partial_+\widehat{\mathrm{C}\cdot\cdot\mathrm{H}}_r = \bigcup_{I\subset r}(\boldsymbol{D}_I \cap \widehat{\mathrm{C}\cdot\cdot\mathrm{H}}_r)$ of the frontiers. A quick look at the definitions reveals that $\boldsymbol{D} = \bigcup_r \nu\partial_+\widehat{\mathrm{C}\cdot\cdot\mathrm{H}}_r$. We will stick to the description in (9.1), though, since it is easier to work with.

Note that the design has a finite and an infinite part coming from the finite and infinite expansions; we call these $\boldsymbol{D}^{<\infty}$ and $\boldsymbol{D}^\infty$. The infinite part $\boldsymbol{D}^\infty$ consist of the end points of all handles $\widehat{\mathrm{C}\cdot\cdot\mathrm{H}}_I$ with infinite expansions, in particular it is a "Cantor set worth of Cantor sets" inside $\widehat{\mathrm{C}\cdot\cdot\mathrm{H}}$. Clearly, the finite part seems more accessible and the good news is that, in some sense, it is enough to know.

Exercise 9.13. Show that the Design $\boldsymbol{D}$ is (a) the closure of $\boldsymbol{D}^{<\infty}$ in $\widehat{\mathrm{C}\cdot\cdot\mathrm{H}}$ and (b) homeomorphic to the end point compactification of $\boldsymbol{D}^{<\infty}$.

Remark 9.14. Strictly speaking we shouldn't speak of *the* Design since our building instructions involve so many choices that it is hard to imagine that two people would end up constructing the same set.

9.4 Embedding the Design in the standard handle

Now that we have found the Design $\boldsymbol{D}$ in our CEQFAS handle $\widehat{\mathrm{C}\cdot\cdot\mathrm{H}} = \widehat{\mathrm{C}\cdot\cdot\mathrm{H}}_{(0)}$ we want to embed it into the standard handle $B^2 \times B^2$. We first focus on the finite part

$$\boldsymbol{D}^{<\infty} = \bigcup_{|I|<\infty} \boldsymbol{D}_I.$$

We denote by $\partial_+^k\widehat{\mathrm{C}\cdot\cdot\mathrm{H}}_I$ and $\partial_+^{\le k}\widehat{\mathrm{C}\cdot\cdot\mathrm{H}}_I$ the intersections of $\partial_+\widehat{\mathrm{C}\cdot\cdot\mathrm{H}}_I$ with the k-th story and the first k stories of $\widehat{\mathrm{C}\cdot\cdot\mathrm{H}}_I$, respectively. With this notation the collars give diffeomorphisms

$$\partial_+^{|I|}\widehat{\mathrm{C}\cdot\cdot\mathrm{H}}_I \times [0,1] \xrightarrow[\cong]{c_I} \boldsymbol{D}_I \subset \widehat{\mathrm{C}\cdot\cdot\mathrm{H}}. \tag{9.2}$$

Moreover, if $I \subset J$ and $k \leq |I|$, then by construction $\widehat{\mathrm{C}\cdot\cdot\mathrm{H}}_J$ is contained in $\widehat{\mathrm{C}\cdot\cdot\mathrm{H}}_I$ and $\partial_+\widehat{\mathrm{C}\cdot\cdot\mathrm{H}}_J$ meets the first k stories of $\widehat{\mathrm{C}\cdot\cdot\mathrm{H}}_I$ in $c_I\big(\partial_+^{\leq k}\widehat{\mathrm{C}\cdot\cdot\mathrm{H}}_I \times \{\rho_J^I\}\big)$ for some $\rho_J^I \in [0,1]$ so that we also have diffeomorphisms

$$\partial_+^{\leq k}\widehat{\mathrm{C}\cdot\cdot\mathrm{H}}_I \underset{\cong}{\longrightarrow} \partial_+^{\leq k}\widehat{\mathrm{C}\cdot\cdot\mathrm{H}}_J \tag{9.3}$$

induced by the collars.

In the light of the above, the our next task is to identify the pieces $\partial_+^k\widehat{\mathrm{C}\cdot\cdot\mathrm{H}}_I$ or, equivalently, $\partial_+^{\leq k}\widehat{\mathrm{C}\cdot\cdot\mathrm{H}}_I$. As in Chapter 7.2, where we studied the boundaries of Casson handles, one can show:

Exercise 9.15. Each $\partial_+^{\leq k}\widehat{\mathrm{C}\cdot\cdot\mathrm{H}}_I$ is diffeomorphic to the complement of a neighborhood of a mixed Bing-Whitehead link in $B^2 \times S^1$ with Whitehead doubles in its last stage.

We can thus choose embeddings

$$\psi_I \colon \partial_+^{\leq |I|}\widehat{\mathrm{C}\cdot\cdot\mathrm{H}}_I \hookrightarrow B^2 \times S^1 \tag{9.4}$$

with the following properties:

(i) ψ_I maps the torus where $\partial_+^{\leq |I|}\widehat{\mathrm{C}\cdot\cdot\mathrm{H}}_I$ meets $\partial_-\widehat{\mathrm{C}\cdot\cdot\mathrm{H}}_I$ to $\partial B^2 \times S^1$.

(ii) Whenever I contains J we have a commutative diagram

$$\begin{array}{ccc} \partial_+^{\leq |I|}\widehat{\mathrm{C}\cdot\cdot\mathrm{H}}_I & \xhookrightarrow{\psi_I} & B^2 \times S^1 \\ \big\downarrow & & \big\| \\ \partial_+^{\leq |J|}\widehat{\mathrm{C}\cdot\cdot\mathrm{H}}_J & \xhookrightarrow[\psi_J]{} & B^2 \times S^1 \end{array} \tag{9.5}$$

where the embeddings $\partial_+^{\leq |I|}\widehat{\mathrm{C}\cdot\cdot\mathrm{H}}_I \hookrightarrow \partial_+^{\leq |J|}\widehat{\mathrm{C}\cdot\cdot\mathrm{H}}_J$ are derived from (9.3).

As a final piece to write down an embedding of $\boldsymbol{D}_I$ into $B^2 \times B^2$ we define a rescaling function $r_I \colon [0,1] \longrightarrow [0,1]$ by the formula

$$r_I(t) = 1 - \sum_{j=1}^{k} \frac{i_j}{3^j} - \frac{1}{3^k}t$$

where $I = (i_1 \dots i_k)$. This maps the unit interval $[0,1]$ affinely onto $[r_I(1), r_I(0)]$ while reversing the direction. Note that for $|I| = k$ these are precisely the intervals in $[\frac{2}{3}, 1]$ that are *not* thrown out in the k-th step of the middle third construction of the Cantor set.

Next we define embeddings $\Psi_I \colon \boldsymbol{D}_I \hookrightarrow B^2 \times B^2$ as a composition

$$\begin{array}{ccc} \boldsymbol{D}_I & \xrightarrow[\cong]{c_I^{-1}} & \partial_+^{|I|}\widehat{\mathrm{C}\cdot\cdot\mathrm{H}}_I \times [0,1] \\ & & \big\downarrow{\scriptstyle \psi_I \times r_I} \\ & & B^2 \times S^1 \times [r_I(1), r_I(0)] \xhookrightarrow{} B^2 \times B^2 \end{array}$$

where the last arrow comes from using polar coordinates in the second factor of $B^2 \times B^2$. Our goal is to patch these embeddings together in order to eventually get an embedding of the whole Design.

Lemma 9.16. *The maps Ψ_I and Ψ_J coincide on $\boldsymbol{D}_I \cap \boldsymbol{D}_J$ and give rise to an embedding*

$$\Psi_I \cup \Psi_J \colon \boldsymbol{D}_I \cup \boldsymbol{D}_J \to B^2 \times B^2.$$

The proof is just a matter of going through the definitions and we leave it as an exercise. This is a good opportunity for the reader to get acquainted with our notation.

Exercise 9.17. Prove Lemma 9.16.

At this point we have found an embedding of the finite part of the Design

$$\Psi^{<\infty} \colon \boldsymbol{D}^{<\infty} \hookrightarrow B^2 \times B^2.$$

It remains to treat the infinite part, that is, the end points of the CEQFAS handles with infinite dyadic expansions.

Lemma 9.18. *Let $I = (i_1 i_2 \dots) \in \{0,2\}^\infty$ be an infinite dyadic expansion. Then the complement of the union $\bigcup_k \operatorname{im} \psi_{(i_1 \dots i_k)} \subset B^2 \times S^1$ is a mixed Bing-Whitehead decomposition $\mathcal{B}_I$ whose elements correspond bijectively to the end points of $\widehat{\mathrm{C}\cdot\cdot\mathrm{H}}_I$. Furthermore, the ψ-maps in* (9.4) *can be chosen such that all decomposition elements of all decompositions $\mathcal{B}_I$ are points.*

Proof. According to Exercise 9.15 the complement of $\operatorname{im} \psi_{(i_1 \dots i_k)}$ is a neighborhood of a mixed Bing-Whitehead link and we denote it by L_I^k. From the compatibility condition (9.5) we see that L_I^{k+1} is contained in L_I^k so that the intersection $\bigcap_k L_I^k$, which is just another way to write the complement of $\bigcup_k \operatorname{im} \psi_{(i_1 \dots i_k)}$, is a mixed Bing-Whitehead decomposition $\mathcal{B}_I$ of $B^2 \times S^1$.

In order to relate this decomposition to $\widehat{\mathrm{C}\cdot\cdot\mathrm{H}}_I$ we note that by construction $\widehat{\mathrm{C}\cdot\cdot\mathrm{H}}_I$ is contained in $\widehat{\mathrm{C}\cdot\cdot\mathrm{H}}_{(i_1 \dots i_k)}$ for each k and it is easy to see that the collar $c_{(i_1 \dots i_k)}$ gives rise to a diffeomorphism

$$\partial_+^{\le k} \widehat{\mathrm{C}\cdot\cdot\mathrm{H}}_{(i_1 \dots i_k)} \longrightarrow \partial_+^{\le k} \widehat{\mathrm{C}\cdot\cdot\mathrm{H}}_I$$

as in (9.3). From here on we can construct a diffeomorphism

$$\partial_+ \mathrm{C}\cdot\cdot\mathrm{H}_I \xrightarrow{\cong} \bigcup_k \operatorname{im} \psi_{(i_1 \dots i_k)} \subset B^2 \times S^1$$

and we see that the ends of $\partial_+ \mathrm{C}\cdot\cdot\mathrm{H}_I$ correspond bijectively with those of $\bigcup_k \operatorname{im} \psi_{(i_1 \dots i_k)}$ which, in turn, correspond to the elements of $\mathcal{B}$. On the other hand, the ends of $\partial_+ \mathrm{C}\cdot\cdot\mathrm{H}_I$ correspond to those of $\mathrm{C}\cdot\cdot\mathrm{H}_I$ as one readily checks.

Moreover, the arguments above show that we can identify the full frontier $\partial_+ \widehat{\mathrm{C}\cdot\cdot\mathrm{H}}_I$ we the decomposition space $B^2 \times S^1 / \mathcal{B}_I$ and, since $\widehat{\mathrm{C}\cdot\cdot\mathrm{H}}_I$ satisfies the Ancel-Starbird property, $\mathcal{B}_I$ is shrinkable. A careful look at the Bing shrinking argument shows that the defining sequence L_I^k can be repositioned by successively applying isotopies in deeper and deeper stages such that all decomposition elements of $\mathcal{B}_I$ are points. Moreover, if two infinite dyadic expansions I, J agree in their first N digits, then for $k \le N$ we can identify L_I^k and L_J^k according to (9.5) and the shrinking isotopies can be chosen compatibly. Finally, these modifications of the L_I^k can be translated into modifications of the ψ-maps. □

Lemma 9.18 shows that the closure of $\Psi^{<\infty}(\boldsymbol{D}^{<\infty})$ inside $B^2 \times B^2$ can be identified with the end point compactification of $\boldsymbol{D}^{<\infty}$ and, according to Exercise 9.13 and its preceding remarks, it follows that $\Psi^{<\infty}$ extends to an embedding of the full Design

$$\Psi \colon \boldsymbol{D} \to B^2 \times B^2 \tag{9.6}$$

by sending the endpoints of $\widehat{\mathrm{C}\cdot\cdot\mathrm{H}}_r$, $r \in \{0,2\}$, which make up $\boldsymbol{D}_r$ to the complement of $\bigcup_k \operatorname{im} \psi_{(i_1 \dots i_k)} \times \{r\} \subset B^2 \times B^2$ assuming that the ψ-maps have been chosen appropriately.

9.5 Holes, gaps and the Endgame

Our strategy is to shrink the complements of the Design in both the standard handle and the Casson handle or, more precisely, the closures of the components of the complements. We will refer to these parts of the standard handle as *holes* and to those in the Casson handle as *gaps*. The holes and gaps are the pieces that are left unexplored and the philosophy is that whenever we can't explore something we try to crush it out and hope that there's enough technology in decomposition space theory so that we can get away with it. To make this a reasonable strategy we should be careful not to crush things that are not cellular.

The problem is that, while there is one "central" hole in the standard handle that is homeomorphic to the 4-ball and is easy to shrink out, we will see that all other holes are homeomorphic to $S^1 \times B^3$ and it would be unproductive to crush them directly into points. To remedy this we try to add spanning disks to these holes to turn them into cellular and potentially more shrinkable decomposition elements. This means that we have to take a step back and give up some pieces that we've already explored but it turns out that what we get in return is worth it.

We first take a closer look at the holes. For that purpose it is useful to understand how the Design in the standard handle intersects the *sleeves* $B^2 \times S^1 \times \{r\}$ where we identify $S^1 \times \{r\}$ with the sphere of radius r in the cocore factor. The first thing to note is that the Design lives in the collar $B^2 \times S^1 \times [\frac{2}{3}, 1]$ of the belt region $B^2 \times S^1$ so that $\boldsymbol{D} \cap B^2 \times S^1 \times \{r\}$ is empty for radii $r < \frac{2}{3}$. For $r \geq \frac{2}{3}$ two things can happen. For a Cantor set radius we get the full sleeve as we've already noted in Remark 9.12. If we're not in a Cantor set radius, then we are in some "middle-third" interval given by some $I \in \{0,2\}^k$ and the lower and upper end points are given by $r_I(0)$ and $r_I(1)$ respectively. In this case the design part in $B^2 \times S^1 \times \{r\}$ is given as the image of ψ_I. Therefore, the holes are given by the components of $L_I \times [r_I(0), r_I(1)]$ for all I, where L_I is the complement of $\operatorname{im} \psi_I$. As already mentioned L_I is a neighborhood of a Bing-Whitehead link. The last Whitehead link components naturally span immersed disks Δ_I^j for $1 \leq j \leq \#$ of link components, as shown in figure **??**. We want to add the disks $\Delta_I^j \times \{r_I(\frac{1}{2})\}$ to the holes to make them birdlike equivalent. But we first have to perturb them in the second factor, to make them embedded disjointly from all other disks and the holes. The disks intersect the associated link component in two disjoint sub disks and themselves in two intervals connecting these sub disks with the boundary. The way we will make them embedded is by pushing a neighborhood of one sub disk to a cantor set level $d_I > r_I(1)$ and a neighborhood of the other to a cantor set level $\hat{d}_I < r_I(0)$. More precise, we will do it in the following inductive way.
We isotope the disk such that they intersect the torus in the sub disks $B_{\frac{1}{4}}(\{\pm\frac{1}{2}\} \times \{0\})$ and themselves in the intervals $[-1, -\frac{3}{4}] \times \{0\}$ and $[\frac{3}{4}, 1] \times \{0\}$. Let $C := B_{\frac{9}{10}}(\{\frac{1}{2}\} \times \{0\}) \cup B_{\frac{9}{10}}(\{-\frac{1}{2}\} \times \{0\})$ and let $b : B^2 \to [0,1]$ be a smooth function with $b \cong 1$ on $B_{\frac{1}{4}}(\{\pm\frac{1}{2}\} \times \{0\})$, $b > 0$ on C and $b \cong 0$ on $B^2 \backslash C$. Now we can start perturbing the disks. Define $C = \{\frac{2}{3}\} \cup \{1\}$. In every step choose one $I \in \{0,2\}^k$ of shortest length where we not yet have spanned disks, then choose points $d_I, \hat{d}_I$ in the cantor set which are no end points and such that $r_I(1) < d_I < \min C \cap [r_I(1), 1]$ and $r_I(0) > \hat{d}_I > \max C \cap [\frac{2}{3}, r_I(0)]$. Define $\phi_I : B^2 \to [0,1]$ by

$$\phi_I(s) = \begin{cases} r_I(\frac{1}{2}) + b(s)(d_I - r_I(\frac{1}{2})) & \text{if } s \in B_{\frac{9}{10}}(\{\frac{1}{2}\} \times \{0\}) \\ r_I(\frac{1}{2}) + b(s)(\hat{d}_I - r_I(\frac{1}{2})) & \text{if } s \in B_{\frac{9}{10}}(\{-\frac{1}{2}\} \times \{0\}) \\ r_I(\frac{1}{2}) & \text{else} \end{cases}$$

For every component of the corresponding hole take the parametrized disks $\Delta_I^j : B^2 \to B^2 \times S^1$ as above and embed disks by $B^2 \xrightarrow{\Delta_I^j \times \phi_I} B^2 \times S^1 \times [0,1]$. At last add the points $\{d_I, \hat{d}_I, r_I(0), r_I(1)\}$ to C. Now we can do the same for the next I.

Exercise 9.19. Check that the disks constructed above are embedded and disjoint from each other and the holes.

10 Epilogue: Edwards' original shrink

Coming soon...

References

[Anc84] F. D. Ancel, *Approximating cell-like maps of S^4 by homeomorphisms*, Four-manifold theory (Durham, N.H., 1982), Contemp. Math., vol. 35, Amer. Math. Soc., Providence, RI, 1984, pp. 143–164.

[AS89] F. D. Ancel and M. P. Starbird, *The shrinkability of Bing-Whitehead decompositions*, Topology **28** (1989), no. 3, 291–304.

[AR65] J. J. Andrews and L. Rubin, *Some spaces whose product with E^1 is E^4*, Bull. Amer. Math. Soc. **71** (1965), 675–677.

[Bea67] R. J. Bean, *Decompositions of E^3 with a null sequence of starlike equivalent non-degenerate elements are E^3*, Illinois J. Math. **11** (1967), 21–23. MR0208581 (34 #8390)

[Bin52] R. H. Bing, *A homeomorphism between the 3-sphere and the sum of two solid horned spheres*, Ann. of Math. (2) **56** (1952), 354–362.

[Bro60] M. Brown, *A proof of the generalized Schoenflies theorem*, Bull. Amer. Math. Soc. **66** (1960), 74–76.

[Cas86] A. J. Casson, *Three lectures on new-infinite constructions in 4-dimensional manifolds*, À la recherche de la topologie perdue, Progr. Math., vol. 62, Birkhäuser Boston, Boston, MA, 1986, pp. 201–244. With an appendix by L. Siebenmann.

[CG78] A. J. Casson and C. McA. Gordon, *On slice knots in dimension three*, Algebraic and geometric topology (Proc. Sympos. Pure Math., Stanford Univ., Stanford, Calif., 1976), Part 2, Proc. Sympos. Pure Math., XXXII, Amer. Math. Soc., Providence, R.I., 1978, pp. 39–53.

[COT03] T. D. Cochran, K. E. Orr, and P. Teichner, *Knot concordance, Whitney towers and L^2-signatures*, Ann. of Math. (2) **157** (2003), no. 2, 433–519.

[COT04] ———, *Structure in the classical knot concordance group*, Comment. Math. Helv. **79** (2004), no. 1, 105–123.

[Dav86] R. J. Daverman, *Decompositions of manifolds*, Pure and Applied Mathematics, vol. 124, Academic Press Inc., Orlando, FL, 1986.

[Edw80] R. D. Edwards, *The topology of manifolds and cell-like maps*, Proceedings of the International Congress of Mathematicians (Helsinki, 1978), Acad. Sci. Fennica, Helsinki, 1980, pp. 111–127, available at `http://www.mathunion.org/ICM/ICM1978.1/`.

[Edw84] ———, *The solution of the 4-dimensional annulus conjecture (after Frank Quinn)*, Four-manifold theory (Durham, N.H., 1982), Contemp. Math., vol. 35, Amer. Math. Soc., Providence, RI, 1984, pp. 211–264.

[Fre82] M. H. Freedman, *The topology of four-dimensional manifolds*, J. Differential Geom. **17** (1982), no. 3, 357–453.

[FQ90] M. H. Freedman and F. Quinn, *Topology of 4-manifolds*, Princeton Mathematical Series, vol. 39, Princeton University Press, Princeton, NJ, 1990.

[GS84] R. E. Gompf and S. Singh, *On Freedman reimbedding theorems*, Four-manifold theory (Durham, N.H., 1982), Contemp. Math., vol. 35, Amer. Math. Soc., Providence, RI, 1984, pp. 277–309.

[Kir89] R. C. Kirby, *The topology of 4-manifolds*, Lecture Notes in Mathematics, vol. 1374, Springer-Verlag, Berlin, 1989.

[Maz59] B. Mazur, *On embeddings of spheres*, Bull. Amer. Math. Soc. **65** (1959), 59–65.

[Mor60] M. Morse, *A reduction of the Schoenflies extension problem*, Bull. Amer. Math. Soc. **66** (1960), 113–115.

[Qui82] F. Quinn, *Ends of maps. III. Dimensions 4 and 5*, J. Differential Geom. **17** (1982), no. 3, 503–521.

[Whi44] H. Whitney, *The self-intersections of a smooth n-manifold in 2n-space*, Ann. of Math. (2) **45** (1944), 220–246.